Coordination of reactive power scheduling in a multi-area power system operated by independent utilities

Yannick Phulpin

COORDINATION OF REACTIVE POWER SCHEDULING IN A MULTI-AREA POWER SYSTEM OPERATED BY INDEPENDENT UTILITIES

A Thesis
Presented to
The Academic Faculty

by

Yannick D. Phulpin

In Partial Fulfillment
of the Requirements for the Degree
Doctor of Philosophy in the
School of ECE

Georgia Institute of Technology
December 2009

COORDINATION OF REACTIVE POWER SCHEDULING IN A MULTI-AREA POWER SYSTEM OPERATED BY INDEPENDENT UTILITIES

Approved by:

Professor Deepak Divan,
Committee Chair
School of ECE
Georgia Institute of Technology

Professor Miroslav Begovic, Advisor
School of ECE
Georgia Institute of Technology

Professor Ron Harley
School of ECE
Georgia Institute of Technology

Professor Erik Verriest
School of ECE
Georgia Institute of Technology

Professor Marc Petit
Department of Power and Energy Systems
SUPELEC

Date Approved: 10/13/2009

PREFACE

This thesis presents research that was done in the framework of a cooperation with Supélec, France. It is co-advised by Marc Petit at Supélec.

ACKNOWLEDGEMENTS

I want to gratefully thank Damien Ernst from the FNRS and University of Liège, Belgium, for his fruitful collaboration. In addition, my recognition goes to Patrick Panciatici and Jean-Baptiste Heyberger, from RTE, for their valuable advice.

TABLE OF CONTENTS

LIST OF TABLES

LIST OF FIGURES

SUMMARY

This thesis addresses the problem of reactive power scheduling in a power system with several areas controlled by independent transmission system operators (TSOs). To design a fair method for optimizing the control settings in the interconnected multi-TSO system, two types of schemes are developed.

First, a centralized multi-TSO optimization scheme is introduced, and it is shown that this scheme has some properties of fairness in the economic sense.

Second, the problem is addressed through a decentralized optimization scheme with no information exchange between the TSOs. In this framework, each TSO assumes an external network equivalent in place of its neighboring TSOs and optimizes the objective function corresponding to its own control area regardless of the impact that its choice may have on the other TSOs.

The thesis presents simulation results obtained with the IEEE 39 bus system and IEEE 118 bus systems partitioned between three TSOs. It also presents some results for a UCTE-like 4141 bus system with seven TSOs. The decentralized control scheme is applied to both time-invariant and time-varying power systems. Nearly optimal performance is obtained in those contexts.

ACRONYMS

AFF	Adaptive forgetting factor
AVR	Automatic voltage regulation
CCC	Centralized control center
CSVC	Coordinated secondary voltage control
ED-ERLS	Environment dependent exponential recursive least squares
ERLS	Exponential recursive least squares
OPF	Optimal power flow
REI	Radial equivalent and independent
SVC	Secondary voltage control
TSO	Transmission system operator
TVC	Tertiary voltage control

CHAPTER I

INTRODUCTION

1.1 Background

Secure operation of large-scale power systems requires appropriate coordination of control actions over the entire system. Despite the development of sophisticated control schemes [1], several recent incidents raise the problem of steady-state optimization of those systems [2, 3]. More specifically, a major issue is to coordinate the control actions of the interconnected entities with respect to their operational objectives and constraints [4].

The influence that the controls of one transmission system operator (TSO) may have on the system variables of the neighboring TSOs has led, as discussed in [5], to two major trends for organization and control of interconnected power systems. On one hand, one has seen the emergence of some Mega TSOs, resulting from the merging of several smaller ones. On the other hand, where the regrouping of TSOs into large entities has not occurred, new strategies to coordinate the actions of the TSOs have been advocated. Those strategies can be classified into two categories, using centralized or decentralized control.

Several papers, such as [6, 7] for example, proposed centralized control strategies for multi-TSO power systems. Those strategies usually rely on the assumption that the TSOs have agreed to transferring some of their prerogatives to a central entity, which is in charge of optimizing the entire system with respect to the operational objectives of the TSOs.

Other research papers also proposed decentralized schemes for multi-TSO power system operation. Y. Li and V. Venkatasubramanian outline in [8] a scheme for

coordinating path transfers with the goal of an increase in transfer capability, while P. Panciatici *et al.* describe in [9] the benefits of inter-TSO coordination for tertiary voltage control. The "UCTE Operation Handbook" [10] also sets some rules for close cooperation between member companies to make the best possible use of the benefits offered by an interconnected operation.

1.2 Problem statement

In the context of a hierarchical voltage control scheme, this thesis addresses the problem of reactive power scheduling. This problem consists of the optimization of the voltage settings for generators and compensators in the entire system with regard to the individual operational objective of every TSO.

Prior to agreeing to optimizing its control area in a coordinated manner, each TSO is likely to require some guarantees regarding the fulfillment of its operational objective(s). As introduced in [11], a scheme with the ability to simultaneously satisfy every party can be qualified "fair." For inter-TSO coordination to be of interest, a new scheme must then be consistent with the fairness properties, which are identified in [12, 13].

As emphasized in [6], a central entity might achieve consensus among the different parties through a specific multi-party optimization scheme. However, this kind of centralized control scheme usually relies on information exchange between the TSOs and the central entity, which could make the scheme more vulnerable with respect to the loss of a communication channel [14]. This vulnerability could raise questions for the TSOs regarding the robustness of the arbitrage strategy chosen by the central entity. Therefore, it may also be of interest to study the performance of decentralized schemes, which would rely less, or not at all, on information exchange.

Indeed, while research in decentralized optimization schemes for power systems is still in its infancy, several papers have already shown the potential outcomes of decentralized optimization schemes in power systems. For example, [15, 16] propose decentralized optimization schemes that can achieve nearly optimal performance through exchange of information concerning the TSOs' network topology and intended control actions. In [17, 18], the decentralized schemes under consideration do not rely on an explicit exchange of information between the TSOs, since the information is implicitly exchanged by observing the influence of the TSO's actions on the other TSOs of the power network. Also, M. Ilic *et al.* highlight in [19] the danger that decentralized optimization may have on power system security, when conflicting local strategies result in a reduction of each TSO's own performance criterion.

As one could think of applying decentralized optimization in the context of reactive power scheduling in multi-TSO power systems, the main issue is therefore to design a scheme that achieves nearly optimal performance with respect to the operational objectives of the TSOs with a high level of robustness.

1.3 Objective of the research

The research is partitioned into four main tasks. First, the problem of reactive power scheduling in a multi-TSO system is formalized. Second, a centralized strategy is proposed to solve the multi-TSO optimization problem. Third, the decentralized control scheme is proposed, and optimal settings for the scheme are identified in the context of two test systems. Fourth, an example of an application to a large-scale system is detailed.

1.4 Thesis outline

In Chapter 2, the theoretical motivation of reactive power scheduling is introduced, practices in the field of voltage control are described and, the need for a higher level of hierarchical voltage control is highlighted. Chapter 3 formulizes the optimization problem for a multi-TSO power system and the relevant evaluation criteria.

In the second part of this thesis, multi-party optimization methods are reviewed in Chapter 4, and Chapter 5 presents a centralized optimization scheme that has some properties of fairness in the economic sense.

The third part of this thesis is dedicated to the decentralized control scheme that is introduced in Chapter 6. Chapter 7 presents an evaluation of the decentralized control scheme in the context of the IEEE 39 bus system and 118 bus system with three TSOs, and Chapter 8 presents some results in the context of a UCTE-like 4141 bus system with seven TSOs. The evaluation is successively carried out for time-invariant and time-varying systems.

Finally, Chapter 9 summarizes the thesis, while the contributions of this research are detailed in Chapter 10, and perspectives for future research are emphasized in Chapter 11.

CHAPTER II

ORIGIN AND HISTORY OF THE PROBLEM

In this chapter, the first section introduces the theoretical motivation of voltage control in power systems. Then, past and current practices in voltage control are analyzed. Finally, the need for a higher-level control layer is emphasized.

2.1 Theoretical motivation of voltage control

One mission of transmission systems operators is to avoid large disturbances and system collapses. When such events occur, an exhaustive analysis is carried out to identify the critical factors, among which voltage stability problems have been recognized for a long time to be a root cause for system failure [20].

As emphasized in [21], voltage instability occurs when the load dynamics fails to restore power consumption at the expected level. In practice, voltage instability is an attribute of a system, whose dynamics does not lead to a constraint-compliant equilibrium. Whereas this attribute involves both short and long term analysis, it has been mainly studied through steady-state modeling of power systems. The fundamentals of long-term voltage stability are introduced in the first part of this section, and the associated concepts are illustrated with the problem of automatic load tap changers. In the second part of this section, the bifurcation theory is detailed, with a particular attention for the saddle node bifurcation.

2.1.1 Long-term voltage stability

The long-term voltage stability problem is introduced in [22] by means of the two bus system that is represented in Figure 1. This system is composed of a generator with a constant voltage output V_G, a transmission line with constant impedance magnitude Z_L and angle φ_L, and a load modeled by an impedance Z, φ. In this context, the active power transmitted to the load P can be written as follows.

$$P - \frac{3 \times Z \times (V_G/Z_L)^2 \times \cos(\varphi)}{1 + (Z/Z_L)^2 + 2 \times Z/Z_L \times \cos(\varphi_L - \varphi)} = 0 \tag{1}$$

Figure 2 depicts the steady-state operation conditions for different values of φ when Z varies from ∞ through 0.

When $Z = \infty$, the active power demand P is zero and the load voltage V is equal to V_G. From this point, one should decrease Z to increase load demand P. This control is effective until a maximum amount of P is reached, which is usually referred to as bifurcation point. It corresponds to $Z = Z_L$, and P_b can be computed as follows.

$$P_b = \frac{3 \times Z_L \times (V_G/Z_L)^2 \times \cos(\varphi)}{4 \times \cos^2(\frac{\varphi_L - \varphi}{2})} \tag{2}$$

The system is said to be unstable if $Z \leq Z_L$. Indeed, with this condition, any new decrease of Z turns into a decrease of P.

To assess power flows in a system where power demands and injections are known, it is usual to compute the bus voltages that correspond to the given operation conditions. When $P < P_b$, one can observe on Figure 2 that two solutions exist. The bifurcation $P = P_b$ is characterized by a single solution for V, and no feasible solution exists for $P > P_b$. Hence, the bifurcation corresponds to an infinite sensitivity of voltage with respect to the power demand [23]. According to [24], this property can be extended to systems, where the loads are represented by more sophisticated models.

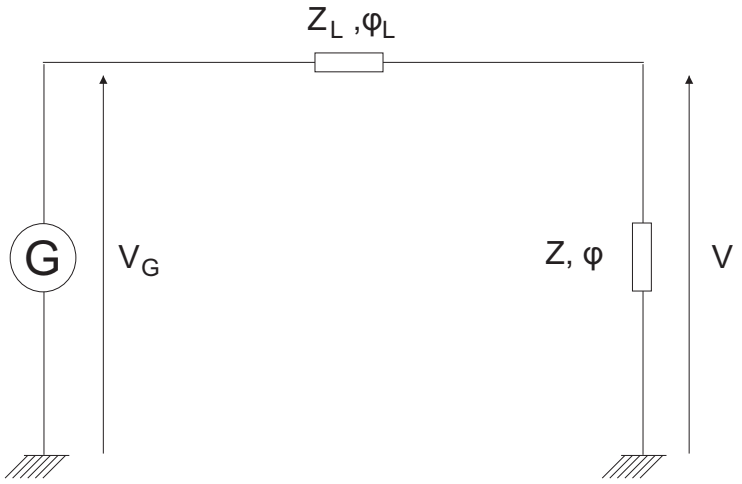

Figure 1: Illustrative two bus system for steady-state voltage stability analysis.

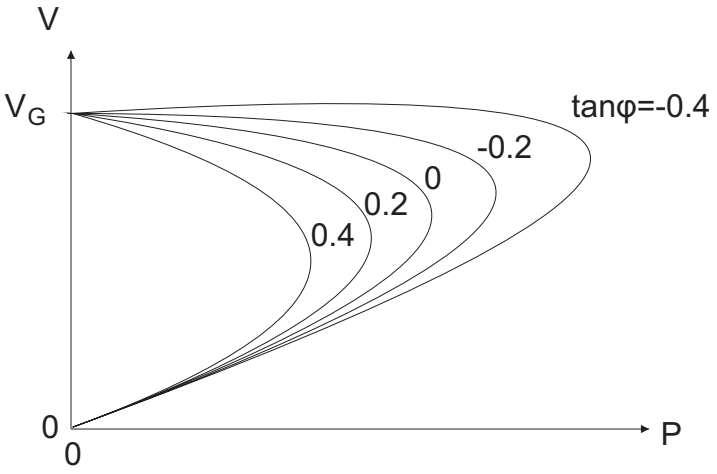

Figure 2: PV curve for the two bus illustrative system with different values of φ.

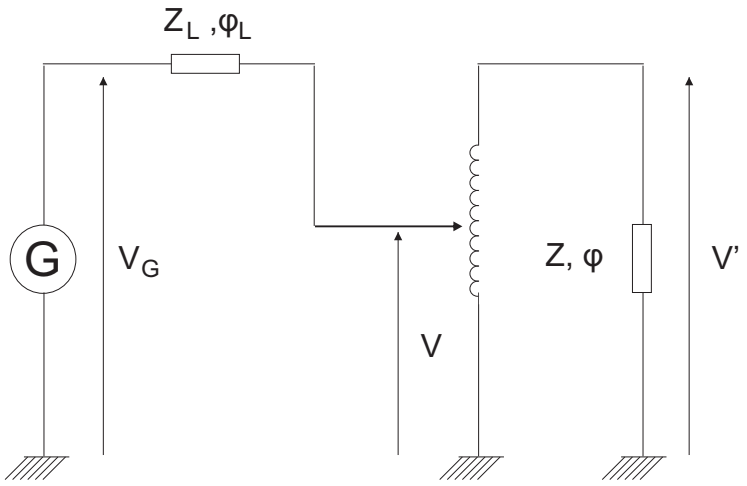

Figure 3: Illustrative two bus system with a load tap changer.

2.1.2 Impact of load tap changers on voltage stability

As emphasized in the previous section, the system stability is directly related to its dynamics. A typical example of this relationship is the load tap changers problem, which was identified as one of the causes of long-term voltage instability in [25]. Those elements aim to restore load demand during low load voltage magnitude conditions. A load tap changer can be modeled as a tap changer, whose setting n is controlled to achieve a specific secondary voltage V_0. In the context of the two bus system that is presented in Section 2.1.1, a load tap changer can be modeled as in Figure 3, where V and V' are the voltage magnitudes at the primary and secondary sides of the load tap changer, respectively.

In this system, the tap changer dynamics can be modeled by the following equation,

$$\frac{dn}{dt} = \frac{K}{T}(V_0 - V') \tag{3}$$

where T is the load tap changer's time constant, which usually amounts ten seconds [26] and K is a control parameter. Although n is a discrete variable in practice, a step in the tap position contributes a relatively small amount of voltage correction. In voltage stability analysis, n is thus considered as a continuous variable [27].

Using the above described model, one can write the steady-state equations of the system.

$$\underline{V'} = \frac{n \times \underline{V_G} \times \underline{Z}}{n^2 \times \underline{Z_L} + \underline{Z}} \tag{4}$$

Based on (3) and (4), the system dynamics is characterized by

$$\frac{dn}{dt} = \frac{K}{T}(V_0 - \frac{n \times \underline{V_G} \times \underline{Z}}{[n^4 \times {Z_L}^2 + 2 \times n^2 \times Z \times Z_L \times \cos(\phi_L - \phi) + Z^2]^{1/2}}) \tag{5}$$

As emphasized in [27], the stability of this non-linear system can be studied by local linearization of the system around the possible equilibrium points, i.e., the values of n, for which $\frac{dn}{dt} = 0$. From (5), it can be deduced that two equilibrium points n_{01} and n_{02} exist if

$$({V_G}^2 \times Z^2 - 2 \times {V_0}^2 \times Z \times Z_0 \times \cos(\varphi_L - \varphi))^2 > 4 \times Z^2 \times {Z_L}^2 \times {Z_0}^4 \tag{6}$$

Under this condition, one can depict $\frac{dn}{dt}$ and V' as functions of n, as in Figures 4 and 5, respectively. Based on this representation, a stability region $0 \leq n < n_{02}$ can be defined, where n converges toward n_{01}. As emphasized in [27], the definition of stability region can be extended to the cases of system with multiple load tap changers.

When the system is operated in conditions where n_{01} is close to n_{02}, an unexpected event is likely to deviate the system from stable to unstable state [28]. A curative approach to maintain long-term voltage stability is then to block load tap changers under low voltage conditions [29]. In addition, as stability margins, i.e. the distance between n_{01} and n_{02} in the illustrative system, depend on voltage settings, a preventive approach could be to optimize voltage settings so as to operate the system under appropriate stability margins.

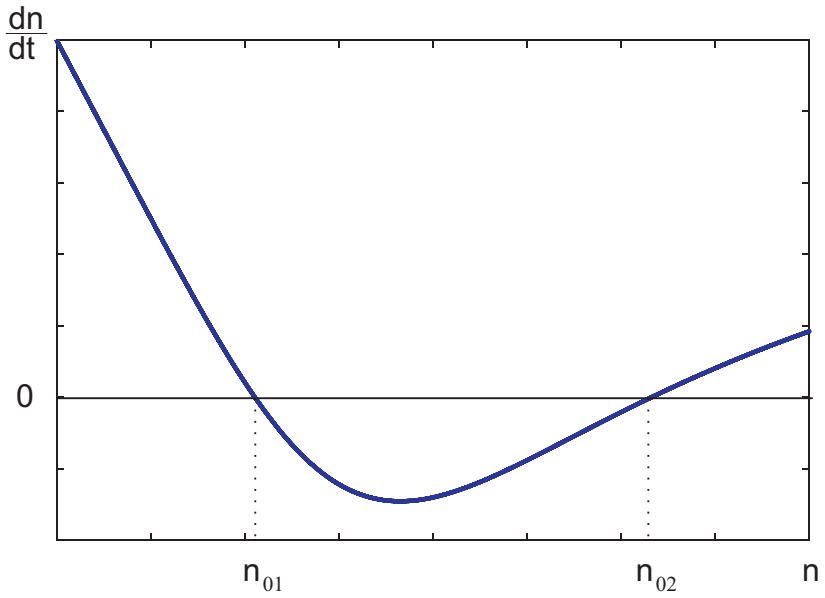

Figure 4: Representation of $\frac{dn}{dt}$ as a function of n for a two bus system with a load tap changer, where two equilibrium points exist.

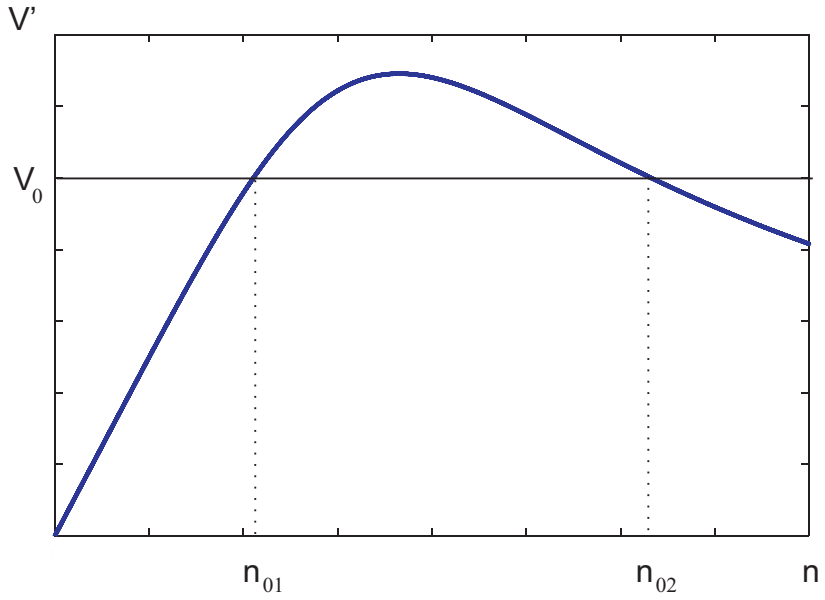

Figure 5: Representation of V' as a function of n for a two bus system with a load tap changer, where two equilibrium points exist.

2.1.3 Bifurcation model of voltage instability

To represent long-term voltage stability problems in a mathematical model, two types of variables should be distinguished, state variables[1] $\mathbf{x} \in \mathbb{R}^n$, and parameters $\lambda \in \mathbb{R}^m$. In power systems, state variables typically include bus voltage magnitude and phase angle, currents in generator windings, and load tap changers' settings. Parameter variations are considered slow compared with the system dynamics. They generally represent real and/or reactive power demand [30]. Using this notation, the power system dynamic model (in the form of differential-algebraic set of equations) is characterized by two functions $\mathbf{F_1} : \mathbb{R}^n \times \mathbb{R}^m \mapsto \mathbb{R}^n$ and $\mathbf{F_2} : \mathbb{R}^n \times \mathbb{R}^m \mapsto \mathbb{R}^m$ as follows [24].

$$\dot{\mathbf{x}} = \mathbf{F_1}(\mathbf{x}, \lambda) \tag{7}$$

$$\mathbf{0} = \mathbf{F_2}(\mathbf{x}, \lambda) \tag{8}$$

In this context, an equilibrium point $(\mathbf{x}^*, \lambda^*)$ corresponds to $\mathbf{F_1}(\mathbf{x}^*, \lambda^*) = \mathbf{0}$, and $\mathbf{F_2}(\mathbf{x}^*, \lambda^*) = \mathbf{0}$, which will be denoted $\mathbf{F}(\mathbf{x}^*, \lambda^*) = \mathbf{0}$ from now on.

Studying the system dynamics with different values of λ leads to the identification of bifurcation points, defined as points in the parameter space for which the qualitative structure of the system changes for a small variation of λ [21]. In [31], a bifurcation point is defined as an equilibrium state $(\mathbf{x}^*, \lambda^*)$, such that

$$\mathbf{F}(\mathbf{x}^*, \lambda^*) = \mathbf{0} \tag{9}$$

$$det[\mathbf{F_x}(\mathbf{x}^*, \lambda^*)] = 0 \tag{10}$$

where $\mathbf{F_x}(\mathbf{x}^*, \lambda^*)$ is the Jacobian matrix of the system model evaluated at point $(\mathbf{x}^*, \lambda^*)$.

In [32], several types of bifurcations are identified, which differ by the types of eigenvalues of $\mathbf{F_x}(\mathbf{x}^*, \lambda^*)$ and can be classified as follows.

[1] In this thesis, bold fonts are used to highlight multidimensional variables, functions, or logical symbols.

- Saddle node bifurcation corresponds to an equilibrium $(\mathbf{x}^*, \lambda^*)$, where $\mathbf{F_x}(\mathbf{x}^*, \lambda^*)$ has a simple zero eigenvalue with left and right eigenvectors $\mathbf{v}^*$ and $\mathbf{w}^*$, respectively. In practice, in a saddle node bifurcation, a stable equilibrium (every eigenvalue of $\mathbf{F_x}(\mathbf{x}^*, \lambda^*)$ has a negative real part) disappears by coalescing with the unstable equilibrium, where one eigenvalue of $\mathbf{F_x}(\mathbf{x}^*, \lambda^*)$ has a positive real part.

- Hopf bifurcation corresponds to an equilibrium $(\mathbf{x}^*, \lambda^*)$, where $\mathbf{F_x}(\mathbf{x}^*, \lambda^*)$ has a pair of (non-zero) purely imaginary eigenvalues [21]. This condition yields that stability of an equilibrium may be lost through its interaction with a limit cycle. In practice, a system whose parameters are nearing Hopf bifurcation will often exhibit a slow onset of sustained oscillations due to the fact that the pair of eigenvalues closest to zero are complex conjugates of each other. Such phenomena have actually been observed in power system and subsequently verified by calculations [33].

- Higher order bifurcations are described in [34], and some third and fourth order bifurcations are discussed in [32]. As power systems dynamic models usually have a single parameter (such as correlated load increase), those types of bifurcations are not generic. This means that they can occur only as isolated exceptions [21]. Hence, they are generally considered unlikely [30].

The system changes induced by a single parameter variation lead to a codimension one bifurcation, the onset of which are large sensitivities of the state variables to parametric changes. As both voltage magnitudes and phase angles compose the state variables, both voltage and angular stability can be affected, depending on the eigenvalues of $\mathbf{F_x}(\mathbf{x}^*, \lambda^*)$ [24]. When voltage magnitudes are particularly affected by parametric changes close to a singularity (bifurcation), it is usually said that the system is close to a voltage collapse.

2.1.4 Saddle node bifurcation

The system can not stay at the saddle node bifurcation equilibrium because any small perturbation in the system $\boldsymbol{\Delta}\lambda$ could induce a loss of voltage and/or angular stability. Indeed, by assuming that the function $\mathbf{F}$ is differentiable around every equilibrium point $(\mathbf{x}^*, \lambda^*)$, and that the system remains in steady-state equilibrium, the following relation can be derived.

$$\frac{\partial \mathbf{F}}{\partial \mathbf{x}}(\mathbf{x}^*, \lambda^*) \times \boldsymbol{\Delta}\mathbf{x} = -\frac{\partial \mathbf{F}}{\partial \lambda}(\mathbf{x}^*, \lambda^*) \times \boldsymbol{\Delta}\lambda \tag{11}$$

This implies that, when $\det[\frac{\partial \mathbf{F}}{\partial \mathbf{x}}(\mathbf{x}^*, \lambda^*)] = 0$, the voltage magnitudes are infinitely sensitive to parameter perturbations.

It is remarkable that, because of the non-linear nature of the systems models, the saddle node bifurcation might be difficult to identify in large-scale power systems. System state trajectories around equilibrium points have thus been studied in [32], so as to design computationally efficient methods to identify stability limits.

Furthermore, to operate power systems more safely, long-term voltage stability indicators have been developed. They usually depict the loading margin of the system, which is defined as the load increase (according to a specific load pattern) that the system can sustain before reaching a bifurcation [35]. Most of the indicators correspond to a measure of singularity (e.g., determinant, smallest eigenvalue, minimum singular value), but none of them is linear up to the point of bifurcation, especially because bifurcation often arises due to hard nonlinearities (such as contingencies or activation of reactive limiters in generators, which is changing the number of states - and the size of Jacobian - in the system). The only linear measure of proximity is the margin itself, which requires more than one evaluation of the system state. Hence, a variety of techniques have been developed, such as continuous power flow [36], which iteratively follow a load trajectory to a point of singularity and assess the metric distance to the point of intersection of the load trajectory in parameter space and the

stability boundary.

A singularity based technique is used in [35], which proposes a method to compute the influence of system controls (e.g., emergency load shedding, reactive power support, interarea redispatch) on the loading margin. More specifically, in a system where parameters λ can be decomposed in (μ, p), with μ the system loading and p control parameters, linearization of the equilibrium curve around the saddle node bifurcation $(\mathbf{x}^*, \mu^*, p^*)$ described by (9) yields.

$$\frac{\partial \mathbf{F}}{\partial \mathbf{x}}(\mathbf{x}^*, \mu^*, \mathbf{p}^*) \times \mathbf{\Delta x} + \frac{\partial \mathbf{F}}{\partial \mu}(\mathbf{x}^*, \mu^*, \mathbf{p}^*) \times \mathbf{\Delta} \mu + \frac{\partial \mathbf{F}}{\partial \mathbf{p}}(\mathbf{x}^*, \mu^*, \mathbf{p}^*) \times \mathbf{\Delta p} = \mathbf{0} \tag{12}$$

Multiplying by the left hand eigenvector $\mathbf{w}^*$ yields the following equation.

$$\mathbf{w}^* \times \frac{\partial \mathbf{F}}{\partial \mu}(\mathbf{x}^*, \mu^*, \mathbf{p}^*) \times \mathbf{\Delta} \mu + \mathbf{w}^* \times \frac{\partial \mathbf{F}}{\partial \mathbf{p}}(\mathbf{x}^*, \mu^*, \mathbf{p}^*) \times \mathbf{\Delta p} = \mathbf{0} \tag{13}$$

This leads to the definition of a sensitivity matrix $\mathbf{L_p}$ for $\Delta\mu$ as a function of Δp.

$$\mathbf{L_p} = -\frac{\mathbf{w}^* \times \frac{\partial \mathbf{F}}{\partial \mathbf{p}}(\mathbf{x}^*, \mu^*, \mathbf{p}^*)}{\mathbf{w}^* \times \frac{\partial \mathbf{F}}{\partial \mu}(\mathbf{x}^*, \mu^*, \mathbf{p}^*)} \tag{14}$$

This matrix can be used to assess optimal settings, so as to maximize loading margin in power systems. They are, however, subject to limitations because of the linearized representation of a complex system, among others.

As emphasized in [37], loading margin sensitivities are applied during imminent situations of voltage collapse to steer away the system from the bifurcation. In such cases, they are used to assess the most effective control actions, among reactive power support changes (e.g., from generators and static or dynamic compensators), freezing of the taps on transformers, reduction of distribution voltage, or load shedding in the worst cases. Those emergency control actions are applied in extreme situations, which are rare in large-scale power systems.

In normal operating conditions, the loading margin is large enough, and reactive power resources are operated with respect to other objectives, such as minimizing transmission losses, or maximizing reserves. The following section and most of the dissertation focus on this aspect of reactive power management, which usually involves a hierarchical organization of voltage control to nest control actions with respect to time scales and domains of influence [38]. While this organization is detailed in the following sections, the remaining of the thesis focuses on the definition of a new layer of hierarchical control to coordinate long-term control actions over several control regions in normal operating conditions.

2.2 A historical perspective on voltage control

Voltage control has been progressively automated [39] and upgraded consequent to new technological developments, further expansion of the network, or more dramatically, some specific incidents, which are reported in [38]. In fact, whereas the voltage stability theory appeared around 1975, consequences of instability were already well known, and the need for voltage control appeared in the early power systems. T. Hughes emphasizes in [40] the existence of a voltage controller in the Pearl Street station system in New York, which was designed by T. Edison and his associates in 1882. At that time, a power station attendant used to control the field resistance according to the signal given by an automatic indicator utilizing an electromagnet connected across the station's main circuit.

The merging of local utilities in the twenties and thirties obliged electricity utilities to deal with new transmission system issues such as voltage control in a regional or national system. The first approaches of automatic voltage control dealing with local correction of generators' excitation are reported in [41].

A regional control dimension appeared in the seventies [39] with the objective of managing a mid-term (10 to 30 min.) dynamic equilibrium within any given area of

the system.

Finally, methods for nationwide regulation have been proposed for the last 40 years. As emphasized in [42], a large body of work reflects this research toward a better large-scale optimization of reactive power management. In [43, 44, 45] a summary of the research activity in this domain is provided. However, reactive power scheduling remains most often heuristic and empirical [46], as intuitive rule-based control usually achieves relatively safe and well-performing operation [47].

2.3 Modern practices in voltage control

Nowadays, voltage control strategies are generally hierarchical. This type of control strategy was introduced in [39] as a three-layer scheme aimed at solving certain issues on three scales of time and distance.

Automatic voltage control is often referred to as automatic voltage regulation (AVR). This closed-loop decentralized scheme provides fast control actions (within several seconds) in the face of local perturbations by adjusting generators' excitation depending on their voltages [48].

Secondary voltage control (SVC) is also a closed-loop control that provides voltage support to an area of the transmission network in a coordinated manner. Its time constant is around one to five minutes.

Tertiary voltage control (TVC) acts every 15 to 30 minutes or as events occur. When not empirically assessed, an off-line optimal power flow program is run to set the reference values of the secondary voltage control.

In some papers, such as [49], secondary and tertiary voltage control are considered collectively as a unique steady-state voltage control layer referred to as centralized voltage control. For the sake of simplicity, the three-layer approach, which is illustrated in Figure 6, is used in this thesis. The different control levels are extensively described in this section.

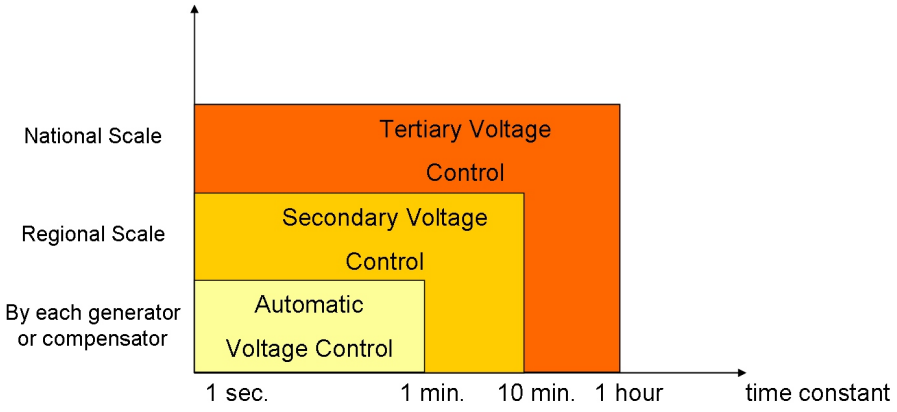

Figure 6: Time-space delineation of the hierarchical voltage control scheme.

2.3.1 Automatic voltage control

The so-called automatic voltage regulation aims to manage a fast, dynamic response to fast voltage changes by maintaining the bus voltage at its expected value [49].

It sets the value of the reactive power injection of every individual generating unit, synchronous condensers, and fast responding static VAr compensators with a short time response (one millisecond to one minute) [50]. Nevertheless, as emphasized in [51], distributed generation is not systematically equipped with AVR.

As described in Equation (15), the AVR modifies the excitation of every generator i under consideration by ΔE_{Gi} for any voltage amplitude variation $\Delta |V_i|$ measured at bus i. The gain of this control loop is K. In this scheme, the reactive power injection is obviously limited to its maximal and minimal values at each bus.

$$\Delta E_{Gi} = K \times \Delta |V_i| \tag{15}$$

2.3.2 Secondary voltage control

As emphasized in [52], AVR alone is not sufficient to lead to a steady-state equilibrium of the system. A regional closed-loop control scheme called secondary voltage control has thus been developed to maintain the pilot bus voltage at its reference value. The

time constant of this control scheme is between 1 and 15 min [53].

The choice of control regions and pilot buses is obviously essential for the performance of the secondary voltage control. Numerous papers have therefore proposed alternative methods for assessing them. For example, global search algorithms [54], electrical distances and sensitivities [55], simulated annealing algorithms [56], or Greedy algorithms have been proposed. An exhaustive comparison of these techniques is provided in [57].

The secondary voltage control sets a reference value for the AVR and acts therefore on the same controls. But, unlike AVR, which is only applied to dynamic devices, it can also deal with slower equipment such as certain synchronous condensers and static VAr compensators. Also, it can act at a substation level and control load tap changers or voltage transformer taps, for instance.

The two major trends for secondary voltage control are detailed hereafter. The classical secondary voltage control (SVC) is the most commonly applied. It is based on complete independence of the control regions. The second scheme, called coordinated secondary voltage control (CSVC), deals with the inter-area influence but is still rarely applied. The only reported application is in western France (Region Pays de Loire).

2.3.2.1 Classical secondary voltage control

Secondary voltage control was introduced in [39]. It ensures that each generator produces, at any loading condition, the same percentage of reactive power with respect to its MVA ratings. Therefore, all generator units in an area contribute, in a coordinated way, to the areas voltage support under both normal operation and during contingencies. This scheme regulates the voltage of the pilot node to a pre-specified value, increasing voltage stability margins.

SVC may be formulated as in Equation (16), where $|V_P|$ is the pilot bus voltage amplitude, $|V_{Pr}|$ is its reference value, K_{SVC} is a parameter, and e_s is the injection

signal that defines the reactive power injection expected from every bus as expressed in Equation (17), where $\mathbf{Q}_G$ is the vector of the reactive power injections at every controlled bus of the region and $\mathbf{Q}_{Gr}$ is its initial value.

$$e_s = K_{SVC} \times \int |V_P| - |V_{Pr}|\, dt \tag{16}$$

$$\mathbf{Q}_G = e_s \times \mathbf{WF} \times \mathbf{Q}_{Gr} \tag{17}$$

A weight factor matrix **WF** may be introduced to amplify the injection signal so as to preserve fast dynamic reactive power reserves for automatic voltage regulation purposes [47].

2.3.2.2 Coordinated secondary voltage control

CSVC was introduced by J.P. Paul *et al.* in [53]. It aims at increasing voltage stability in highly constrained areas [58]. The influence that one region can have on its neighboring regions is considered under the conditions defined by M. Ilic *et al.* in [59]. In addition, it consists of an optimization problem, which can be written in the form

$$\begin{aligned} \min_{\mathbf{Q}_G} & \lambda_p \times \|\alpha(|V_P| - |V_{Pr}|) - \mathbf{C_p \Delta}\,|\mathbf{V_c}|\|^2 \\ & + \lambda_q \times \|\alpha(\mathbf{Q}_G - \mathbf{Q}_{Gr}) - \mathbf{C_q \Delta}\,|\mathbf{V_c}|\|^2 \\ & + \lambda_v \times \|\alpha(|\mathbf{V}| - |\mathbf{V}_r|) - \mathbf{\Delta}\,|\mathbf{V_c}|\|^2 \end{aligned} \tag{18}$$

where α is the gain of CSVC, $\mathbf{C_p}$ the voltage sensitivity matrix, $\mathbf{\Delta}\,|\mathbf{V_c}|$ the vector of stator voltage amplitude variations, $\mathbf{C_q}$ the reactive power sensitivity matrix, $|\mathbf{V}|$ and $|\mathbf{V}_r|$ the vectors of bus voltage amplitudes and their reference values, respectively, and finally λ_p, λ_q and λ_v are the weight factors of each criteria. Other optimization functions have been proposed for CSVC, like the minimization of changes in reactive power output [60].

The solution of this optimization problem must comply with the security constraints such as minimal and maximal bus voltages, reactive power injection, and real

power flows.

2.3.3 Tertiary voltage control

Tertiary voltage control (TVC), also called "reactive power scheduling," refreshes the reference values of bus voltages $\mathbf{V}_r$ and their reactive power injections $\mathbf{Q}_{Gr}$ based on the scheduled operating conditions of the power system. Those operating conditions are typically characterized by a given load demand, active power generation pattern, and network topology.

Tertiary voltage control consists therefore of a steady-state optimization of the control settings, which is most often run every 15 to 30 minutes, or when events occur. The entire network is therefore considered.

For this optimization problem, the control variables are the vector $\mathbf{V}_{PV}$ of voltage amplitude at every generating unit or compensation device and the vector $\mathbf{T}$ of tap settings. Those two vectors are appended into $\mathbf{u}$, which will be referred to from now on as the vector of control variables.

The state variables are the voltage amplitude and angle at every bus. They are denoted by the state variable vector $\mathbf{x}$.

Most often, heuristic and empirical methods are used to assess the control vector $\mathbf{u}$ [46]. Indeed, C. Taylor describes in [47] the empirical method for maximizing the voltage profile that is employed by the Bonneville Power Administration. However, recent technical developments have led TSOs to use an off-line optimal power flow whose specifications are detailed in the following subsection.

2.3.3.1 Objective function

The objective function is based on one or several of the following criteria.

- A possible objective of TVC is to maximize short-term voltage stability margins, although short-term voltage stability, whose definition is provided in [21], is principally addressed by the secondary and automatic voltage control. Some

studies propose solutions for maximizing stability margins through TVC [61, 62]. Prior to this, some TSOs, like the Belgian one [63], have applied a maximization of reactive power reserves. This cost function can be expressed as the minimization of reactive power support, which is defined in [7] as follows.

$$C_Q(\mathbf{u}, \mathbf{x}) = \sum_i {Q_{Gi}}^2 \tag{19}$$

- Another possible objective is the minimization of operation costs. Most TSOs consider only active power losses whose costs are mainly supported by the TSOs in their objective function [64, 65]. In this case, the TSO minimizes

$$C_L(\mathbf{u}, \mathbf{x}) = \sum_i (P_{Gi} - P_{Di}) \tag{20}$$

  where P_{Di} is the active power demand at bus i. Some TSOs maximize the voltage profile across the network [66, 47]. As emphasized in Section 3.2, this strategy is similar to a minimization of active power losses.

- Other formulations, like the maximization of transmission capacity or long-term voltage stability margins, could also be used. However, as the set of possible formulations is extremely large, those have not been considered in this thesis.

2.3.3.2 Constraints

The optimization solution must satisfy load flow Equations (21) and (22). For each bus i, they are written as follows

$$P_{Gi} - P_{Di} - \sum_j (|V_i|\,|V_j|\,(\mathbf{G}(i,j)\cos(\delta_i - \delta_k) + \mathbf{B}(i,j)\sin(\delta_i - \delta_k))) = 0 \tag{21}$$

$$Q_{Gi} - Q_{Di} - \sum_j (|V_i|\,|V_j|\,(\mathbf{G}(i,j)\sin(\delta_i - \delta_k) - \mathbf{B}(i,j)\cos(\delta_i - \delta_k))) = 0 \tag{22}$$

where P_{Di} is the actual active power demand at bus i, δ_i the voltage angle, j can be any other bus in the power system and, $\mathbf{G}$ and $\mathbf{B}$ are the real and imaginary parts of the admittance matrix of the power system, respectively.

Additional inequality constraints (23) and (24) assure that bus voltages and reactive power injections are in their normal range, respectively. For any bus i, the optimization solution must thus satisfy.

$$V_{mini} \leq |V_i| \leq V_{maxi} \tag{23}$$

$$Q_{Gmini} \leq Q_{Gi} \leq Q_{Gmaxi} \tag{24}$$

Another inequality constraint assures that real power flows do not exceed the maximal admitted values. For any pair (i, j), this can be formulated as follows

$$|V_i|^2 |V_j|^2 ((\mathbf{G}(i,j))^2 + (\mathbf{B}(i,j))^2) \leq (\mathbf{S_{max}}(i,j))^2 \tag{25}$$

where $\mathbf{S_{max}}$ is the matrix of maximal real power flows in the system. The set of constraints defined by Equations (21)-(24) is generally referred to as "N constraints." These constraints may also have to be satisfied with any contingency or after an unexpected incident [67]. In this case, the OPF is said to verify "$N-1$ constraints."

2.3.4 A panorama of practices in voltage control

It is remarkable that every TSO has required generators and fast dynamic compensators to be equipped with AVR, even if the gain K may be different from one TSO to another. However, every TSO has developed its own strategy for SVC and TVC. Table 1 summarizes the centralized voltage control practices of the following TSOs: RTE [58, 9], REE [65], ENEL [44], ELIA [63], and RWE [64].

2.4 Need for a higher level of voltage control

The recent past has seen an evolution toward the continental interconnection of power systems. By way of example, 23 countries and 450 million people are connected to the UCTE network in Europe. This evolution is motivated by the fact that increasing the quantity of interconnections should enhance energy supply security, flexibility, and quality for the entire system [68]. Actually, the globalization process of the economy

Table 1: Practices in the field of hierarchical voltage control.

TSO	RTE	REE
Country	France	Spain
SVC mode	SVC or CSVC	SVC
SVC controls	**PV** and T	**PV** and $T_{<220kV}$
TVC mode	Manual	OPF + Expert System
TVC Controls	**PV** and T	**PV** and $T_{\geq 220kV}$
TVC Objective	maximize voltage profile	$C_L(\mathbf{u}, \mathbf{x})$
TVC Constraints	$N-1$	N, Expert System

TSO	ENEL	ELIA	RWE
Country	Italy	Belgium	Germany
SVC mode	SVC	SVC	SVC
SVC controls	**PV** and T	**PV** and $T_{<150kV}$	**PV** and $T_{<220kV}$
TVC mode	closed-loop OPF	OPF	OPF
TVC Controls	**PV** and T	**PV** and $T_{\geq 150kV}$	**PV** and $T_{\geq 220kV}$
TVC Objective	$C_L(\mathbf{u}, \mathbf{x})$	$C_Q(\mathbf{u}, \mathbf{x})$	$C_L(\mathbf{u}, \mathbf{x})$
TVC Constraints	N	N	N

allows former national utilities to go further with a merging trend that was initiated in the beginning of the last century [40]. This evolution has not only been profitable for electricity markets, but also for operating power systems more safely. For instance, A. Adamson *et al.* emphasize in [69] that large-scale power systems can be operated with higher security margins than independent regional ones because active power reserves are shared.

2.4.1 Coordination issues

However, interconnections may also have some drawbacks when the system is operated by non-coordinated regional utilities. J.W. Bialek states in [2] that poorly coordinated operation may even increase the risk of blackouts for multi-TSO power systems. His thesis is also supported by the fact that significant flaws in the German active and reactive power scheduling were responsible for a large-scale disturbance on

4 November 2006 in Western Europe [3]. The UCTE official report actually states that the disturbance was leveraged by the lack of coordination between the TSOs.

Moreover, interconnected independent TSOs may choose different optimization functions, as in the UCTE network for example, where France, Germany, and Belgium have different objectives (see Table 1). In [70], it is demonstrated that this case may be an issue, as the choice of a particular objective function by one TSO can significantly increase the costs of the interconnected utilities. Some interconnection lines may also face greater reactive power flows, limiting the transmission capacities and stressing the entire interconnected power system.

2.4.2 Toward a higher level of voltage control

As discussed in [5], the lack of coordination between strategies developed by independent TSOs has led to two major trends for the organization and control of interconnected power systems.

On one hand, one has seen the emergence of some Mega TSOs, resulting from the merging of several smaller ones (e.g., the regional transmission organization PJM has gradually expanded its operation in the United States over the last few years and now ensures the reliability of the electric power supply system in 13 states and the District of Columbia). On the other hand, where the regrouping of TSOs into large entities has not occurred, new strategies to coordinate the actions of the TSOs have been studied and implemented.

Considering that in TVC, the interactions between the TSOs is difficult in practice, the "UCTE Operation Handbook" [10] proposes basic rules as "good practices": while active power exchanges are separately assessed, TSOs are advocated to assume that there must be no reactive power flow at the interconnections when scheduling their reactive power dispatch. This rule, however, is difficult to apply, as observations show that reactive power flows are rarely negligible at interconnections.

The research presented in this thesis aims to design a suitable method for coordinating TVC in a multi-TSO context. This can be seen as a new layer of hierarchical voltage control, which can then be presented as in Figure 7.

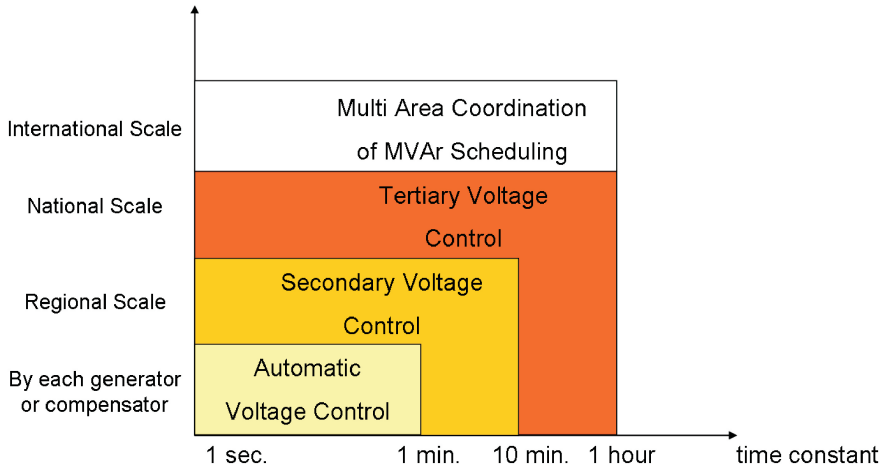

Figure 7: Time-space delineation of a four-layer hierarchical voltage control scheme.

CHAPTER III

FORMULATION OF THE PROBLEM

This chapter is dedicated to the formalization of the multi-TSO reactive power scheduling problem and description of the optimization methodology. It is organized as follows. First, a mathematical formulation of the single-TSO reactive power scheduling problem is proposed, its practical implementation is detailed, and the optimization tools are presented. Second, a mathematical formulation of the multi-TSO problem is proposed.

3.1 Formalization of the single-TSO problem

This section provides a mathematical formulation of the single-TSO reactive power scheduling problem, and details the optimization tools that have been used to run the simulations.

3.1.1 Single-TSO problem

As introduced in [43], the reactive power dispatch problem refers to the optimization of a steady-state system, where the load demand, active power generation pattern, and network topology are considered fixed.

In a real system, operating conditions are constantly varying with respect to time. As AVR and SVC are supposed to undertake fast variations, those variations are not considered in TVC. However, slow variations are represented by different operation conditions from one discrete instant to another. Hence, reactive power scheduling of a time-varying system can be modeled by the successive optimizations of different operating conditions.

It is supposed hereafter that the reactive power dispatch is periodically scheduled,

based on the steady-state operating conditions scheduled for the next iteration. More specifically, it consists of the computation, at the instant $k-1$, of the optimal control settings that will be applied at the next instant k. It is assumed that every TSO perfectly predicts the operating conditions at the instant $k-1$, under which its control area will be operated at the instant k.

In a single-TSO system, the optimal power flow problem (OPF) faced by the TSO at the instant $k-1$ is usually written as follows [71, 72]

$$\min_{\mathbf{u},\mathbf{x}} C^k(\mathbf{u},\mathbf{x}) \tag{26}$$

under the equality and inequality constraints

$$\mathbf{f^k}(\mathbf{u},\mathbf{x}) = \mathbf{0} \tag{27}$$

$$\mathbf{g^k}(\mathbf{u},\mathbf{x}) \leq \mathbf{0} \tag{28}$$

where $\mathbf{u}$ and $\mathbf{x}$ are vectors of control variables and state variables, respectively, $C^k(\mathbf{u},\mathbf{x})$ is the objective function and $\mathbf{f^k}(\mathbf{u},\mathbf{x})$ and $\mathbf{g^k}(\mathbf{u},\mathbf{x})$ represent the constraint functions. The superscript ^{k} denotes the fact that the associated function depends on the scheduled operating conditions at the instant k. To ease the reading of this thesis, the superscript ^{k} will be omitted when dealing with only one particular operating condition (with $k=0$, for example).

In the context of reactive power scheduling, the practical meaning of the different terms used to formalize the optimization problem is detailed in Section 2.3.3.

3.1.2 Practical formulation

To simplify the practical implementation of the multi-TSO optimization problem, several assumptions were made. They are related to the formulation of the objective functions, control variables, and constraints. They are summarized in this section.

3.1.2.1 Objective functions

While there exists an infinite number of possible formulations for the objective function, only the formulations relying on a weighted sum of active power losses $C_L^k(\mathbf{u})$ and reactive power support $C_Q^k(\mathbf{u})$ are considered in this thesis. Actually, as emphasized in [73], those criteria are the most common for reactive power scheduling.

Therefore, a general formulation for the cost function is adopted

$$C^k(\mathbf{u}) = \gamma \times C_L^k(\mathbf{u}) + (1-\gamma) \times C_Q^k(\mathbf{u}) \tag{29}$$

where $\gamma \in [0,1]$ is supposed as being constant with respect to time.

As the general formulation includes objectives of different natures, $C^k(\mathbf{u})$ will be expressed with no physical unit.

3.1.2.2 Control variables

To model a real system, some of the control actions should be discrete variables, as in [74], for example. However, as the use of discrete and continuous variables would result in a mixed-integer, non-linear programming problem, whose solution is difficult to compute, only continuous control variables have been considered in the simulations.

Moreover, for the sake of simplicity, phase-shifter settings are considered constant here. Therefore, in this thesis, $\mathbf{u}$ refers only to the voltage settings for generators and compensation devices, and tap settings.

3.1.2.3 Constraints

As emphasized in [75], in the context of multi-area systems, a new constraint must be introduced in the equality constraints (27) to set active power export between the areas at its scheduled level.

3.2 Optimization methodology

As most traditional power system optimization programs are not able to handle the specific constraints and objectives of this problem, a new optimization program had to be developed. AMPL [76] appeared to be an appropriate software since RTE, the French TSO, uses it for benchmarking in power system analysis. Also, R. Vanderbei has developed several models for power system optimization [77].

The optimization methodology is based on three files, namely the main file, data file, and model file. The main file (typically, "problem.run") details the names of the data file ("problem.dat") and model file ("problem.mod"). It also describes the objective function, and designs the optimization output file ("problem.out"). The main file can be easily called from the Matlab workspace by using the command "!ampl problem.run." A practical example of those AMPL files is provided in Appendix A.

3.3 Validation of the methodology

This section presents some results obtained when applying the single-TSO scheme to the IEEE 118 bus system. The performance of the solver, and algorithm are also analyzed. Results of the single-TSO optimization process that corresponds to the AMPL file "problem.run" are presented hereafter in the case of the single-TSO IEEE 118 bus system, whose numerical data are provided in [78]. It is considered that those data correspond to the prediction of the operating conditions at the instant $k = 0$ for the instant $k = 1$.

Figures 8 and 9 represent the voltage in the IEEE 118 bus system, where active power losses and reactive power support have been minimized, respectively. Results show that a minimization of active power losses tends to maximize the voltage profile, whose mean value is equal to 1.0432 per unit (p.u.), while a minimization of reactive power support induces more contrast for the voltage, whose mean value is 1.0139 p.u.

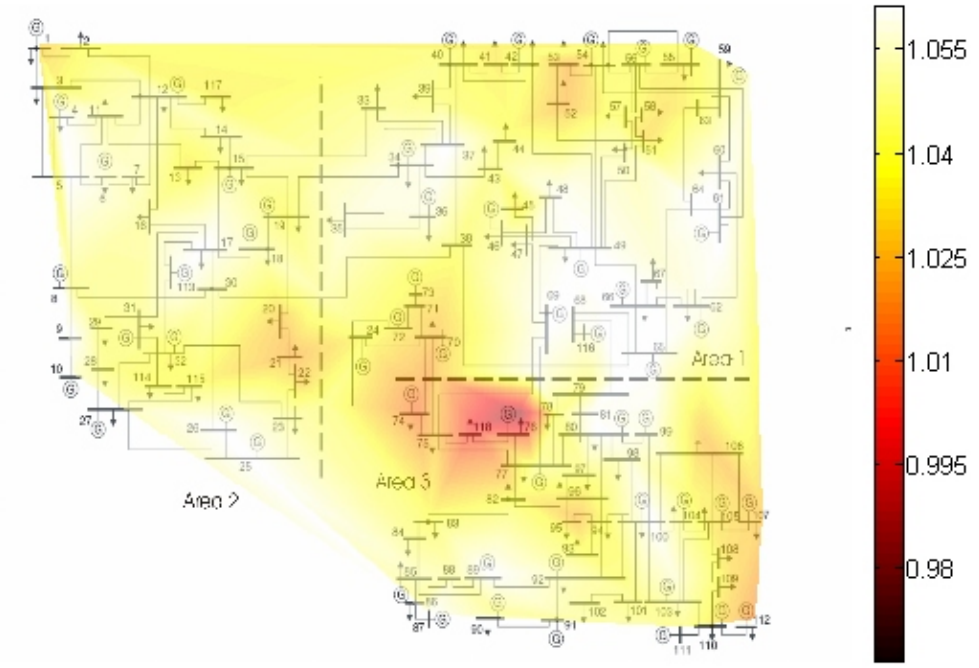

Figure 8: Voltage (in p.u.) in the IEEE 118 bus system with the minimization of active power losses. The optimization is run with the solver MINOS in AMPL.

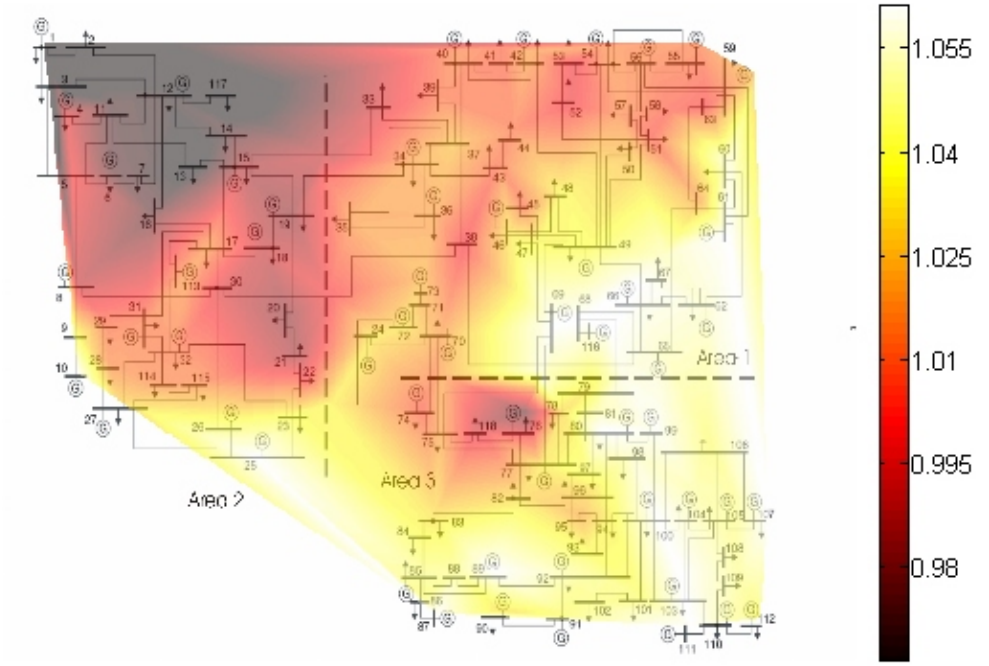

Figure 9: Voltage (in p.u.) in the IEEE 118 bus system with the minimization of reactive power support. The optimization is run with the solver MINOS in AMPL.

3.3.1 Validation of the solver

Different solvers are offered in the AMPL student edition package. For the non-linear optimization problem under consideration, solvers using interior-point methods seem to be most relevant according to [79]. The following solvers could thus be possibly chosen.

- MINOS is a solver for sparse linear programming and non-linear programming problems. Linear models are solved using an efficient reduced gradient technique, while non-linear models are solved using a method that iteratively solves subproblems with linearized constraints and an augmented Lagrangian objective function. It was developed by B.A. Murtagh and M.A. Saunders [80]. MINOS is described in [81] as the fastest solver for small-scale OPF problems.

- LOQO was developed by R. Vanderbei in 1997, especially for solving linear and quadratic problems [82].

- SPI is a solver that was developed by RTE for large-scale power system optimization applications.

MINOS and LOQO are compared in the case of the single-TSO optimization problem for the IEEE 118 bus system. The optimizations are run on a PC with Intel Core 2 T7200 2.0 GHz P2 processor and 2 GB memory. Computation times and optimal costs $C(\mathbf{u}, \mathbf{x})$ are represented in Table 2.

As MINOS proves a higher speed and better results than LOQO, the optimizations of small-scale systems (such as the IEEE 118 bus system and the IEEE 39 bus system) have been run using this solver.

Table 2: A comparison of different algorithms for the single-TSO optimization of the IEEE 118 bus system. Computation time for solver SPI is non-significant since this solver runs on a different machine than MINOS and LOQO.

Solver	MINOS	LOQO
γ	1	1
computation time (seconds)	1.23	45.50
$C(\mathbf{u}, \mathbf{x})$	115.5696	115.5696
γ	0	0
computation time (seconds)	1.125	27.78
$C(\mathbf{u}, \mathbf{x})$	108.82	123.30

3.3.2 Validation of the algorithm

To check that the optimization algorithm is errorless, the output of the optimization has been applied to a commercial power flow software, namely Matpower [78]. Afterward, the outcome of the power flow has been compared with the optimization output.

For all cases met, no error has been reported, i.e. the optimization output were indeed respecting Constraints (27) and (28).

When applying the scheme to a large-scale UCTE-like system, the formulation of the constraints was checked and the results were compared with measurements on the real system. No error has been reported in this case.

3.4 Multi-TSO problem

This section details the reactive power scheduling problem formulation in the context of a system with $NbTSO$ TSOs, referred to as TSO_1, TSO_2,... , TSO_{NbTSO}.

3.4.1 Mathematical formulation

The problem to be addressed is the coordination of voltage settings optimization in a system, where every TSO_i is unaware of the operating conditions in the other

control areas. In practice, every TSO_i can formulate its own objective function $\hat{C_i^k}(\mathbf{u}_{TSO_i}, \mathbf{x}_{TSO_i})$, and constraint functions $\hat{\mathbf{f}_\mathbf{i}^\mathbf{k}}(\mathbf{u_{TSO_i}}, \mathbf{x_{TSO_i}})$ and $\hat{\mathbf{g}_\mathbf{i}^\mathbf{k}}(\mathbf{u_{TSO_i}}, \mathbf{x_{TSO_i}})$ as functions of its internal control and state variables $\mathbf{u}_{TSO_i}$ and $\mathbf{x}_{TSO_i}$ only[1].

As introduced in Section 2.3.3, the type of operational objective is likely to differ from one TSO to another, since they may be influenced by local topology, system architecture, generation capacity, or reliance on traditional engineering practices [1]. As for the single-TSO problem, the individual cost functions are characterized by γ_i, which weights active power losses with respect to reactive power support in the area controlled by TSO_i. The objective of TSO_i will thus be formulated as follows

$$\hat{C_i^k}(\mathbf{u}_{TSO_i}, \mathbf{x}_{TSO_i}) = \gamma_i \times \hat{C_{Li}}^k(\mathbf{u}_{TSO_i}, \mathbf{x}_{TSO_i}) + (1 - \gamma_i) \times \hat{C_{Qi}}^k(\mathbf{u}_{TSO_i}, \mathbf{x}_{TSO_i}) \quad (30)$$

where $\gamma_i \in [0, 1]$ is constant with respect to time.

With knowledge of the scheduled operating conditions in the entire system, one could formulate the individual objectives and constraint functions as functions of the control variable $\mathbf{u}$, which appends the individual vectors of control variables $\mathbf{u}_{TSO_1}$, $\mathbf{u}_{TSO_2}$,..., $\mathbf{u}_{TSO_{NbTSO}}$, and state variable $\mathbf{x}$, which appends the individual vectors of state variables $\mathbf{x}_{TSO_1}$, $\mathbf{x}_{TSO_2}$,..., $\mathbf{x}_{TSO_{NbTSO}}$. Those functions will be referred to as $C_i^k(\mathbf{u}, \mathbf{x})$, $\mathbf{g_i^k}(\mathbf{u}, \mathbf{x})$, and $\mathbf{h_i^k}(\mathbf{u}, \mathbf{x})$, $\forall i \in [1, 2, \ldots, NbTSO]$. Also, by appending the $NbTSO$ respective constraint functions, one can define constraints for the entire system $\mathbf{f^k}(\mathbf{u}, \mathbf{x})$, and $\mathbf{g^k}(\mathbf{u}, \mathbf{x})$. One can note that the objective and constraint functions only depend on the control variables $\mathbf{u}$ for the entire system. The state variable $\mathbf{x}$ will therefore be removed from the formulation of the functions $C_i^k(\mathbf{u})$ $\forall i \in [1, 2, \ldots, NbTSO]$, $\mathbf{f^k}(\mathbf{u})$, and $\mathbf{g^k}(\mathbf{u})$. The multi-TSO reactive power scheduling problem faced at the instant $k - 1$ can then be written as follows

[1]The symbol $\hat{}$ on $C_i{}^k$, $\mathbf{f_i^k}$, and $\mathbf{g_i^k}$ specifies that, since a TSO_i does not systematically know the system topology, generation pattern, and load demand in the other areas, it can only formulate its own objective and constraints as functions of its own system state, defined by $\mathbf{u}_{TSO_i}$ and $\mathbf{x}_{TSO_i}$.

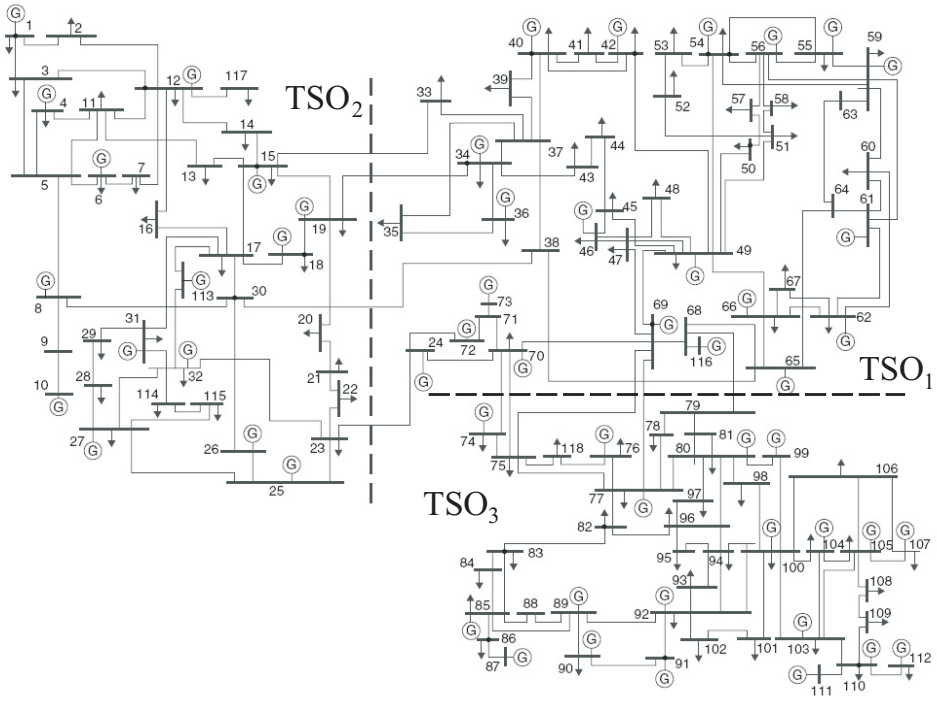

Figure 10: IEEE 118 bus system partitioned into three areas.

$$\min_{\mathbf{u}}[C_1^k(\mathbf{u}), C_2^k(\mathbf{u}), \ldots, C_{NbTSO}^k(\mathbf{u})] \tag{31}$$

subject to

$$\mathbf{f^k}(\mathbf{u}) = \mathbf{0} \tag{32}$$

$$\mathbf{g^k}(\mathbf{u}) \leq \mathbf{0} \tag{33}$$

where $\mathbf{f^k}(\mathbf{u}) = \mathbf{0}$ represents the equality constraints, and $\mathbf{g^k}(\mathbf{u}) \leq \mathbf{0}$ represents the inequality constraints. From now on, the set of solutions $\mathbf{u}$, such that $\mathbf{u}$ verifies Equality (32) and Inequality (33) will be referred to as $U[k]$.

3.5 Benchmark system

The benchmark power system used herewith is the IEEE 118 bus system partitioned into three areas referred to as TSO_1, TSO_2, and TSO_3. This system is shown in Figure 10 and its data is provided in Appendix B.

To illustrate the description of the centralized and decentralized algorithms, it will be assumed that TSO_1 minimizes reactive power in its control area ($\gamma_1 = 0$), TSO_2 focuses on a weighted sum of active power losses and reactive power support ($\gamma_2 = 0.9$), and TSO_3 focuses on active power losses only ($\gamma_3 = 1$).

The slow changes in load demand are modeled by a discrete-time variation of the load demand, and it is assumed that the "real" time interval between two successive discrete instants $k-1$ and k is 30 minutes. At each instant k, the active power demand $P_{D_j}(k)$ and the corresponding reactive power demand $Q_{D_j}(k)$ are obtained by multiplying their respective initial values by a load factor $r(k)$. They can thus be expressed as follows

$$P_{D_j}(k) = P_{D_j}(0) \times r(k) \tag{34}$$

$$Q_{D_j}(k) = Q_{D_j}(0) \times r(k) \tag{35}$$

where $P_{D_j}(0)$ and $Q_{D_j}(0)$ represent the active and reactive power demand as defined in [78], respectively.

First, to model a time-invariant system, the load factor is chosen as constant, $r(k) = 1 \ \forall k \geq 0$. Second, for a convenient and realistic modeling of the load demand variations in the IEEE 118 bus system, the load factor $r(k)$ is associated with real observations on the French power system during the period January 1st-31st, 2008. More precisely, the French power demand is averaged over this period and the load factor $r(k)$ is computed as the ratio between the demand at the instant k and this average. As emphasized in Section 3.1.1, it is assumed that no prediction error occurs, and $r(k)$ is to be accurately predicted at instant $k-1$ using short-term load forecasting methods. It is also assumed that the active power injections homothetically grow with the load factor. Moreover, a decentralized slack bus is used in our simulations, which may slightly change the generation pattern depending on active power losses.

CHAPTER IV

MULTI-OBJECTIVE OPTIMIZATION

As emphasized in Chapter 3, the reactive power scheduling problem can be formalized as a particular type of multi-objective optimization. This chapter is dedicated to the theory of multi-objective optimization, and investigate qualitative criteria to evaluate potential coordination schemes. It is organized as follows. First, the theoretical background on multi-objective optimization is presented, and a basic two-party problem is introduced. Second, a classification of multi-objective optimization methods is outlined. Finally, the evaluation criteria are described.

4.1 Theoretical background

Let us assume that a single decision maker must design a control action $\mathbf{u}$ with knowledge of the entire system so as to minimize a set of N objectives $C_i(\mathbf{u})$ $\forall i \in [1, \ldots, N]$. This problem can be formalized as follows

$$\min_{\mathbf{u} \in U} [C_1(\mathbf{u}), C_2(\mathbf{u}), \ldots, C_N(\mathbf{u})] \tag{36}$$

where U is the set of control actions that are consistent with the system constraints.

Every control action $\mathbf{u} \in U$ can be represented in a N-dimensional cost space by a vector $[C_1(\mathbf{u}), C_2(\mathbf{u}), \ldots, C_N(\mathbf{u})]$. Hence, the representation function v, $U \mapsto V$, where V is the N-dimensional space of the cost vectors $[C_1(\mathbf{u}), \ldots, C_N(\mathbf{u})]$ $\forall \mathbf{u} \in U$, is defined as follows

$$\mathbf{v}(\mathbf{u}) = [C_1(\mathbf{u}), C_2(\mathbf{u}), \ldots, C_N(\mathbf{u})] \tag{37}$$

By definition, a control action $\mathbf{u}_n \in U$ is non-dominated, if there exists no other action $\mathbf{u} \in U$ such that, $\forall i \in [1, 2, \ldots, N]$, $C_i(\mathbf{u}) \leq C_i(\mathbf{u}_n)$ and $C_i(\mathbf{u}) < C_i(\mathbf{u}_n)$

for at least one $i \in [1, 2, \ldots, N]$. In the N-dimensional cost space, the set of non-dominated control actions represents the Pareto-front of the multi-objective problem.

4.2 Illustrative example

To illustrate multi-objective optimization methods, a two-party optimization problem is introduced in this section. The two objective functions are defined as follows

$$C_{mo1}(x, y) = 2 \times x + y \tag{38}$$

$$C_{mo2}(x, y) = x + 2 \times y \tag{39}$$

with $(x, y) \in [0, 2]^2$ such that $(x - 1)^2 + (y - 1)^2 \leq 1$. It is supposed that party 1 has $C_{mo1}(x, y)$ for objective and controls x. Reciprocally, party 2 has $C_{mo2}(x, y)$ for objective and controls y.

The illustrative problem is characterized by a continuous set of control variables U and a convex set of solution representations V, i.e., every element m on a segment between two elements $m_1 \in V$ and $m_2 \in V$ is also in V.

4.3 Multi-objective optimization methods

As emphasized in [83], there exist three main trends to solve multi-objective optimization problems, namely *a posteriori*, *interactive*, and *a priori* approaches. Those categories are described hereafter, and the associated techniques are presented.

4.3.1 A posteriori methods

A posteriori methods are to provide a set of non-dominated solutions, or a graphical representation of the Pareto-front, so that the independent decision maker can choose one of these solutions. As a variety of *a posteriori* methods have been developed, the most popular of them are described hereafter.

4.3.1.1 Scalar method

Continuous optimization methods have been developed to identify non-dominated solutions of multi-objective problems. Many of these techniques (e.g., [84, 85]) consist of weighting the individual objectives to optimize a single scalar objective

$$C_{scalar}(\mathbf{u}) = \sum_{i=1}^{N} \alpha_i \times C_i(\mathbf{u}) \tag{40}$$

where $\mathbf{u} \in U$, and $(\alpha_1, \ldots, \alpha_N) \in \mathbb{R}^N$ such that $\alpha_i \geq 0, \forall i \in [1, \ldots, N]$ and $\sum_{i=1}^{N} \alpha_i = 1$.

As emphasized in [86], for a particular distribution of weight factors $(\alpha_1, \ldots, \alpha_N)$, solving the multi-objective optimization problem is equivalent to minimizing $C \in \mathbb{R}$ such that there exists a solution $\mathbf{u} \in U$ such that $\mathbf{v}(\mathbf{u})$ belongs to the hyperplane defined by

$$\sum_{i=1}^{N} \alpha_i \times C_i + C = 0 \tag{41}$$

In the context of the two-objective example introduced in Section 4.1, the scalar objective can be written

$$C_{scalar_{mo}}(x, y) = \alpha_{mo} C_{mo1}(x, y) + (1 - \alpha_{mo}) C_{mo2}(x, y) \tag{42}$$

with $\alpha_{mo} \in [0, 1]$. In the N-dimensional cost space, the hyperplane equation corresponds to a line such that

$$C_{mo2} = -\frac{\alpha_{mo}}{(1 - \alpha_{mo})} C_{mo1} - C \tag{43}$$

Figure 11 represents both the set of solutions $(x, y) \in [0, 2]^2$ such that $(x-1)^2 + (y-1)^2 \leq 1$ and a hyperplane $L_{0.5}$ that corresponds to $\alpha_{mo} = 0.5$ in Equation (43).

This technique has two main flaws. First, its outcome may be composed of solutions that are unevenly distributed, which might induce missing a potential compromise between the objectives. Second, as shown in Figure 12, the scalar technique may fail to identify some Pareto solutions in a non-convex vector space V.

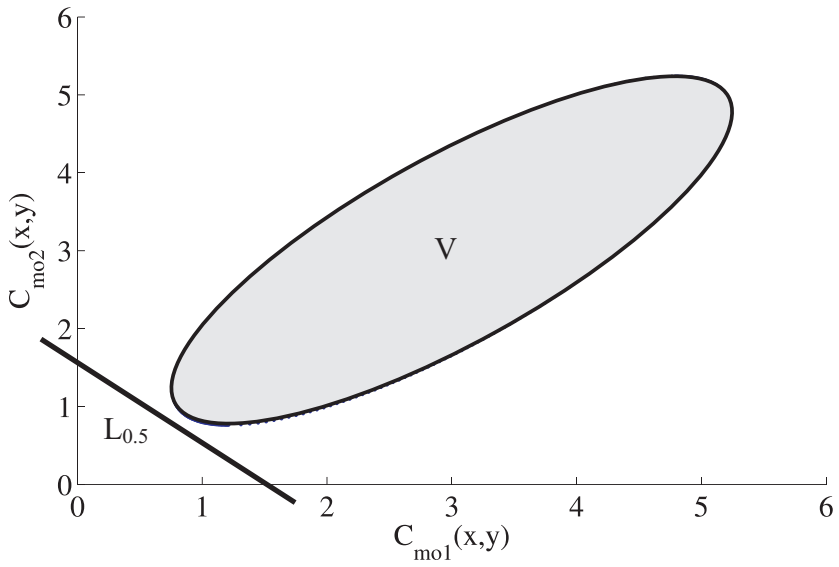

Figure 11: Representation of the set of solution vectors V and hyperplane $L_{0.5}$ in the two-dimensional cost space for the basic two-objective problem.

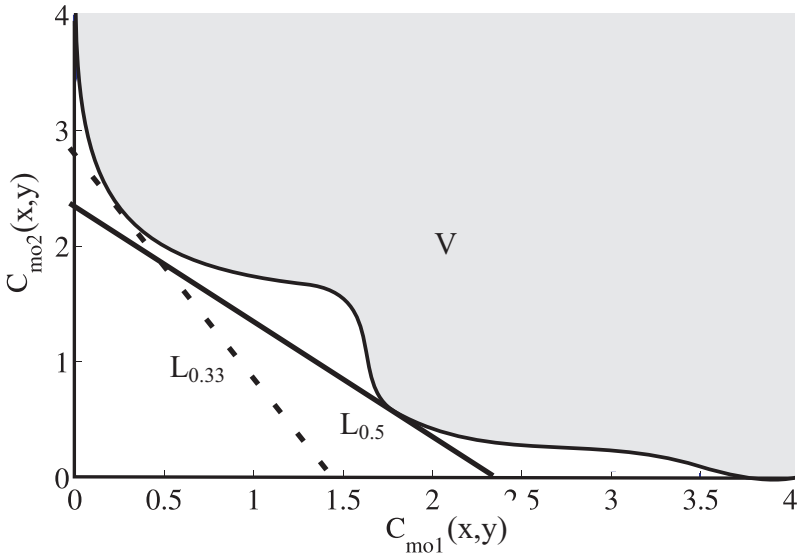

Figure 12: Representation of a Pareto-front and hyperplanes $L_{0.5}$ and $L_{0.33}$ in the two-dimensional for a non-convex set of solutions.

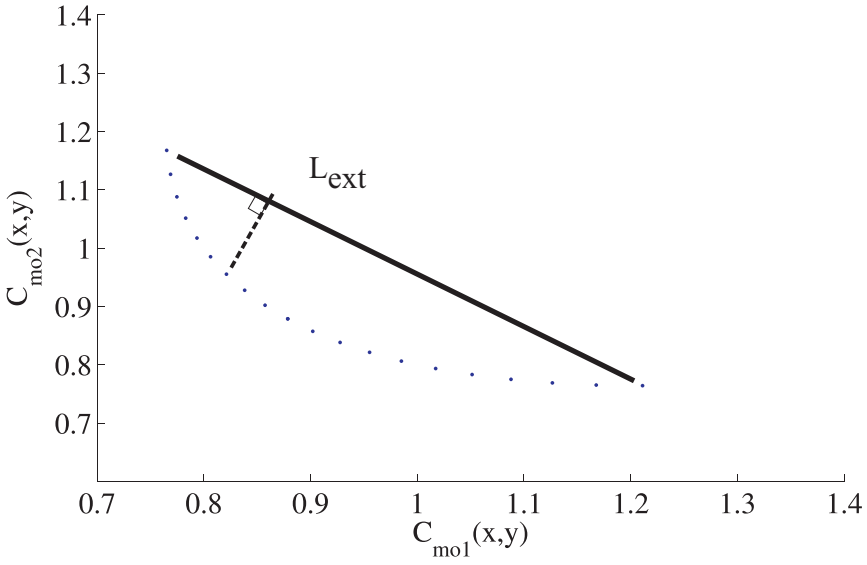

Figure 13: Solutions obtained with the normal boundary intersection approach applied to the basic two-objective problem.

4.3.1.2 Normal boundary intersection method

To address those issues, the so-called normal boundary intersection approach, which is presented in [87], is used to obtain evenly-distributed non-dominated solutions. This method is applied to a two-objective OPF problem in [88]. It is based on the identification of the extreme points of the Pareto-front, i.e. the solutions of the N single objective optimization problems $\min_{\mathbf{u}} C_i(\mathbf{u})\ \forall i \in [1,\ldots,N]$. To identify N_p particular solutions, $N_p - N$ evenly-distributed points are defined in the hyperplane L_{ext} that contains the N extreme points. For every point $p \in L_{ext}$, a single objective (typically the algebraic sum of the N objective functions) is minimized subject to the extended constraint $\mathbf{u} \in U$ such that the vector $[C_1(\mathbf{u}), C_2(\mathbf{u}), \ldots, C_N(\mathbf{u})] - \mathbf{p}$ is orthogonal to the hyperplane L_{ext}.

For example, Figure 13 depicts the application of the normal boundary intersection approach to the illustrative two-objective problem that is presented in Section 4.2.

As emphasized in [87], an additional step must be included in the normal boundary

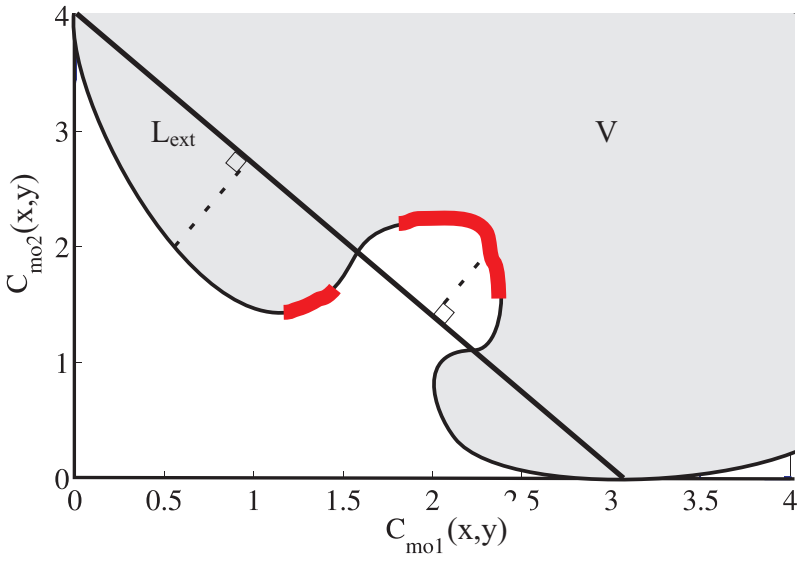

Figure 14: Set of solution vectors V for a non-convex problem. The area, where the normal boundary intersection approach could elect dominated solutions is depicted as a thick red line.

intersection approach to avoid designing dominated solutions. This could happen in the case of non-convex sets V, whose boundary contains dominated solutions, as represented in Figure 14. In this case, the optimization scheme must include a final test to state whether the intersections are dominated.

4.3.1.3 Metaheuristic approaches

A number of research papers investigate metaheuristic algorithms to design the set of non-dominated solutions of multi-objective problems. For example, a simulated annealing approach is proposed in [89] and a tabu search technique is presented in [90]. Multi-objective optimization methods based on genetic algorithms have also been developed to take advantage of the heuristic process to identify non-dominated solutions. In [91], a sorting technique is developed to obtain evenly-distributed Pareto-optimal solutions. This approach is applied to multi-objective reactive power planning in [92].

4.3.2 Interactive methods

Interactive methods involve interactions between an optimization process and a decision maker [93]. In practice, the decision maker alternatively receives potential solutions and gives directions for further improvement, until the most preferred solution is identified. Because of the interactions, this optimization approach is usually avoided for short term optimization [94].

A comprehensive review of *interactive* methods is provided in [93]. This book provides a classification of those methods, among which the trade-off based, reference point, and classification-based methods. Because of the subjectivity of the decision maker, it is usually agreed that no interactive method is better than the others.

4.3.3 A priori methods

A priori solution methods have been designed to elect a single solution based on prespecified preferences. While *a posteriori* methods could be used with an arbitrary weight [95] or priority [96] assignment for the objectives, specific methods have also been proposed. Those are detailed hereafter.

4.3.3.1 ϵ-constraint method

The ϵ-constraint was introduced in [97]. It is based on the formulation of objectives as constraints, so as to reduce the multi-objective optimization to a single-objective problem.

In particular, in the case of Problem (36), the ϵ-constraint would lead to the following optimization

$$\min_{\mathbf{u}\in U} C_k(\mathbf{u}) \tag{44}$$

subject to

$$C_i(\mathbf{u}) \leq \epsilon_i, \forall i \in [1, \ldots, N], i \neq k \tag{45}$$

with ϵ_i $\forall i \in [1, \ldots, N]$, $i \neq k$, a priori defined.

This method is subjective in essence, as it involves a prioritization of the objective and the choice of specific constraints $\epsilon_i, \forall i \in [1, \ldots, N]$ such that $i \neq k$, which must be relaxed enough to guarantee the existence of a solution.

In the illustrative example, the optimal solution with $\epsilon_2 = 1$ is $x^* = 0.2$ and $y^* = 0.4$, which yields $C_{mo1}(x^*, y^*) = 0.8$ and $C_{mo2}(x^*, y^*) = 1$.

4.3.3.2 Goal attainment methods

The goal attainment method was proposed in [98]. The approach is based on the minimization of the distance between a solution and a reference point V^0, along a pre-specified direction $\mathbf{w} = [w_1, \ldots, w_N]$. In this case, the decision maker is to solve the following single-objective problem.

$$\min_{\mathbf{u} \in U} \lambda \tag{46}$$

subject to

$$C_i(\mathbf{u}) - \lambda \times w_i = V_i^0, \forall i \in [1, \ldots, N] \tag{47}$$

In the illustrative example, the optimal solution with $V^0 = [0, 0]$ and $w = [1.2, 1]$ is $x^* = 0.379$ and $y^* = 0.216$, which yields $C_{mo1}(x^2, y^*) = 0.974$ and $C_{mo2}(x^2, y^*) = 0.811$.

4.3.3.3 Compromise methods

The compromise methods consist of minimizing the distance to a reference point in the cost space. This approach is described in [99]. It is remarkable that the outcome of those approaches obviously depends on the reference point and metrics chosen. A comprehensive review of those criteria is presented in [100], and [83] comments on the influence of the distance metrics.

In the case of multi-party optimization, the reference point and metrics are likely to be the outcome of a preliminary negotiation between the parties. The application

of the optimization method is then straightforward, and does not require additional input from the decision maker.

In the illustrative example, minimizing the Euclidean distance to $V^0 = [0, 0]$ leads to $x^* = 0.293$ and $y^* = 0.293$, which yields $C_{mo1}(x^2, y^*) = 0.879$ and $C_{mo2}(x^2, y^*) = 0.879$.

4.4 Evaluation criteria

As introduced in Section 2.4, making the best use of the resources offered by an interconnected system requires a coordination scheme to pick a control action $\mathbf{u} \in U$, which can be compared to the solutions of the multi-objective optimization problem (31).

As emphasized in Section 4.3, a number of multi-objective optimization methods could be used to achieve a non-dominated solution. In addition, decentralized coordination schemes that do not involve transferring some control prerogatives to a single decision maker could be advocated, although they might lead to dominated control actions. As it was shown with the illustrative example, every coordination scheme leads to a different control action, which can be more a less favorable to one party or the others. Hence, this section proposes some qualitative criteria to evaluate the outcome of coordination methods.

4.4.1 Pareto-optimality

It is commonly adopted in the multi-objective optimization literature that the solution of a multi-objective problem should be on, or as close as possible to its Pareto-front [101]. Thus, one can evaluate a particular coordination with respect to its ability to constantly lead to a solution that is close to the Pareto-front. As the notion of distance is subjective in essence, different Pareto-optimality measures may be proposed.

In practice, the Pareto-optimality indexes usually rely on the computation of a large number of evenly-distributed non-dominated solutions. The Pareto-optimality of a control action $\mathbf{u} \in U$ can then be computed as the minimum Euclidean distance

between $\mathbf{v}(\mathbf{u})$ and every point of the Pareto-front.

4.4.2 Fairness criteria

As introduced in [11], Pareto-optimality is not sufficient to lead to consensus among different parties. Indeed, a resource allocation scheme must also have some properties of fairness to be of potential interest for all parties. The notion of fairness is doubtlessly subjective [102] and relies on multiple criteria. Hence, different arbitrages can be simultaneously qualified as fair for any given situation. As discussed in [12], freedom from envy is an important property of fairness. In addition, the classification proposed by J. Konow in [13] provides some criteria for assessing the fairness of a particular allocation, namely "efficiency," "accountability," and "altruism." Those latter criteria have been defined by analyzing experimental data obtained by polling people on their opinions concerning fairness of different types of allocations. The above mentioned fairness criteria are detailed in this section.

4.4.2.1 Freedom from envy

As introduced in [12], freedom from envy is a necessary condition of fairness for an allocation scheme. Indeed, an envy-free procedure makes no *a priori* difference between the different parties, such that no party would prefer to be in the place of another. In practice, all individual objectives must be treated through the same procedure that does not rely on any specific preference among the TSOs.

4.4.2.2 Efficiency

According to J. Konow, an arbitrage can not be qualified as fair if it is poorly efficient, i.e. if considerable resources are not allocated. While the level of efficiency of a given arbitrage for a multi-objective problem is not explicitly defined in [13], efficiency is assumed maximal if there exists no control action in U that leads to a better outcome for all parties. As suggested in Section 4.4.1, in the case of individual objectives

expressed by real-valued functions, the efficiency of an arbitrage may be related to a specific distance in a well-defined cost-space between a solution vector and the Pareto-front of the problem.

4.4.2.3 Accountability

In the context of multi-party resource allocation, a scheme is accountable if the party investing more effort earns its superior position. An example of an accountable arbitrage is given in [13]: consider two individuals with the same abilities and a global earning that should be divided between them. If one chooses to work less, an accountable notion of fairness would allocate less earnings to him than the other individual.

4.4.2.4 Altruism

The notion of "altruism" is defined by J. Konow in [13]. He states that what parties can not influence should not affect the allocation, and proposes the following example of altruism: if two individuals having different abilities each work at 100% of their capabilities, an altruist notion of fairness would allocate them the same share of the global earnings. This notion is also developed by M. Rabin, who associates fairness with "reciprocity," in [103].

Hence, altruism reflects two properties. On the one hand, a parameter that does not depend on the TSOs' actions should not affect the allocation. On the other hand, the allocations should not be biased toward the TSOs with the greatest "abilities."

CHAPTER V

CENTRALIZED APPROACH

Designing a higher-level entity to solve the multi-TSO reactive power scheduling problem in a centralized manner is emphasized in [6] as an intriguing alternative. This approach relies on the creation of a centralized control center (CCC), which would be in charge of scheduling the reactive power dispatch in the multi-TSO system.

In fact, even with the creation of a CCC, it is expected that every TSO will preserve some prerogatives of its own system operation. More specifically, as introduced in Chapter 3, operational objectives are likely to remain defined by the TSOs. In this context, prior to agreeing to transferring some of their competencies to a higher decision level, the TSOs may require some guarantees regarding the fulfillment of their own objectives by the CCC. There may be a conflicting issue, as satisfying the objective of a single TSO may adversely affect other TSOs.

Negotiations are usually advocated to reach a fair solution for multi-party resource allocation problems [104]. In the case of multi-TSO reactive power scheduling, as the optimization scheme should handle short-term operation, negotiating can not be considered a suitable solution. However, the choice of a multi-TSO optimization procedure that would satisfy every party may be subjected to negotiations between the different TSOs.

As introduced in Section 4.1, *a posteriori* and *interactive* methods involve an arbitrary choice at each iteration. As this could be questioned by the different parties, those strategies are inappropriate for multi-TSO operation. *A priori* methods that depend on an arbitrary prioritization between the different objectives may also not be acceptable for every party. Therefore, a new compromise method is proposed in this

chapter, which could be used by the CCC to solve the multi-party optimization problems, where the objective of every TSO can be represented by a real-valued function. The scheme relies on the formulation of the problem as a multi-objective optimization problem and picks a solution that could, at least in principle, bring consensus among the different TSOs. Indeed, besides the fact that the solution minimizes a specific distance from the utopian minimum in a normalized multi-dimensional space, it is shown that the scheme has some properties of fairness. In addition, it is also shown that the scheme is robust with respect to certain biased behavior by the different parties.

This chapter is organized as follows. In Section 5.1, a normalization of the multi-objective problem and a procedure for identifying the best solution in the normalized space are proposed. Section 5.2 shows that the scheme has some properties of fairness in an economic sense, while Section 5.3 analyzes certain biased behaviors, which can be adopted by the TSOs to turn the optimization scheme in their favor. Finally, Section 5.4 emphasizes the technical issues that need to be addressed prior to applying the scheme to real systems.

5.1 Proposed method

In this section, an approach for electing the point on the Pareto-front that could satisfy the different parties is proposed. The optimization procedure was designed as follows. First, it is supposed that every TSO_i provides the CCC with its objective and constraint functions $\hat{C}_i(\mathbf{u}_{TSO_i}, \mathbf{x}_{TSO_i})$, $\hat{\mathbf{f}}_\mathbf{i}(\mathbf{u_{TSO_i}}, \mathbf{x_{TSO_i}})$, and $\hat{\mathbf{g}}_\mathbf{i}(\mathbf{u_{TSO_i}}, \mathbf{x_{TSO_i}})$. After receiving the information from every TSO_i on its objective and constraint functions $\hat{C}_i(\mathbf{u}_{TSO_i}, \mathbf{x}_{TSO_i})$, $\hat{\mathbf{f}}_\mathbf{i}(\mathbf{u_{TSO_i}}, \mathbf{x_{TSO_i}})$, and $\hat{\mathbf{g}}_\mathbf{i}(\mathbf{u_{TSO_i}}, \mathbf{x_{TSO_i}})$, the CCC defines the multi-objective problem ($C_i(\mathbf{u})$, $\forall i \in [1, 2, \ldots, NbTSO]$, $\mathbf{f}(\mathbf{u})$, and $\mathbf{g}(\mathbf{u})$), and, afterward, faces the problem of electing the fairest solution on its Pareto-front.

The proposed approach relies on finding a solution as close as possible to the

"utopian minimum" C^{ut} defined in [87] as

$$C^{ut} = [C_1(\mathbf{u}_1^*), C_2(\mathbf{u}_2^*), \ldots, C_{NbTSO}(\mathbf{u}_{NbTSO}^*)] \tag{48}$$

where $\mathbf{u}_i^*$ is the solution of Problem (49), which optimizes the entire system with the unique objective $C_i(\mathbf{u})$ under constraints (32)-(33), that is

$$\mathbf{u}_i^* = \arg\min_{\mathbf{u}\in U} C_i(\mathbf{u}) \tag{49}$$

It is supposed hereafter that Problem (49) admits a unique solution $\mathbf{u}_i^*$ that is different for every $i \in [1, \ldots, NbTSO]$. If several solutions minimize Problem (49), a secondary optimization step, with respect to the sum of individual objectives for example, could be run. Nevertheless, this case is not detailed in this thesis.

The approach is based on the compromise principle introduced in [100]: should a "utopian minimum" exist, it would then be chosen as the solution since each one of the TSOs' objectives are minimized with that solution. However, except for the case where the Pareto-front is reduced to a single element, there is no $\mathbf{u} \in U$ that corresponds to the "utopian minimum." Hence, the solution $\mathbf{u}^* \in U$ is chosen so as to minimize the distance − related to an Euclidean norm − between $[C_1(\mathbf{u}^*), C_2(\mathbf{u}^*), \ldots, C_{NbTSO}(\mathbf{u}^*)]$ and the "utopian minimum" C^{ut}. The method is also based on a normalization of the cost space that has fairness properties.

The procedure for normalizing the cost functions is presented in Section 5.1.1. Section 5.1.2 describes the procedure for computing the solution that is closest to the utopian minimum in the normalized space. Finally, the approach is illustrated in Section 5.2 with the benchmark system presented in Section 3.5.

5.1.1 Normalization of the cost space

The normalization process that can be adopted to obtain a fair arbitrage is explained hereafter. Its rationale is twofold. First, every local objective can be of a different nature (e.g., minimization of active power losses, maximization of reactive power

reserves, etc). This problem should naturally be addressed by the normalization process. Second, it also makes sense to normalize the cost functions to penalize the TSOs whose objective fulfillment is detrimental to other TSOs' objectives and favor those whose objectives are particularly compatible with the others.

For a particular cost function $C_i(\mathbf{u})$, the normalization factor will be the product of the two terms C_i° and χ_i. The normalized cost function $\overline{C}_i(\mathbf{u})$ will thus be computed using the following equation

$$\overline{C_i}(\mathbf{u}) = \frac{C_i(\mathbf{u})}{C_i^\circ \times \chi_i} \tag{50}$$

One can note that − since the solution that stands closest to the utopian minimum will be picked after the normalization of the cost-space − a small normalization factor for TSO_i will have the effect of giving more weight to its own objective function C_i and then favoring it. Moreover, as it will be demonstrated hereafter, C_i° and χ_i are null only if the utopian minimum corresponds to a solution $\mathbf{u}^{ut} \in U$. In this case, $\mathbf{u}^{ut}$ should be elected as a solution to the centralized problem.

The term C_i° is defined as follows.

$$C_i^\circ = \sum_{j=1}^{NbTSO} \frac{C_i(\mathbf{u}_j^*) - C_i(\mathbf{u}_i^*)}{NbTSO} \tag{51}$$

It has been introduced for two main reasons. First, it is expressed in the same unit as C_i and will therefore make the comparison possible between objective functions having different natures. In particular, it will make the approach independent of any scaling factor that may affect the different cost functions C_i. Second, the term C_i° will also favor a TSO whose objective fulfillment is weakly penalized by the fulfillment of the other objectives. Indeed, C_i° being the average value of the overcosts[1] supported by TSO_i for the $NbTSO$ control variables $\mathbf{u}_1^*$, $\mathbf{u}_2^*$, ..., $\mathbf{u}_{NbTSO}^*$, this term will be particularly small if the overcosts induced by other objective fulfillments $C_i(\mathbf{u}_j^*)$ are small.

[1]The term "overcosts" refers, in this thesis, to the difference between the actual costs $C_i(\mathbf{u})$ and their minimal value $C_i(\mathbf{u}_i^*)$.

The term χ_i is defined as follows.

$$\chi_i = \sum_{j=1}^{NbTSO} \frac{C_j(\mathbf{u}_i^*) - C_j(\mathbf{u}_j^*)}{C_j^\circ} \tag{52}$$

It has been introduced to penalize the detrimental impact of TSO_i's objective achievement on the other TSOs' costs, represented by the term $C_j(\mathbf{u}_i^*) - C_j(\mathbf{u}_j^*)$. One can note that this difference term is divided by C_j°. Thus, this division allows to sum up overcosts having different natures. Also, this normalization aims to leverage the penalization that TSO_i endures when its optimal control variables are detrimental to the objective of another TSO_j, which is itself compatible with the other TSO's objectives.

By anticipating the results of Section 5.2, it is found that, by using the normalization factor $C_i^\circ \times \chi_i$, the solution of the arbitrage has some properties of fairness in the economic sense.

5.1.2 Optimization of the normalized problem

As mentioned earlier, the presented approach will elect the solution $\mathbf{u}^*$, for which the cost vector $C(\mathbf{u}^*)$ minimizes (in the normalized cost space) the Euclidean distance to the "utopian minimum" under Constraints (32)-(33). This problem can be formulated as follows

$$\mathbf{u}^* = \arg\min_{\mathbf{u}\in U} \sum_{i=1}^{NbTSO} (\overline{C_i}(\mathbf{u}) - \overline{C_i}(\mathbf{u}_i^*))^2 \tag{53}$$

Solving this problem is indeed equivalent to finding the point on the Pareto-front that minimizes the distance to the utopian minimum. As a proof, suppose that $\mathbf{u}^*$ is not on the Pareto-front but solution of (53) under Constraints (32)-(33). Then, there would exist a solution $\mathbf{u}'$ such that $C_i(\mathbf{u}') \leq C_i(\mathbf{u}^*)$ for every $i \leq NbTSO$. In this case, for every area i, one could write the inequality $\overline{C_i}(\mathbf{u}') \leq \overline{C_i}(\mathbf{u}^*)$, and consequently $\sum_{i=1}^{NbTSO} (\overline{C_i}(\mathbf{u}') - \overline{C_i}(\mathbf{u}_i^*))^2 \leq \sum_{i=1}^{NbTSO} (\overline{C_i}(\mathbf{u}^*) - \overline{C_i}(\mathbf{u}_i^*))^2$. Therefore, $\mathbf{u}^*$ would not be the solution of (53), and the equivalence is proved.

Table 3: An algorithm for identifying a fair solution of the multi-objective optimization problem.

Input: For every TSO_i, a real-valued objective function $\hat{C}_i(\mathbf{u_{TSO_i}}, \mathbf{x_{TSO_i}})$ and the constraint functions $\hat{f}_i(\mathbf{u_{TSO_i}}, \mathbf{x_{TSO_i}})$, $\hat{g}_i(\mathbf{u_{TSO_i}}, \mathbf{x_{TSO_i}})$.
Output: A vector of control variables $\mathbf{u}^*$.
Step 1: Define the objective and constraint functions $C_i(\mathbf{u})$, $\forall i \in [1, 2, \ldots, NbTSO]$, $f(\mathbf{u})$, and $g(\mathbf{u})$, respectively.
Step 2: For every TSO_i, compute $\mathbf{u}_i^*$, solution of $\arg\min_{\mathbf{u}\in U} C_i(\mathbf{u})$.
Step 3: Compute the solution $\mathbf{u}^*$ of $\arg\min_{\mathbf{u}\in U} \sum_{i=1}^{NbTSO} (\overline{C_i}(\mathbf{u}) - \overline{C_i}(\mathbf{u}_i^*))^2$ where $\overline{C_i}(\mathbf{u}) = \frac{C_i(\mathbf{u})}{C_i^\circ \times \chi_i}$ with $C_i^\circ = \sum_j \frac{C_i(\mathbf{u}_j^*) - C_i(\mathbf{u}_i^*)}{NbTSO}$ and $\chi_i = \sum_j \frac{(C_j(\mathbf{u}_i^*) - C_j(\mathbf{u}_j^*))}{C_j^\circ}$.

Table 3 summarizes the procedure for computing, according to the proposed strategy, the point on the Pareto-front that could displease the different TSOs the least. This procedure implies solving the optimization problem (53) under Constraints (32)-(33), which can be solved using a standard single-TSO optimal power flow algorithm, as described in Section 3.1.1.

5.1.3 Example

The proposed method is illustrated here with the benchmark system presented in Section 3.5. Table 4 gives the different costs $C_i(\mathbf{u}_j^*)$, the normalized overcosts $\overline{C_i}(\mathbf{u}_j^*) - \overline{C_i}(\mathbf{u}_i^*)$ and the terms involved in the computation of the normalization factors. The bottom of the table also gives the costs $C_i(\mathbf{u}^*)$ and the normalized overcosts $\overline{C_i}(\mathbf{u}^*) - \overline{C_i}(\mathbf{u}_i^*)$ supported by each TSO. As one can see, those overcosts are particularly small. Figure 15 represents the localization of the normalized costs corresponding to $\mathbf{u}^*$ on the normalized Pareto-front.

Table 4: Values of the different costs $C_i(\mathbf{u})$ and normalized overcosts $\overline{C_i}(\mathbf{u}) - \overline{C_i}(\mathbf{u}_i^*)$ for every solution $\mathbf{u}_j^*$ of the single objective optimizations and for the solution $\mathbf{u}^*$ of the centralized decision making scheme. Values of C_i° and χ_i for TSO_i are also reported.

	$i=1$	$i=2$	$i=3$
$C_i(\mathbf{u}_1^*)$	4.36	134.82	44.40
$C_i(\mathbf{u}_2^*)$	1381.00	34.64	47.97
$C_i(\mathbf{u}_3^*)$	1278.28	302.00	37.92
C_i°	883.52	122.51	5.51
χ_i	1.99	3.38	3.62
$\overline{C_i}(\mathbf{u}_1^*) - \overline{C_i}(\mathbf{u}_i^*)$	0	0.2418	0.3245
$\overline{C_i}(\mathbf{u}_2^*) - \overline{C_i}(\mathbf{u}_i^*)$	0.7815	0	0.5032
$\overline{C_i}(\mathbf{u}_3^*) - \overline{C_i}(\mathbf{u}_i^*)$	0.7232	0.6453	0
$C_i(\mathbf{u}^*)$	20.01	37.7	38.13
$\overline{C_i}(\mathbf{u}^*) - \overline{C_i}(\mathbf{u}_i^*)$	0.0089	0.0071	0.0106

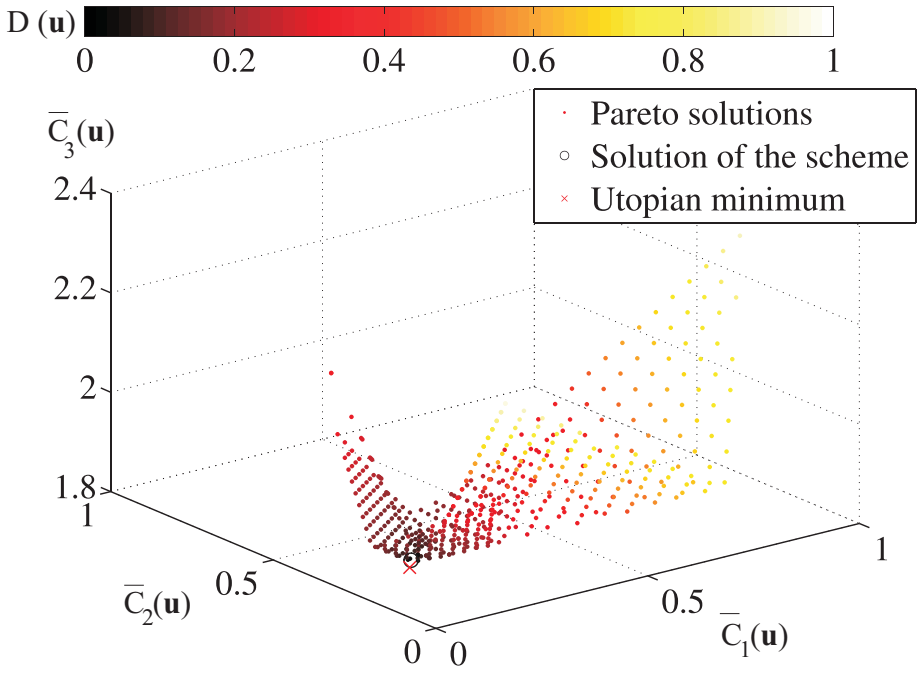

Figure 15: Localization of the centralized scheme's solution on the normalized Pareto-front for the IEEE 118 bus system partitioned between three TSOs. The color mapping represents the Euclidean distance $D(\mathbf{u})$ (in the normalized cost space) between each solution $\mathbf{u}$ and the utopian minimum.

5.2 Fairness evaluation

In Section 5.1, a new method was presented for choosing a single solution of the multi-TSO optimization problem described in Chapter 3. As introduced in Section 4.4, this method must have some properties of fairness to be potentially adopted by the TSOs, namely freedom from envy, efficiency, accountability, and altruism. This section assesses whether the optimization scheme proposed in Section 5.1 satisfies those criteria in the context of reactive power dispatch in a multi-TSO system.

5.2.1 Freedom from envy

As introduced in Section 4.4.2.1, with an envy-free procedure, all individual objectives of the TSOs must be treated through the same procedure, which must not rely on any specific information on the TSOs. This is obviously the case with the proposed approach. Indeed, since the procedure has been designed independently of any specific information related to the TSOs, every TSO is equally treated.

5.2.2 Efficiency

As described in Section 4.4.2.2, the efficiency of an arbitrage is related to a distance measure (e.g., the Euclidean distance in the normalized cost space) between an outcome and the Pareto-front of the problem. In practice, as proved in Section 5.1.2, the solution of the optimization scheme is on the Pareto-front. Consequently, the elected solution has the property of maximum efficiency, regardless of the objective functions and the constraints.

5.2.3 Accountability

In the context of multi-party resource allocation, a scheme is accountable if the party investing more effort earns its superior position. With the interpretation of accountability proposed in [7], an "effort" of TSO_i could be to make the constraints $g_i(\mathbf{u}) \leq 0$ less strict. It can be considered, for example, that an effort from one TSO would be

the increase of the range of possible bus voltages in its entire control area (say, from $[0.94, 1.06]$ to $[0.92, 1.08]$).

To study the accountability of the arbitrage strategy, the benchmark system was optimized with no effort and with an effort from each TSO, successively. Table 5 presents the costs and normalized overcosts supported by each TSO in every case. Those simulation results confirm the observations in [7] that the final allocation is generally more profitable for the TSO that makes more effort, at least in the original cost space. This "accountability" can also be observed in the normalized space, where the overcosts $\overline{C_i}(\mathbf{u}^*) - \overline{C_i}(\mathbf{u}_i^*)$ tend to decrease when TSO_i makes an effort (except for TSO_1 in this example).

However, those observations can not be generalized since there are some cases in which the final allocation is not accountable. For example, one can consider the case where a TSO_i makes an effort from which it does not directly benefit ($C_i(\mathbf{u}_i^*)$ does not significantly decrease). In such a context, its effort could allow the other TSOs to increase their possible benefits by increasing their use of TSO_i's resources. This could change the normalization factors, especially C_i°, and the location of the utopian minimum so that the final allocation could be less profitable for TSO_i. In particular, this situation happens when TSO_1 increases the range of possible bus voltages within its control area. For such a case, the decrease of $C_1(\mathbf{u}_1^*)$ is limited, as $\mathbf{u}_1^*$ is not really constrained by the bus voltage limits. In the meantime, $C_1(\mathbf{u}_2^*)$ and $C_1(\mathbf{u}_3^*)$ increase significantly, as the effort made by TSO_1 can be exploited by TSO_2 and TSO_3 in a detrimental way for TSO_1. Consequently, C_1° increases (from 883.52 to 1469.2), while χ_1 does not significantly decrease (from 1.99 to 1.56), and the other normalization factors tend to decrease. Hence, despite its higher effort, TSO_1 is penalized - $C_1(\mathbf{u}^*)$ increases from 20.01 to 30.80.

Table 5: Values of the cost functions $C_i(\mathbf{u}^*)$ and normalized overcosts $\overline{C_i}(\mathbf{u}^*) - \overline{C_i}(\mathbf{u}_i^*)$ in every area of the test system. Four cases have been studied: no extra effort, effort from TSO_1, effort from TSO_2, and effort from TSO_3.

Effort	$C_1(\mathbf{u}^*)$	$C_2(\mathbf{u}^*)$	$C_3(\mathbf{u}^*)$
None	20.01	37.70	38.13
TSO_1	30.80	37.02	37.91
TSO_2	15.65	36.71	38.12
TSO_3	19.61	36.95	36.96
Effort	$\overline{C_1}(\mathbf{u}^*) - \overline{C_1}(\mathbf{u}_1^*)$	$\overline{C_2}(\mathbf{u}^*) - \overline{C_2}(\mathbf{u}_2^*)$	$\overline{C_3}(\mathbf{u}^*) - \overline{C_3}(\mathbf{u}_3^*)$
None	0.0089	0.0071	0.0106
TSO_1	0.0125	0.0067	0.0172
TSO_2	0.0087	0.0061	0.0120
TSO_3	0.0070	0.0101	0.0059

The allocation is also non-accountable if applied to a system with only two parties. The normalization factors for TSO_1 and TSO_2 would then be $C_1^\circ \times \chi_1 = C_1(\mathbf{u}_2^*) - C_1(\mathbf{u}_1^*)$ and $C_2^\circ \times \chi_2 = C_2(\mathbf{u}_1^*) - C_2(\mathbf{u}_2^*)$, respectively. Therefore, one TSO would be rewarded if its objective fulfillment is highly penalizing its neighbor and the arbitrage could not be accountable. This flaw disappears, however, when considering systems with three TSOs or more. Indeed, the more TSOs participate in the process, the more importance is given to a local objective that only slightly affects the other TSOs' objectives.

5.2.4 Altruism

As introduced in Section 4.4.2.4, one property of altruism is that a parameter that does not depend on TSOs' actions should not affect the allocations. The interpretation made here is that an optimal control settings for a TSO_i, whose control variables have much influence on the objective fulfillment of the other TSOs, should be consistent with the other TSOs' objectives, regardless of the objective function $C_i(\mathbf{u})$. It is, however, difficult to check whether this concept is indeed satisfied.

Another property of altruism is that the allocations should not be biased toward the TSOs with the greatest "abilities." Indeed, as written in Chapter 1, the overcosts should rather be shared according to the effort made by the different TSOs. In the context of reactive power scheduling, it can be considered that the ability of a TSO is related to its influence on the costs of the other TSOs. Thus, the TSOs that have a strong influence on the system should not have a highly negative impact on the other TSOs. In this respect, the allocation scheme clearly has some altruism properties since the terms χ_i and C_i^0 penalize TSO_i, when its objective is not compatible with the other objectives.

5.3 Sensitivity to biased information

If a CCC were to apply the proposed resource allocation scheme, some TSOs might be tempted to exercise strategic behavior to turn the scheme in their favor. This section discusses how sensitive the optimization scheme is with respect to biased information concerning the constraints (e.g., limitations on voltage or reactive power injections) and objective functions.

5.3.1 Biased formulation of the constraints

A way for the parties to bias the arbitrage scheme in their favor is to report accountable efforts only. In particular, every TSO_i may be interested in declaring more restrictive constraints $g_i(\mathbf{u})$ than those faced in reality, when it does not directly benefit from the relaxation of those constraints. A numerical example of the outcome for a TSO, when it provides wrong information about its voltage constraints, is presented in Section 5.2.3.

Although the lack of accountability of the scheme with respect to certain types of effort may induce such types of gaming, this non-collaborative strategy might be avoided by continuous monitoring of the power system state by the CCC. For example, a statistical analysis of the bus voltages could inform the CCC about real voltage

control abilities of every generator in the power system. The practical implementation of such a policy is, however, particularly complex, and is not discussed in this thesis.

5.3.2 Biased formulation of the objectives

Finally, a TSO_i may be tempted to declare a biased formulation of its cost function. More precisely, a TSO_i could provide the CCC with a function $\hat{C}_i^w(\mathbf{u})$ rather than $\hat{C}_i(\mathbf{u})$.

If $C_i^w(\mathbf{u}) = a \times C_i(\mathbf{u}) + b$ with $a, b \in \Re$, the allocation strategy is not affected since, as emphasized in Section 5.1.2, the arbitrage strategy has the property of being immune to any linear transformation of the objective functions[2].

One can also consider the case where $C_i^w(\mathbf{u}) = C_i(\mathbf{u}) \times C_i(\mathbf{u})$. Intuitively, with such a biased formulation of its objective function, TSO_i could obtain a better allocation, since it may give the CCC the impression that a deviation from $\mathbf{u}_i^*$ is worse for it than it is in reality. However, such a strategy is not systematically beneficial for a TSO. For example, if TSO_1, which focuses on the minimization of reactive power support in its control area, asks the CCC to minimize the square of $\sum_{j \in TSO_1} Q_j^2$, the arbitrage leads to a solution were $C_1(\mathbf{u}^*) = 97.07$ rather than 20.01 if TSO_1 were to provide its true objective function. Hence, such a strategy of overestimating its costs may be counter-productive.

Even if it is clear that, by truncating their objective function, the TSOs might bias the allocation in their favor, such a problem could be avoided in practice by constraining the TSOs to select their cost function in a set of reasonable formulations for the objectives, and report data and constraints truthfully.

[2]The independence of the arbitrage with respect to a translation $+b$ is due to the fact that only overcosts are used to define the normalization factors.

5.4 Limitations of the method

Previous sections demonstrate that the proposed method has some properties of fairness in an economic sense and robustness with respect to some types of strategic behavior from the interconnected TSOs. Those observations should be considered with care since they have been limited to a single case and counter examples have been identified. However, one could think of applying the proposed scheme to schedule reactive power in a multi-area power system, where every TSO has real-valued objective function.

Prior to applying the proposed scheme to real systems, some practical issues need to be addressed. In particular, the computational costs of the scheme may be higher than those needed for a single-objective optimal power flow. Indeed, as emphasized in [105], a sophisticated formulation of the objective may induce more computational complexity, which could be critical, when the scheme is applied to large-scale systems.

One may also consider other issues in relation to the application of the scheme to real systems. By way of example, with large-scale systems, the individual objectives of the TSOs may almost be independent of a large number of control variables, such as those located very far from the area under consideration. This could induce a high sensitivity of the normalization factors with respect to some small changes in the system operating conditions, which could be questioned by the different parties.

While the number of potential applications of the proposed method is large (any allocation that can be formulated as a multi-objective problem could be solved through the centralized method), its Achilles' heel is related to the way the "fairest allocation" is defined and, more specifically, to the cost functions normalization procedure. In essence, this definition is subjective. It may perhaps even be naive to assess the fairness of an allocation without consulting the different parties.

CHAPTER VI

DECENTRALIZED APPROACH

Decentralized optimization schemes may appear as another promising solution for multi-area power system scheduling, as their intrinsic accountability and freedom from envy make them easily accepted by all parties. Moreover, their implementation may be easier, since decentralized control schemes usually involve a restricted amount of information exchange. However, some decentralized schemes may be less effective in terms of altruism and efficiency. Hence, there seems to be an overall consensus that decentralized optimization control schemes should exhibit several characteristics such as *simplicity* and *robustness* with respect to various configurations of the power system and loss of communication channels. They should also give *close-to-optimal performance* with the optimal performance being achieved when the solution of the scheme is on the Pareto-front of the problem.

This chapter presents an iterative control scheme, where the different TSOs concurrently schedule, at each iteration, the reactive power dispatch within their own control area, while representing the neighboring areas with external network equivalents. Afterward, the TSOs apply the locally optimized control actions in their own control area, and, before the next iteration, the TSOs update the parameters of the external network equivalents used to represent their neighboring areas based on the observations made at the interconnections. The scheme is obviously simple since, among others, it requires no need for communication between the different TSOs or for a centralized authority to coordinate their actions. Two key elements of this iterative control scheme are the type of equivalents used by each TSO to represent

its neighboring areas, and the procedure the TSOs adopt to refresh, in every iteration, the parameters of those equivalents to "best" fit the observations made at the interconnections.

The goal of this chapter is to provide a mathematical formulation of the scheme, while its performance and robustness are analyzed in Chapter 7. While the set of *a priori* plausible equivalents may be extremely large, the study will mainly focus on the cases, where every TSO models its neighboring areas by associating to every interconnection line an equivalent that can be formulated as a set of parametric equality constraints depending only on the current and the voltage at the interconnection. Those equivalents will be referred to as *single interconnection-based equivalents*. Similarly, while many mechanisms could be thought of to compute the parameters of those equivalents from the observations, the study will be limited to procedures that fit the parameters of an equivalent associated with a particular interconnection to the past measurements of the current and voltage at this interconnection. Also, the type of equivalent used as well as the mechanism to fit their parameters will be constrained to be identical everywhere, regardless of the interconnection under consideration.

The chapter is organized as follows. First, the outline of the iterative decentralized control scheme is provided in Section 6.1. Second, in Section 6.2, the mathematical formulation of the equivalents under consideration is detailed. Third, Section 6.3 proposes three adaptive fitting procedures.

6.1 Outline of the algorithm

The main features of the decentralized control scheme are sketched on Figure 16. The scheme is iterative in nature, and every TSO concurrently solves at instant $k-1$ the scheduling problem corresponding to its own area, and then, applies its control actions on the system at instant k.

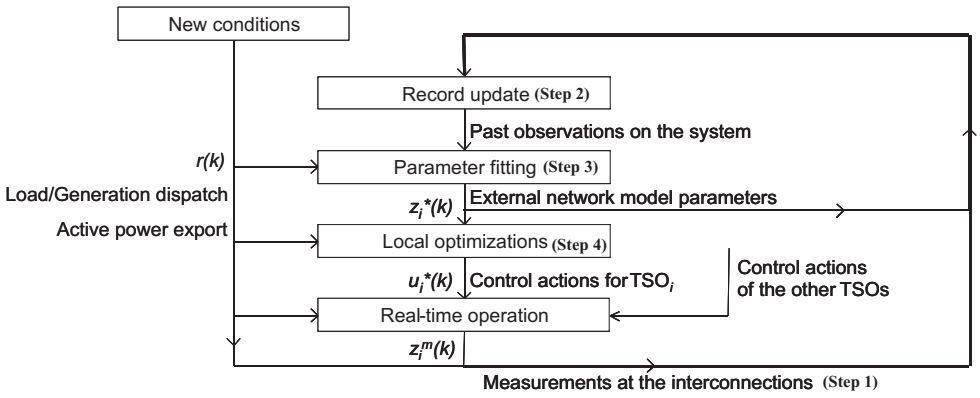

Figure 16: The role of TSO_i in the decentralized optimization scheme. The four steps of the decentralized optimization scheme are marked in brackets. A tabular version of the algorithm is provided in Section 6.4

The coordination relies on the fact that every TSO is recommended to model the external system with a set of parametric equality constraints $\hat{h}_i^k(\mathbf{u}_{TSO_i}, \mathbf{x}_{TSO_i}, \mathbf{z}_{TSO_i}^k{}^*)$, which correspond to an external network model, whose parameters are denoted by $\mathbf{z}_{TSO_i}^k{}^*$. Then, every TSO solves the optimization problem corresponding to its control area in a greedy way. The scheme is obviously simple since, among others, it requires no need for communication between the different TSOs or for a centralized authority to coordinate their actions.

While different types of external network models could be advocated, this thesis only focuses on three single interconnection-based equivalents, namely the PQ, PV, and PQ(V) equivalents. The practical formulation of $\hat{h}_i^k(\mathbf{u}_{TSO_i}, \mathbf{x}_{TSO_i}, \mathbf{z}_{TSO_i}^k{}^*)$ and the components of the parameter vector $\mathbf{z}_{TSO_i}^k{}^*$ are described in Section 6.2.

At instant $k-1$, every TSO_i thus solves the following optimization problem

$$\min_{\mathbf{u}_{TSO_i}, \mathbf{x}_{TSO_i}} \hat{C}_i^k(\mathbf{u}_{TSO_i}, \mathbf{x}_{TSO_i}) \tag{54}$$

under the inequality and equality constraints

$$\hat{f}_i^k(\mathbf{u}_{TSO_i}, \mathbf{x}_{TSO_i}) \leq 0 \tag{55}$$

$$\hat{g}_i^k(\mathbf{u}_{TSO_i}, \mathbf{x}_{TSO_i}) = 0 \tag{56}$$

$$\hat{h}_i^k(\mathbf{u}_{TSO_i}, \mathbf{x}_{TSO_i}, \mathbf{z}_{TSO_i}^{k\,*}) = 0 \tag{57}$$

The solutions $\mathbf{u}_{TSO_1}^{k\,*}$, $\mathbf{u}_{TSO_2}^{k\,*}$,..., $\mathbf{u}_{TSO_{NbTSO}}^{k\,*}$ are appended onto $\mathbf{u}^{k*}$, which is applied to the interconnected system at instant k. To model the impact of those control actions on real-time system operation, it is considered here that operation conditions are as steady with the same values as predicted. Nevertheless, it may happen that those actions $\mathbf{u}_{TSO_1}^{k\,*}$, $\mathbf{u}_{TSO_2}^{k\,*}$,..., $\mathbf{u}_{TSO_{NbTSO}}^{k\,*}$ correspond to a state that does not satisfy[1] Constraints (32) and (33). Usually, as shown in [106], the constraints, if violated, are only slightly passed over, and, in practice, the secondary voltage control may accordingly change the operation conditions of the system to make sure that the constraints are satisfied. In this thesis, the assumption of a hierarchical voltage control scheme implies the existence of such control actions. Moreover, it is considered that their combined action is equivalent to choosing, instead of $\mathbf{u}^{k*}$, a vector of control variables $\mathbf{u}^{km}$ solution of

$$\min_{\mathbf{u}} \left|\left|\mathbf{u}^{k*} - \mathbf{u}\right|\right| \tag{58}$$

under Equality (32) and Inequality (33). One can note that this definition is slightly different from the definition of SVC that is detailed in Section 2.3.2. This results from the steady-state modeling of this dynamic control, which here allows to assess the secondary voltage control effort at instant k as the value $\left|\left|\mathbf{u}^{k*} - \mathbf{u}^{km}\right|\right|$.

Among the state variables $\mathbf{x}^{km}$, the values of power flows and voltage at each interconnection are then measured by each TSO, and the record of measurements $\mathbf{H}\mathbf{x}^k$ is updated.

[1] This may be checked in a simulation environment by running a load flow.

It will be supposed in this thesis that every TSO proceeds fairly, according to the recommended procedure, and uses the same type of equivalent and procedure to compute its parameters ${\mathbf{z}^k_{TSO_i}}^*$.

6.2 Mathematical formulation of the equivalents

In this section, the practical formulation of $\hat{h}^k_i(\mathbf{u}_{TSO_i}, \mathbf{x}_{TSO_i}, {\mathbf{z}^k_{TSO_i}}^*)$ is detailed for three types of external network models, namely the PQ, PV, and PQ(V) equivalent. An evaluation of the equivalents is proposed in Section 7.2.

6.2.1 PQ equivalent

A PQ equivalent replaces the power system beyond an interconnection l of TSO_i by a bus, whose active and reactive power demand is constant. Figure 17 illustrates the use of three PQ equivalents by TSO_i.

The set of parametric equality constraints $\hat{h}^k_i(\mathbf{u}_{TSO_i}, \mathbf{x}_{TSO_i}, {\mathbf{z}^k_{TSO_i}}^*) = \mathbf{0}$ corresponding to this equivalent can be written in the form[2]

$$\Re(V_{i,l} \cdot conj(I_{i,l})) - ZP^k_{i,l} = 0 \tag{59}$$

$$\Im(V_{i,l} \cdot conj(I_{i,l})) - ZQ^k_{i,l} = 0 \tag{60}$$

where $V^k_{i,l}$ and $I^k_{i,l}$ are the voltage and current at the interconnection l of TSO_i at instant k. Their values depend on $\mathbf{x}_{TSO_i}$. Also, the two parameters $ZP^k_{i,l}$ and $ZQ^k_{i,l}$ represent the scheduled active and reactive power consumption of the PQ equivalent. This information is included into ${\mathbf{z}^k_{TSO_i}}^*$.

6.2.2 PV equivalent

The PV equivalents are used to represent the power system areas beyond the interconnections as buses, whose voltage magnitudes and active power consumptions are constant. Figure 18 illustrates the use of three PQ equivalents by TSO_i.

[2] $conj(a)$ denotes the conjugate of the complex number a, $\Re(a)$ its real part, and $\Im(a)$ its imaginary part.

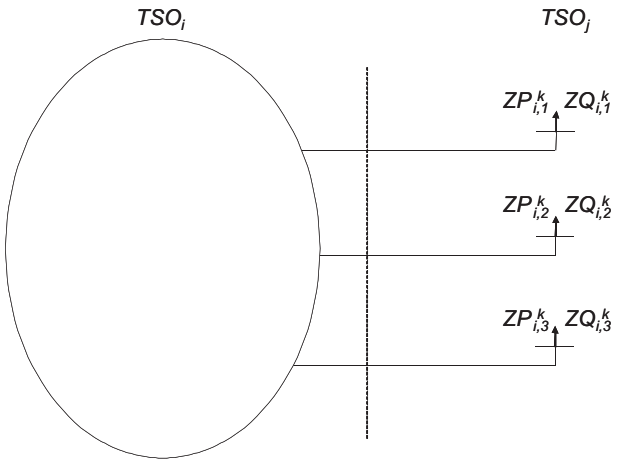

Figure 17: A TSO_i relying on PQ equivalents to model a neighboring area controlled by TSO_j, with which it has three interconnections.

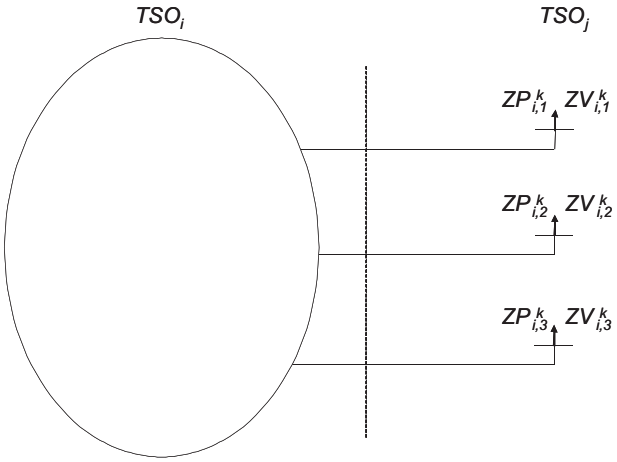

Figure 18: A TSO_i relying on PV equivalents to model a neighboring area controlled by TSO_j, with which it has three interconnections.

The set of parametric equality constraints $\hat{h}_i^k(\mathbf{u}_{TSO_i}, \mathbf{x}_{TSO_i}, \mathbf{z}_{TSO_i}^k{}^*) = \mathbf{0}$ corresponding to this equivalent can be written in the form

$$\Re(V_{i,l} \cdot conj(I_{i,l})) - ZP_{i,l}^k = 0 \tag{61}$$

$$\|V_{i,l}\| - ZV_{i,l}^k = 0 \tag{62}$$

Those equality constraints have two parameters $ZP_{i,l}^k$ and $ZV_{i,l}^k$ that represent the active power and voltage magnitude related to the PV equivalent. This information is included into $\mathbf{z}_{TSO_i}^k{}^*$.

6.2.3 PQ(V) equivalent

A PQ(V) equivalent replaces the power system seen beyond an interconnection l of a TSO_i by a bus, whose reactive power injection is proportional to the bus voltage. Figure 19 illustrates the use of those equivalents by a TSO_i.

The set of parametric equality constraints $\hat{h}_i^k(\mathbf{u}_{TSO_i}, \mathbf{x}_{TSO_i}, \mathbf{z}_{TSO_i}^k{}^*) = \mathbf{0}$ corresponding to this equivalent can be written in the form

$$\Re(V_{i,l} \cdot conj(I_{i,l})) - ZP_{i,l}^k = 0 \tag{63}$$

$$\Im(V_{i,l} \cdot conj(I_{i,l})) - ZA_{i,l}^k \times V_{i,l} = ZB_{i,l}^k \tag{64}$$

where $ZPth_{i,l}^k$, $ZAth_{i,l}^k$, and $ZBth_{i,l}^k$ are the parameters of the PQ(V) equivalent. They represent the active power, and the Q(V) linear coefficients related to the interconnection i, l, respectively. This information is included into $\mathbf{z}_{TSO_i}^k{}^*$.

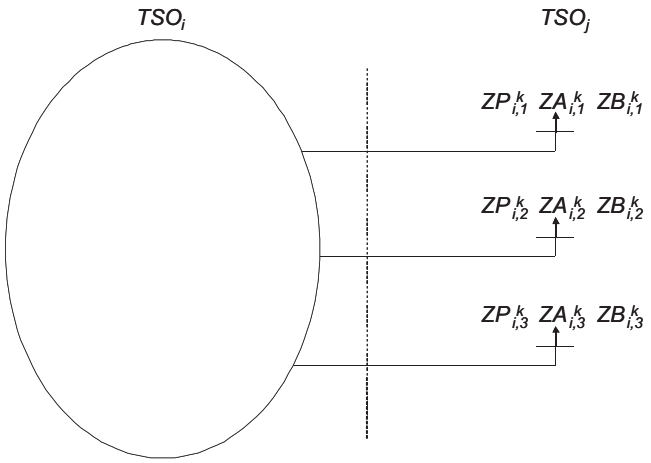

Figure 19: A TSO_i relying on PQ(V) equivalents to model a neighboring area controlled by TSO_j, with which it has three interconnections.

6.3 Parameter fitting procedures

Another key element of the decentralized control scheme is the procedure to best fit the parameters of the equivalents to past measurements at the interconnection so that the final allocation leads to nearly optimal performance.

As represented in Figure 16, several types of inputs may be considered in the design of parameter tracking procedure. Those are, for example, the past observations of the power system, load predictions, and past values of the equivalents' parameters. In this thesis, for computing the parameters of a PQ equivalent related to a particular interconnection, only the past measurements of active and reactive power at this interconnection will be considered as input. The parameter tracking issue is tackled by using three different adaptive parameter fitting approaches, which are detailed hereafter. As outlined in [107, 108], those tracking strategies have already been widely used to design adaptive control schemes for power systems. In particular, they have led to the design of efficient control strategies for damping inter-area oscillations [109, 110].

6.3.1 Exponential recursive least squares approach

The exponential recursive least squares (ERLS) strategy computes $\mathbf{z}_i^{k*}$ by solving the following minimization problem

$$\min_{\mathbf{z}} \sum_{j=0}^{k-1} \beta^{1+j-k} \times \left|\left|\mathbf{z}^{jm} - \mathbf{z}\right|\right|^2 \tag{65}$$

where β is a memory factor such that $\beta \in [0, 1]$, and $\mathbf{z}_i^{jm}$ the parameters' on-site measurement at instant j. As the choice of the memory factor β affects the value of $\mathbf{z}_i^{k*}$, this choice may be subject to some tuning. This choice is thus discussed in Section 7.3.

6.3.2 Environment-dependent exponential recursive least squares approach

While the ERLS approach emphasizes the importance of recent measurements, those measurements may correspond to a power system state that is particularly different from the scheduled one. A solution could be to use an environment-dependent exponential recursive least squares approach (ED-ERLS), where the memory factor $\xi(k, j)$ would weight the measurements at instant j according to the similarity between the power system state at instant j and the one scheduled for instant k. For the sake of simplicity, the state at instant j is assumed to be similar to the state at instant k if the associated load factor $r(j)$ is close to $r(k)$.

The term $\xi(k, j)$ can thus be typically written as follows

$$\xi(k, j) = N_{r(k)}^{\sigma}(r(j)) \tag{66}$$

where $N_{r(k)}^{\sigma}(\cdot)$ is a Gaussian function with mean $r(k)$ and variance σ.

In this context, $\mathbf{z}_i^{k*}$ is the solution of the following problem

$$\min_{\mathbf{z}} \sum_{j=0}^{k-1} [\xi(k, j)]^{1+j-k} \times \left|\left|\mathbf{z}^{jm} - \mathbf{z}\right|\right|^2 \tag{67}$$

6.3.3 Adaptive forgetting factor approach

The previous approaches do not allow a fast tracking of specific changes in the system configuration (e.g. change in the system topology), which could significantly affect the steady-state values of the parameters at the interconnections. Therefore, an adaptive forgetting factor (AFF) approach, which is introduced in [111], is proposed for tracking non-linear systems in both slow and fast time-varying environments. The rationale of this method is to use, as a weighting factor, the product of two terms $\psi(k) \times \xi(k,j)$, where $\xi(k,j)$ is defined by Equation (66), and where $\psi(k) \in]0,1[$ is close to 1, when there is no fast change in the system between instants $k-1$ and k, and close to 0 otherwise.

More specifically, $\psi(k)$ depends on the prediction error observed at instant $k-1$, $\epsilon_i(k-1) = \left|\left|\mathbf{z}_i^{k-1^m} - \mathbf{z}_i^{k-1^*}\right|\right|$, in the following way

$$\psi(k) = exp(-\tau \times \epsilon_i(k-1)) \tag{68}$$

where τ is a forgetting factor.

Therefore, $\mathbf{z}_i^{k^*}$ is the solution of the following problem

$$\min_{\mathbf{z}} \sum_{j=0}^{k-1} [\psi(k) \times \xi(k,j)]^{1+j-k} \times \left|\left|\mathbf{z}^{j^m} - \mathbf{z}\right|\right|^2 \tag{69}$$

6.4 A tabular version of the decentralized control scheme

In this thesis, it is assumed that every TSO_i computes, at the instant $k-1$, the values of the control actions it will apply to the system at time k by solving the optimization problem described by Equations (54)-(57). Those values are denoted by $\mathbf{u}_{TSO_i}^{k^*}$. At the next instant k, after implementation of the control actions and, if necessary, actions by the SVC controllers, TSOs measure the state variables again within their control area to update the parameters of their equivalents. This update is realized by adding the values of $x_{TSO_i}^{k^m}$ to the record of the state variables $\mathbf{H}\mathbf{x}_{TSO_i}^{k-1}$.

After having updated the record of state variables, the TSOs solve their respective optimization problems and update their control actions as depicted in the tabular version of the algorithm that is given in Table 6.

Table 6: A generic algorithm for simulating the decentralized control scheme. The expression $a = b \oplus c$ sets first the vector a equal to the vector b, and then, adds at the end of a the element c.

1. Set $k = 1$.

2. For every TSO_i, do the following operations:

   Step 1: Measure $\mathbf{u}_{TSO_i}^{k-1\ m}$, and $\mathbf{x}_{TSO_i}^{k-1\ m}$.

   Step 2: Update of the record of the measurements: $\mathbf{Hu}_{TSO_i}^{k} = \mathbf{Hu}_{TSO_i}^{k-1} \oplus \mathbf{u}_{TSO_i}^{k-1\ m}$ and $\mathbf{Hx}_{TSO_i}^{k} = \mathbf{Hx}_{TSO_i}^{k-1} \oplus \mathbf{x}_{TSO_i}^{k-1\ m}$.

   Step 3:Compute the values of $\mathbf{z}_{TSO_i}^{k\ *}$ based on a weighted least squares approach.

   Step 4: Solve the optimization problem defined by Equations (54)-(57), and let $\mathbf{u}_{TSO_i}^{k\ *}$ denote its solution.

3. Simulate secondary voltage control by using $\mathbf{u}^{k*}$ as input of a power flow algorithm $\min_{\mathbf{u} \in U[k]} \left|\left|\mathbf{u}^{k*} - \mathbf{u}\right|\right|$ subject to Constraints (32) and (33).

4. Set $k \leftarrow k + 1$, and go back to **Step 2**.

CHAPTER VII

EVALUATION OF THE DECENTRALIZED APPROACH

This chapter is dedicated to the evaluation of the decentralized control scheme. It also aims to design the pair equivalent-fitting procedure that constantly leads to close to optimal solutions. The chapter is organized as follows. First, the evaluation criteria are designed. Second, the performance of the scheme is detailed for a time-invariant power system. Third, the robustness of the scheme is studied for a time-invariant system. Fourth, the performance of the scheme is analyzed in the context of a time-varying power system.

7.1 Evaluation criteria

To study the influence of the equivalents and fitting procedures described in Chapter 6, Section 7.1.1 introduces some performance evaluation criteria. In the second part of the section, additional criteria are introduced for time-invariant systems.

7.1.1 Definition of the performance indexes

As introduced in Section 4.4, a performance analysis for a particular coordination scheme should take several criteria into account, namely, freedom from envy, efficiency, accountability, and altruism. Assessing the efficiency of an allocation as a distance measure (according to a specific metric) to the Pareto-front of the problem could be difficult in practice due to the large number of Pareto-solutions that would then need to be computed. Therefore, it is proposed here to run the performance analysis based on the fairness index that is used in the centralized control scheme presented in Chapter 5. More precisely, the performance of the decentralized scheme is related to the euclidean distance to the utopian minimum of the problem, in the normalized cost

space. At instant k, the performance of the scheme can thus be assessed as follows

$$D(k) = \sqrt{\sum_{i=1}^{NbTSO} (\overline{C_i^k}(\mathbf{u}^{k^m}) - \overline{C_i^k}(\mathbf{u}_i^*))^2} \tag{70}$$

It may be observed that the normalization factors depend on the operating conditions. They are thus computed at each instant k. Also, as a large period of time may be considered, only the average (AD) and variance (VD) of $D(k)$ will be reported. Obviously, the scheme will be said to perform well, when AD is small.

As one could argue that the performance criteria is subjective in nature (see Section 5.4), it must be recalled at this stage that, even if the objective of every TSO_i has the same nature (for instance, every TSO seeks to minimize active power losses), summing the individual costs into a single objective function would also be subjective. Nevertheless, this latter approach has been chosen in [106, 112], for example.

Another evaluation criterion relies on the secondary voltage control effort that is necessary to change the actions $\mathbf{u}^{k^*}$ to make them satisfy the Constraints (32) and (33) (see Stage **3** of the algorithm of Table 6). In particular, the performance of the decentralized scheme is higher, when the corresponding SVC effort is small. The effort will be denoted by $E(k)$, which is computed as follows

$$E(k) = \left|\left|\mathbf{u}^{k^m} - \mathbf{u}^{k^*}\right|\right| \tag{71}$$

The maximum value E_{max} of $E(k)$ will be reported. The scheme will be said to perform well, when E_{max} is small.

7.1.2 Evaluation criteria for a time-invariant system

First, the decentralized control scheme will be applied to a time-invariant system, where the load demand does not change with respect to time. In this particular context, additional evaluation criteria can be defined. As these criteria may depend on the evolution of the control actions over the iterations, two classes of evolution have

been designed. These two classes and the associated evaluation criteria are defined hereafter.

7.1.2.1 Convergent

When considering a time-invariant system, the process is said to be convergent if there exists a set of control actions $\mathbf{u}_A \in U$ such that $\lim_{k\to\infty} \left\|\mathbf{u}^{k^m} - \mathbf{u}_A\right\| \to 0$, i.e. the sequence of actions taken by the different TSOs converges toward $\mathbf{u}_A$.

In such a case, the following criteria are reported.

- Average performance AD
- Maximum SVC effort E_{max}
- Time to convergence (TC), which is defined as the highest value of k for which $D(k) \leq 0.9 \times AD$ or $1.1 \times AD \leq D(k)$.

7.1.2.2 Non-convergent

A process is said to be non-convergent if it does not converge. If one of the optimizations involved in the scheme is singular (i.e., the optimization does not converge), then the simulation process is stopped and the evaluation criteria are automatically assigned an infinite value. However, as emphasized in Section 7.2.4.1, this case is particularly unlikely. Otherwise, if no singular case is reported, the following criteria are reported.

- Average performance AD
- Performance variance VD
- Time to convergence TC, which is computed as for convergent cases despite the fact the process is non-convergent. A small value of TC shows that the performance is almost stationary in the long term.
- Maximum SVC effort E_{max}

7.1.2.3 Classification in practice

To limit computation time, a maximum number of iterations equal to 500 has been used in the simulations as a substitute for $k \to \infty$. If $D(k)$ is not constant over the last iterations, it is considered that the process is non-convergent. With such a relatively high limit on the number of iterations, it is likely that very few cases have been misclassified in the simulation results.

7.1.2.4 Illustration of the process classification through didactic examples

To illustrate the criteria defined in Section 7.1.1, simulations have been run on the benchmark system presented in Section 3.5.

Figure 20 represents the simulation results, when the interconnections are represented by PV equivalents together with a ERLS fitting procedure with $\beta = 0.5$, and $[\gamma_1, \gamma_2, \gamma_3] = [0, 0, 0]$. For this convergent process, AD is equal to 0.0651, the time to convergence index (TC) is 22, the maximum SVC effort (E_{max}) is 0.00035.

Figure 21 represents the simulation results, when the interconnections are represented by PQ(V) equivalents together with a ERLS fitting procedure with $\beta = 0.75$, and $[\gamma_1, \gamma_2, \gamma_3] = [0, 0, 0]$. This case illustrates a typical non-convergent behavior, where the AD is equal to 0.067. Also, the maximum SVC effort is 0.0012.

7.1.3 Evaluation criteria in a time-varying system

The above defined classification may not be meaningful for time-varying power systems. In this particular context, a "training period" of 26 days is used to set a consistent record of measurements so as to provide insightful input into the fitting procedure. After that training period, simulation results only focus on a specific "test period," during which the average performance AD and its variance VD are reported. In addition, the average effort AE and its variance VE over the test period are presented.

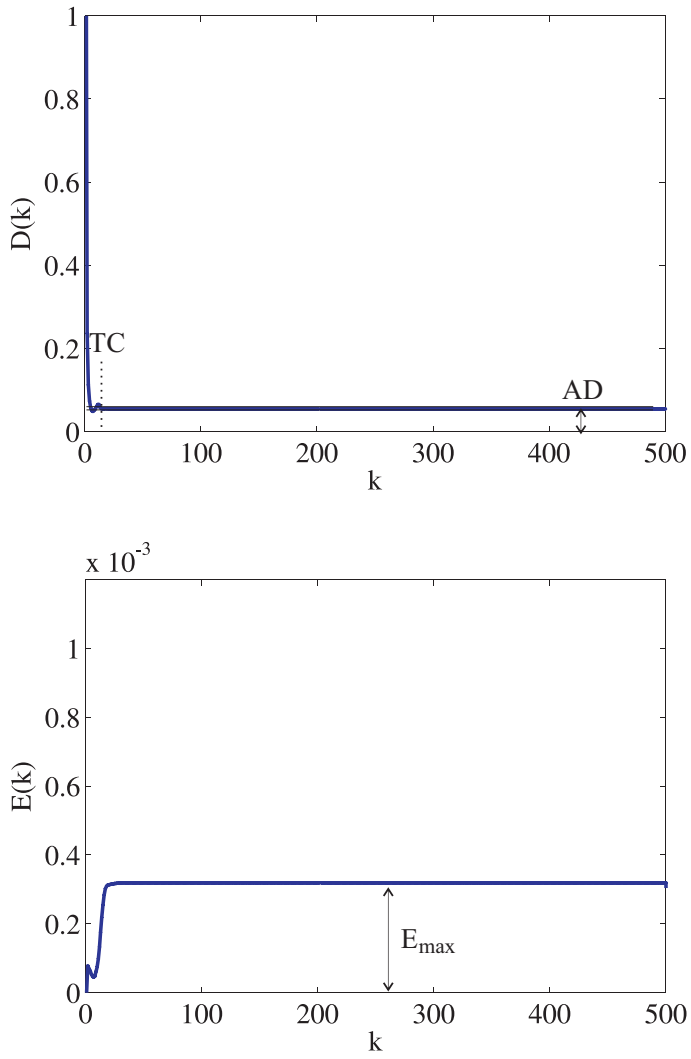

Figure 20: The decentralized optimization scheme is run on the IEEE 118 bus system with three TSOs. The cost functions represent only reactive power support for each TSO_i. PV equivalents are used. The memory factor is chosen equal to 0.5. The top figure represents the evolution of $D(k)$ with respect to k. The bottom figure plots the evolution of $E(k)$ with respect to k.

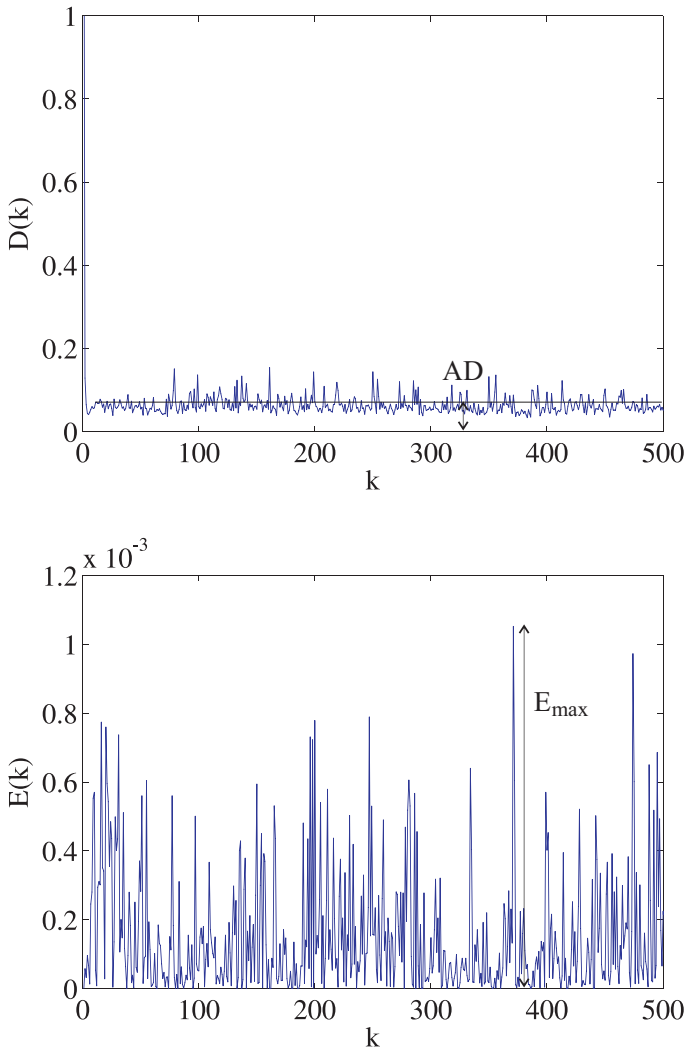

Figure 21: The decentralized optimization scheme is run on the IEEE 118 bus system with three TSOs. The cost function represents only reactive power support for each TSO_i. PQ(V) equivalents are used. The memory factor is chosen equal to 0.75. The top figure represents the evolution of $D(k)$ with respect to k. The bottom figure plots the evolution of $E(k)$ with respect to k.

7.2 Application to a time-invariant system

This section analyzes the performance of the decentralized control scheme introduced in Chapter 6 in the particular context of a time-invariant power system. It aims at evaluating the performance that can be obtained with the different equivalents, and assessing the influence of simulation parameters. The study considers four types of equivalents with an ERLS Fitting procedure, for which three values of the memory factor β are evaluated. To assess the performance of a specific pair, two power systems were chosen to be considered, 27 sets of objective functions, and three types of initial conditions (i.e., the state of the system at $t = 0$). For each pair "equivalent-fitting procedure," this amounts to analyzing 162 cases.

The remainder of this section is organized as follows. First the equivalents and fitting functions are detailed. Then, the different study cases are described, and, finally, the results are discussed.

7.2.1 Equivalents and fitting functions

7.2.1.1 Equivalents

The performance evaluation considers three "single-interconnection based equivalents," namely the PQ, PV, and PQ(V). Their description, together with the formulation of Constraint (57), is given in Section 6.2. Additionally, one more advanced equivalent, namely the non-reduced power system (NPS), has been considered. Its description and mathematical formulation is provided in [106].

Other types of equivalents could be evaluated. Indeed, the Thévenin-like equivalent, which is introduced in [113], and the REI equivalent [114, 115] could be seen as potentially interesting alternatives. However, simulation results have shown that such equivalents usually induce relatively high SVC efforts [106]. Indeed, those equivalents set voltage angle differences between interconnections, and it was found that those voltage angle differences "predicted" at time t by the fitting procedure are

significantly different from those that can be measured at time $t+1$, when local controls $\mathbf{u}_1^{t+1^m}$, $\mathbf{u}_2^{t+1^m}$,..., $\mathbf{u}_{NbTSO}^{t+1}{}^m$ are applied to the power system. As emphasized in [106], this strong difference may be the root cause for the volatility induced by the Thévenin-like and REI equivalents. To avoid such variations, those equivalents are qualified inappropriate for use with the decentralized control scheme and will not be evaluated hereafter.

7.2.1.2 Fitting functions

In this section, the decentralized approach is applied to a time-invariant power system. In this context, the ERLS fitting procedure, which is described in Section 6.3, is used with different values of the memory factor $\beta \in [0, 1]$. Hence, a past observation obtained at instant k is weighted with respect to the current observation at instant t by a factor β^{t-k}. The following values of β are considered hereafter.

- $\beta = 0.5$ (low memory factor)
- $\beta = 0.75$ (medium memory factor)
- $\beta = 0.95$ (high memory factor)

Values of $\beta = 0$ and $\beta = 1$ have not been considered on purpose. Indeed, if $\beta = 0$, that is only the last measurements are taken into account, then the solution of the ERLS problem is undefined for the PQ(V) equivalent. On the other hand, with a value of $\beta = 1$, the function to be minimized using the ERLS procedure can not be bounded. Thus, $\beta = 1$ is not considered in this thesis.

7.2.2 Conditions of simulations

To assess the influence of the simulation conditions, the evaluation has been run with two power systems. With each power system, three types of objective function were applied for each TSO_i. In each case, three initial operation states were considered.

7.2.2.1 Benchmarks

Two power system benchmarks have been considered, namely:

- the IEEE 118 bus system with three different TSOs, which is introduced in Section 3.5 and detailed in Appendix B.
- the IEEE 39 bus New England system with three different TSOs. This system is depicted in [17] and its numerical data is provided in Appendix C.

7.2.2.2 Optimization functions

For every TSO_i, three types of optimization functions have been considered. As described in Section 3.4, the type of objective function of TSO_i depends on the value of the weight factor γ_i. The results for nine combinations of weight factors $[\gamma_1, \gamma_2, \gamma_3]$, with γ_i equal to 0, 0.9, or 1 for each $i \in [1, 2, 3]$ are presented in Section 7.2.3.4.

7.2.2.3 Initial state

The state of the system at time $t = 0$ may influence the outcome of the first optimization problem solved by the TSOs. Subsequently, every action $\mathbf{u}^{k^m}$ results from the initial state since $\mathbf{u}^{k^m}$ is a function of $\mathbf{u}^{0^m}, \mathbf{u}^{1^m}, \ldots, \mathbf{u}^{k-1^m}$. The influence of three types of initial states is thus studied.

- High-voltage state: The initial state is the solution of an optimization problem, whose objective is to maximize the average bus voltage under Constraints (27)-(28).

- Medium-voltage state: The initial state is the solution of an optimization problem, whose objective is to bring the average bus voltage as close as possible to 1 p.u.
- Low-voltage state: The initial state corresponds to the minimum average bus voltage.

7.2.3 Simulation Results

This section presents the simulation results in the context of a time-invariant system. After analyzing the performance of each pair equivalent-fitting procedure, the impact of the simulation conditions is studied.

7.2.3.1 Average performance of each pair "equivalent-fitting function"

To analyze the average performance of every pair "equivalent-fitting function" over the 162 simulation cases, the frequency of each type of dynamics (convergent, non-convergent) and the relevant evaluation indexes (introduced in Section 7.1.2) are reported in Table 7.

The processes induced by the PQ, PV, PQ(V), and NPS equivalents can be either classified as convergent or non-convergent. Convergence is almost always observed with PQ and PV equivalents, and in almost 80% of the cases with NPS equivalents. Non-convergence is almost systematic with PQ(V) equivalents. Within the classification of dynamics, a certain influence of β was observed. Also, with the investigated values, it was found that increasing β could either increase or decrease the amount of convergent cases.

In terms of the performance index, the PQ equivalent offers the best performance with a low AD (average distance to the utopian minimum) of around 0.19. It is followed by the NPS equivalent, for which the AD is around 0.25 for convergent cases and varies between 0.66 and 0.70 for non-convergent ones. The PV equivalent leads to the highest distances to the utopian minimum, which are in average more than

ten times higher than with the PQ equivalent. This result can be explained by the fact that the competition between different TSOs is stronger when they have more accurate information on other TSOs' network and past actions. Here, the stronger competition leads to local optimization relying more on external TSOs' control actions, which results in a less efficient state after several iterations.

As for the SVC effort associated with different types of equivalents, it is remarkable to observe that, even if the TSOs choose actions only by considering their own constraints, violations induced by the decentralized control schemes are small. Also, the required SVC effort strongly depends on the equivalent. PQ equivalents lead to a maximum effort of $0.0001 p.u.$, while PV equivalents and NPS equivalents are around $0.0020 p.u.$. The higher volatility obtained with PQ(V) equivalents induces a superior effort of around $0.0100 p.u.$.

The parameter β, which weights long term measurements with respect to short-term ones, was not found to strongly influence the performance of the different schemes, at least for the values under consideration. However, it can be observed that for PQ equivalents, which offer the best performance, large values of β lead to more convergent cases, even if the time to convergence increases with β. In the rest of this section, only a single value of β equal to 0.75 will be considered.

Table 7: An analysis of the dynamics induced by 12 pairs of "equivalents/fitting functions." For each pair, 162 cases are studied (2 power systems × 27 sets of objective functions × 3 initial states). The classification and the average values of the indexes introduced in Section 7.1.2 are reported. Also, the performance obtained with the centralized control scheme proposed in Chapter 5 is presented.

Equiv.–Fit. funct.		Classification		Convergent cases			Non-convergent cases			
Equiv.	β	Conv.	Non-conv.	AD	TC	E_max	AD	VD	TC	E_{max}
PQ	0.50	44.4%	55.6%	0.2168	4.7	0.0000	0.1913	0.0015	155	0.0002
PQ	0.75	94.4%	5.6%	0.1886	8.3	0.0001	0.4174	0.0157	500	0.0000
PQ	0.95	94.4%	5.6%	0.1887	18.0	0.0001	0.4165	0.0173	500	0.0000
PV	0.50	94.4%	5.6%	0.4527	13.1	0.0014	1.4584	0.0003	7	0.0005
PV	0.75	94.4%	5.6%	0.4527	24.7	0.0014	1.4592	0.0005	11	0.0006
PV	0.95	83.3%	16.7%	0.3190	29.6	0.0016	1.1556	0.0347	341	0.0002
PQ(V)	0.50	0.0%	100.0%				0.6841	0.0321	498	0.0393
PQ(V)	0.75	0.0%	100.0%				0.6795	0.0291	500	0.0237
PQ(V)	0.95	5.6%	94.4%	0.2491	446.3	0.0099	0.6890	0.0276	500	0.0158
NPS	0.50	81.5%	18.5%	0.2556	5.2	0.0036	0.6666	0.0031	196	0.0125
NPS	0.75	80.9%	19.1%	0.2431	3.0	0.0020	0.7059	0.0109	198	0.0217
NPS	0.95	83.3%	16.7%	0.2570	4.7	0.0020	0.7047	0.0066	201	0.0242
Cent.				0.1023						

7.2.3.2 Impact of the initial state

Table 8 represents the collection of mean values of the main evaluation indexes for PQ, PV, PQ(V), and NPS equivalents with a memory factor $\beta = 0.75$. Every benchmark power system and optimization function has been considered when computing those values.

Simulation results show that the initial state does not impact the final result, when considering decentralized schemes based on PQ equivalents. Indeed, with PQ equivalents, an average value for AD equal to 0.189 is obtained for every initial state considered. The initial state impacts, however, the time to convergence. Hence, a lower initial voltage induces a longer time to convergence. Some non-convergent processes are also observed.

With PV, PQ(V), and NPS equivalents, the initial state slightly impacts the process classification: the percentage of convergent cases is a bit lower with a low-voltage, or a medium-voltage initial state, than with a high-voltage initial state. The average performance index AD does not significantly depend on the initial state. For the PV equivalent, it should be stressed that comparing the average values of AD for the convergent cases is not meaningful since they have been computed for different cases. If the average value of AD for the non-convergent cases were integrated into the average values of AD for the convergent case, it would not depend on initial state.

Table 8: An analysis of the influence of three initial states on the performance obtained with four pairs of "equivalents/fitting functions." For each equivalent, the fitting function corresponds to a memory factor $\beta = 0.75$. For each pair, 54 cases are studied (2 power systems $\times$ 27 sets of objective functions). The classification and the average value of the indexes introduced in Section 7.1.2 are reported. Also, the performance obtained with the centralized control scheme proposed in Chapter 5 is presented.

		Classification		Convergent cases			Non-convergent cases			
Equiv.	Init.	Conv.	Non-conv.	AD	TC	E_max	AD	VD	TC	E_{max}
PQ	*Low*	83.3%	16.7%	0.1869	16.0	0.0000	0.4174	0.0157	500	0.0000
PQ	*Med.*	100.0%	0.0%	0.1892	5.4	0.0001	0.0000	0.0000	0	0.0000
PQ	*High*	100.0%	0.0%	0.1892	4.6	0.0001	0.0000	0.0000	0	0.0000
PV	*Low*	83.3%	16.7%	0.3189	14.9	0.0013	1.4592	0.0005	11	0.0006
PV	*Med.*	100.0%	0.0%	0.5084	37.4	0.0013	0.0000	0.0000	0	0.0000
PV	*High*	100.0%	0.0%	0.5084	20.2	0.0015	0.0000	0.0000	0	0.0000
PQ(V)	*Low*	0.0%	100.0%				0.6801	0.0141	500	0.0084
PQ(V)	*Med.*	0.0%	100.0%				0.6806	0.0602	500	0.0532
PQ(V)	*High*	0.0%	100.0%				0.6779	0.0131	500	0.0095
NPS	*Low*	81.5%	18.5%	0.2372	3.3	0.0024	0.7328	0.0007	228	0.0026
NPS	*Med.*	81.5%	18.5%	0.2515	2.9	0.0018	0.7037	0.0320	188	0.0556
NPS	*High*	79.6%	20.4%	0.2406	2.9	0.0019	0.6834	0.0009	181	0.0083
Cent.				0.1023						

7.2.3.3 Impact of the power system

Table 9 illustrates the influence of the power system on the performance obtained with different types of equivalents.

On the one hand, with the IEEE 118 bus system with three TSOs, the best performance is observed with the PV equivalent ($AD = 0.155$), but at a higher cost in terms of SVC effort. The distance obtained with the PQ equivalent is slightly greater ($AD = 0.165$), with a smaller SVC effort. On the other hand, the PQ equivalent leads to similar performance when applied to the IEEE 39 bus system with three TSOs, while the PV equivalent leads to a much greater distance to the utopian minimum ($AD = 0.86$).

In general, the performance of the scheme depends on the ratio between the number of interconnections divided by the size of the power system. The higher that ratio is, the more difficult it is to design a solution that can satisfy every TSO.

Table 9: An analysis of the performance obtained on two power systems, while using three different equivalents, a memory factor $\beta = 0.75$, and a medium-voltage initial state. For each case, 27 sets of objective functions are considered. Also, the performance obtained with the centralized control scheme proposed in Chapter 5 is presented.

		Classification		Convergent cases			Non-convergent cases			
Equiv.	Sys.	Conv.	Non-conv.	AD	TC	E_max	AD	VD	TC	E_{max}
PQ	118/3	100.0%	0.0%	0.1635	8.9	0.0001	0.0000	0.0000	0	0.0000
PQ	39/3	100.0%	0.0%	0.2150	2.0	0.0000	0.0000	0.0000	0	0.0000
PV	118/3	100.0%	0.0%	0.1553	8.9	0.0011	0.0000	0.0000	0	0.0000
PV	39/3	100.0%	0.0%	0.8615	65.9	0.0015	0.0000	0.0000	0	0.0000
PQ(V)	118/3	0.0%	100.0%				0.3426	0.0143	500	0.0043
PQ(V)	39/3	0.0%	100.0%				1.0186	0.1061	500	0.1020
NPS	118/3	100.0%	0.0%	0.1073	3.1	0.0006	0.0000	0.0000	0	0.0000
NPS	39/3	63.0%	37.0%	0.4804	2.5	0.0036	0.7037	0.0320	188	0.0556
Cent.	118/3			0.0233						
Cent.	39/3			0.1813						

7.2.3.4 Impact of the optimization function

The influence of the optimization functions on the performance of the control scheme has also been studied. As introduced in Section 3.4, the optimization function of a TSO_i is characterized by the value of $\gamma_i \in [0, 1]$, which weights active power losses with respect to reactive power support. Thus, Table 10 presents the main evaluation indexes for different sets of objective functions in the IEEE 118 bus system with three TSOs. As the evaluation index AD refers to the normalized cost space instead of the real values of the individual objectives, it induces some slight changes with respect to the observations in [106].

One can note that the maximum SVC effort does not strongly depend on the set of objective functions. However, it is remarkable that the set of objective functions has a significant impact on the performance obtained. Indeed, when the objective of TSO_1 is only focused on active power losses, best performance is observed with NPS and PV equivalents. PQ equivalents are better when the objective of TSO_1 also considers reactive power support.

Table 10: An analysis of the performance obtained for eight sets of objective functions, while using three different equivalents, a memory factor $\beta = 0.75$, and a medium-voltage initial state. For each TSO_i, two values of γ_i are considered ($\gamma_i = 0$ or $\gamma_i = 1$). Also, the performance obtained with the centralized control scheme proposed in Chapter 5 is presented.

	Objective			Convergent cases		
Equiv.	γ_1	γ_2	γ_3	AD	TC	E_max
PQ	0	0	0	0.2301	2	0.0000
PQ	0	0	1	0.1800	2	0.0000
PQ	0	1	0	0.2395	2	0.0000
PQ	0	1	1	0.2050	3	0.0000
PQ	1	0	0	0.2062	1	0.0000
PQ	1	0	1	0.0603	4	0.0000
PQ	1	1	0	0.2870	1	0.0000
PQ	1	1	1	0.1050	3	0.0000
PV	0	0	0	0.2830	18	0.0025
PV	0	0	1	0.8150	16	0.0025
PV	0	1	0	0.5948	18	0.0025
PV	0	1	1	0.9831	17	0.0025
PV	1	0	0	0.7936	170	0.0001
PV	1	0	1	0.8163	163	0.0001
PV	1	1	0	0.7414	172	0.0001
PV	1	1	1	0.7367	161	0.0001
NPS	0	0	0	0.3552	1	0.0093
NPS	0	0	1			
NPS	0	1	0	0.6113	5	0.0027
NPS	0	1	1	0.5357	2	0.0000
NPS	1	0	0	0.2631	3	0.0011
NPS	1	0	1	0.3671	3	0.0011
NPS	1	1	0			
NPS	1	1	1			

7.2.4 Convergence properties of the scheme

The existence of different classes of processes raises the issue of robustness of the decentralized control scheme. More specifically, the convergence properties of the decentralized scheme may be questioned in the particular context of a time-invariant system. This section aims to provide useful information to identify the conditions that can lead to a convergent process. It is organized as follows. First, the conditions for singularity of the scheme are detailed. Second, the conditions for the convergence of the scheme are analyzed.

7.2.4.1 Potential singularity of the scheme

Whereas modeling the SVC by a second OPF should avoid the singular processes identified in [106], it is remarkable that restricting the set of possible control values U^k for the SVC could induce singular cases at **Step 3** of the algorithm presented in Table 6. This might occur in real systems, where the SVC is managed as described in Section 2.3.2.1. Indeed, the voltage settings of the generators within one area may vary only in a coordinated manner based on the pilot bus voltage amplitude regardless of the needs of the interconnected system. Hence, this could result in non-sustainable control settings, and eventually load-shedding or line-tripping. However, simulation results tend to show that the SVC effort is limited when using adequate equivalents and fitting procedures, which reduces the risk of a singular process.

Furthermore, using a decentralized control scheme with simple equivalents should ease the computation of the OPF, as it involves less computation resource than a large-scale OPF that considers the entire system. Indeed, as described in [105], the computation costs strongly increase with the size of the system. Under the assumption of sustainable constraints at the interconnections, using the decentralized optimization scheme instead of the centralized scheme proposed in Chapter 5 should thus reduce the risk of singularity in the system optimization.

7.2.4.2 Conditions for convergence

The existence of non-convergent processes for every pair of equivalent/fitting procedure tends to show that the decentralized scheme does not systematically converge to a single solution. It may thus be of interest to identify the convergence properties of a time-invariant system controlled with the iterative decentralized optimization schemes, which can be formalized as follows

$$\mathbf{u}^{k+1^m} = f_{sys}(\mathbf{u}^{k^m}, \mathbf{H}\mathbf{u}^{k^m}) \tag{72}$$

where $\mathbf{u}^{k^m} \in U^k$ is the control action (after SVC correction) that is applied at iteration k, $\mathbf{H}\mathbf{u}^{k^m}$ is the record of such actions at previous iterations, and $f_{sys}(\mathbf{u}^{k^m}, \mathbf{H}\mathbf{u}^{k^m})$ characterizes the evolution of the control actions from an iteration to ananother.

The existence of control settings for which the system is stable is a necessary condition for convergence of the iterative process. In control theory, the stability analysis is usually based on the state representation of a system [116, 117]. This approach is, however, hardly applicable in the case of the decentralized optimization scheme, as the system dynamics is characterized by a discrete time process that involves the record of actions at previous iterations. Furthermore, as $f_{sys}(\mathbf{u}^{k^m}, \mathbf{H}\mathbf{u}^{k^m})$ can not be explicitly formalized, most available analysis methods are inappropriate.

In the context of an iterative multi-party optimization, a stable equilibrium is usually referred to as "Nash equilibrium." In game theory, this refers to a solution $u^N \in U$, such that $\hat{C_i}^N(\mathbf{u}_{TSO_i}) \geq \hat{C_i}^N(\mathbf{u}^N_{TSO_i})$ for all $\mathbf{u}_{TSO_i} \in U_{TSO_i}$ and $i \in [1, 2, ..., NbTSO]$, where $\hat{C_i}^N$ corresponds to the objective function of TSO_i, when considering $\mathbf{u}^N$ as the initial state to define the parameters of the equivalents, $\mathbf{u}_{TSO_i}$ is the vector of control settings for TSO_i, and $\mathbf{u}^N_{TSO_i}$ is the set of control settings in $\mathbf{u}^N$ that corresponds to TSO_i. In [118, 119], it is proved that a single Nash equilibrium exists when U is convex and $C_i(\mathbf{u})$ is concave $\forall i \in [1, ..., NbTSO]$. Other assumptions on U and $C_i(\mathbf{u}), \forall i \in [1, ..., NbTSO]$, such as local convexity or weak interconnection,

may be sufficient to guarantee the existence of a Nash equilibrium [120].

In a large-scale multi-TSO system operated with a decentralized optimization scheme, those conditions are unlikely, and hard to check, as the dimension of the systems under consideration makes the stability analysis uncertain. In addition, even if stability conditions were satisfied with a particular control setting $\mathbf{u} \in U$, it would not be sufficient to guarantee that the decentralized optimization scheme converges toward this solution. In this matter, the dimension of the system and non-deterministic nature of reactive power scheduling makes the convergence analysis strenuous.

7.3 Application to a time-varying system

In the previous section, it has been assumed, mostly for the sake of simplicity, that the load consumption, generation dispatch and network topology remain constant from one instant k to another. With such an assumption, it has been shown that the performance of the decentralized control scheme with PQ equivalents and an ERLS fitting procedure is nearly optimal. Before adopting such a scheme for implementation in a large scale power system, its performance should be analyzed in "time-varying" systems.

The relatively fast convergence properties of the control scheme shown in the previous section suggest that such an application could be feasible. Indeed, suppose that at one instant, a sudden change of topology occurs (e.g., loss of a transmission line). Then, due to its fast convergence properties, the scheme should converge again within a few iterations to new control settings that correspond to a nearly optimal solution for the new configuration of the system. Moreover, if the time between two iterations is small, the transient period during which the system operates in higher suboptimal conditions is short. However, it is important to mention that, as shown in the previous section (and more particularly in Table 7), the time to convergence may depend on the memory factor β (or more generally on the parameter

fitting procedure). This weights past observations with respect to the current ones in the parameter fitting procedure. In the case of a "time-varying" system, choosing a consistent fitting procedure is important in addressing the trade-off between the adaptivity of the scheme and the efficiency of the values of control variables.

To design an appropriate fitting procedure, this section presents some simulation results in the context of a time-varying power system. Simulations focus on three adaptive parameter tracking procedures, which are presented in Section 6.3. They are evaluated on the IEEE 118 bus system with three TSOs, where the load demand $r(k)$ changes at each discrete time instant k (see Section 3.5 for more details). The objectives of the TSOs are defined as follows: $\gamma_1 = 0$, $\gamma_2 = 0.9$, and $\gamma_3 = 1$. A "training period" (from January 1 to January 27, 2008) is used to initialize the history of measurements and control variables. Therefore, only results corresponding to the period January 28-31, 2008 are presented. To consider rapid changes in the system configuration, a line outage is introduced for the branch between bus 19 and 20 on January 28 at 12.00 am. The line is reconnected on January 28 at noon.

Although it is informative to study the evolution of $D(k)$ and $E(k)$ with respect to k, the performance analysis of the control scheme will only focus on the average performance measure AD, and the maximum SVC effort E_{max} over the period January 27th-31st, 2008. The AD obtained with the different parameter fitting techniques will be compared with the average performance measurements that would be obtained if the centralized control scheme proposed in Chapter 5 were applied at every instant k. With the centralized control scheme proposed in Chapter 5, this index has the following values $AD = 0.0272$. By definition, $E_{max} = 0$ with the centralized control scheme.

7.3.1 Performance with ERLS-algorithm

Figure 22 depicts the performance index AD obtained with the exponential recursive least squares algorithm presented in Section 6.3 on the 118 bus benchmark system. It can be observed that the memory factor β has a significant influence on AD. The lowest AD is reported for $\beta = 0.575$, i.e. the equivalents' parameters are set at a value that is close to the three last measurements at the interconnections. Even with such a memory factor, the AD is higher than the one that would be obtained with the centralized control scheme (0.0871 vs 0.0272).

Figure 23 presents the maximal value of the SVC effort during the evaluation period with an ERLS-algorithm. As for the performance index, it can be observed that the memory factor β impacts the SVC effort. The lowest effort $E_{max} = 0.3e^{-3}$ is obtained with $\beta = 0.6$. It is noticeable that AD and E_{max} are strongly correlated.

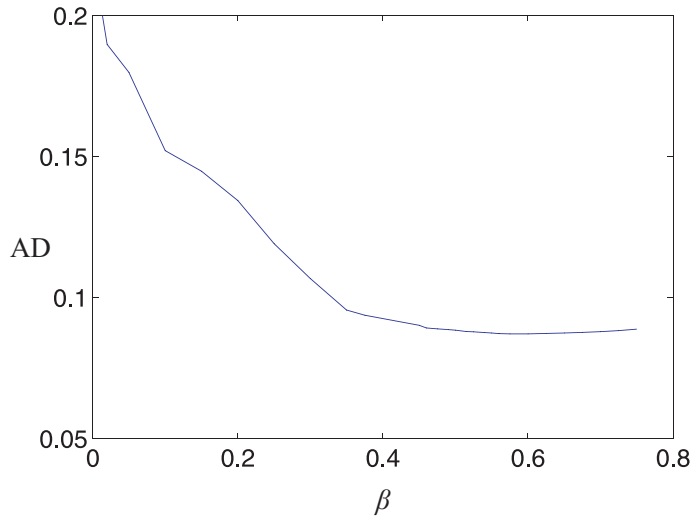

Figure 22: Average performance index as a function of β on the time-varying 118 bus benchmark system with an ERLS fitting algorithm.

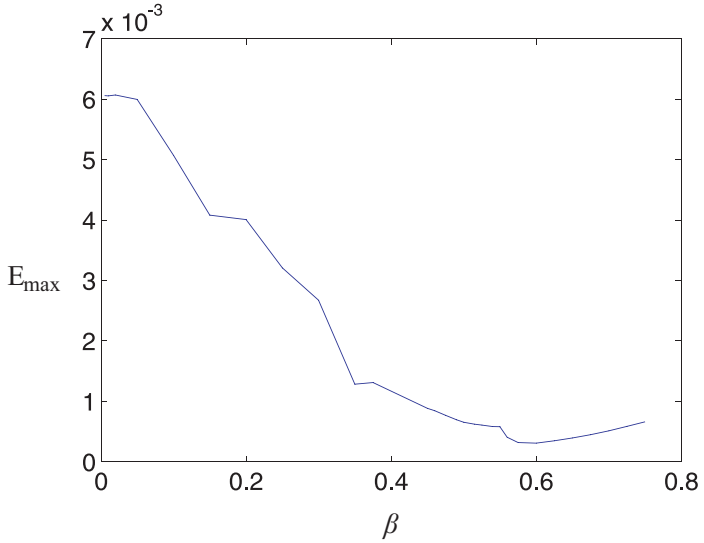

Figure 23: Maximum SVC effort as a function of β on the time-varying 118 bus benchmark system with an ERLS fitting algorithm.

7.3.2 Performance with ED-ERLS-algorithm

The performance of the decentralized control scheme with the environment dependent exponential recursive least squares algorithm presented in Section 6.3 is reported in Figure 24. The impact of the similarity factor σ is significant, and one can observe that the best performance is reached with $\sigma \simeq 0.025$. In this case, the average performance index, AD, is around 0.875, which represents no improvement over the performance observed with the ERLS algorithm.

Figure 25 presents the maximal value of SVC effort during the evaluation period with an ED-ERLS parameter fitting procedure. As for the performance index, it can be observed that the similarity factor σ impacts the SVC effort. The lowest effort $E_{max} = 8e^{-6}$ is obtained with $\sigma = 0.095$. It is also noticeable that AD and E_{max} are slightly correlated.

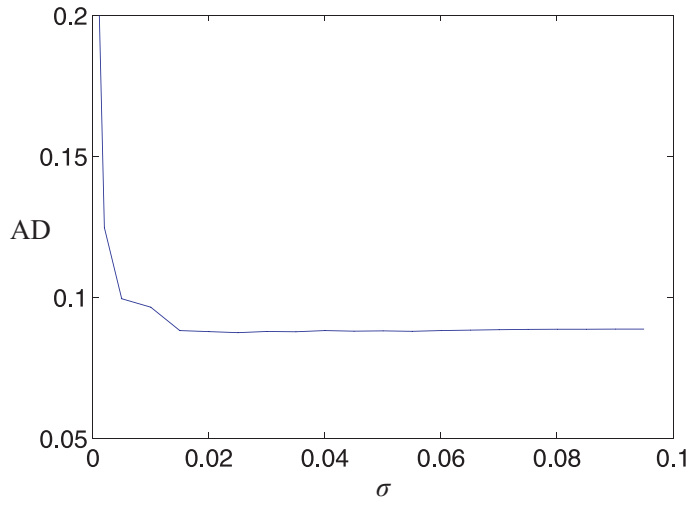

Figure 24: Average performance index as a function of σ on the time-varying 118 bus benchmark system with an ED-ERLS fitting algorithm.

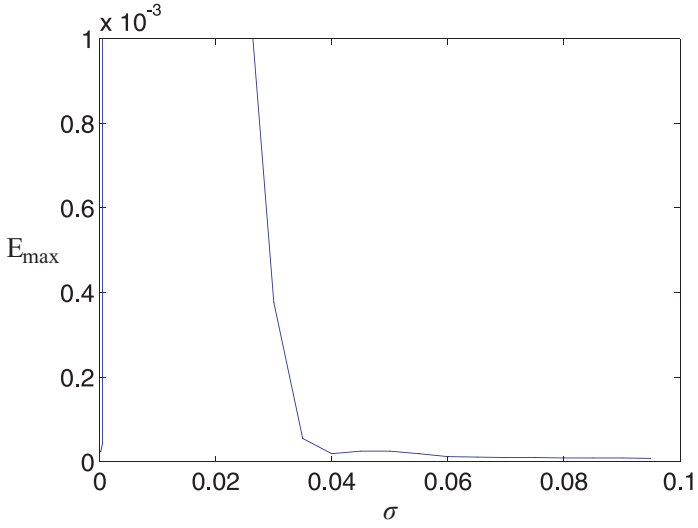

Figure 25: Maximum SVC effort as a function of σ on the time-varying 118 bus benchmark system with an ED-ERLS fitting algorithm.

7.3.3 Performance with AFF-algorithm

The performance of the decentralized control scheme with the adaptive forgetting factor algorithm presented in Section 6.3 is reported on Figure 26. This figure highlights the impact of the similarity factor σ and deviation factor τ on the performance of the control scheme. More specifically, in this case, the best performance is reached with $\sigma = 0.095$ and $\tau = 0.35$. Those values of σ and τ lead to an average performance index AD equal to 0.0860, which is better when compared to the ED-ERLS fitting procedure.

Figure 27 presents the maximal value of an SVC effort during the evaluation period with an AFF parameter fitting procedure. As for the performance index it can be observed that the similarity factor σ and deviation factor τ impact the SVC effort. The lowest effort $E_{max} = 1e^{-5}$ is obtained with $\sigma = 0.095$ and $\tau = 0.0001$. It is also noticeable that AD and E_{max} are correlated.

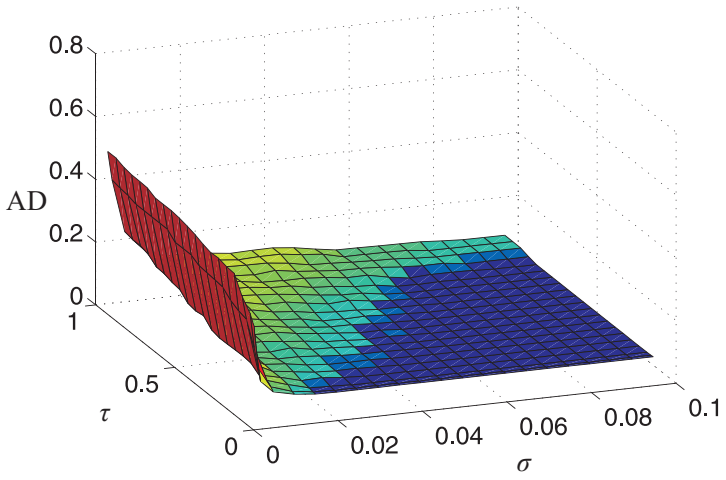

Figure 26: Average performance index as a function of σ and τ on the time-varying 118 bus benchmark system with an AFF fitting algorithm.

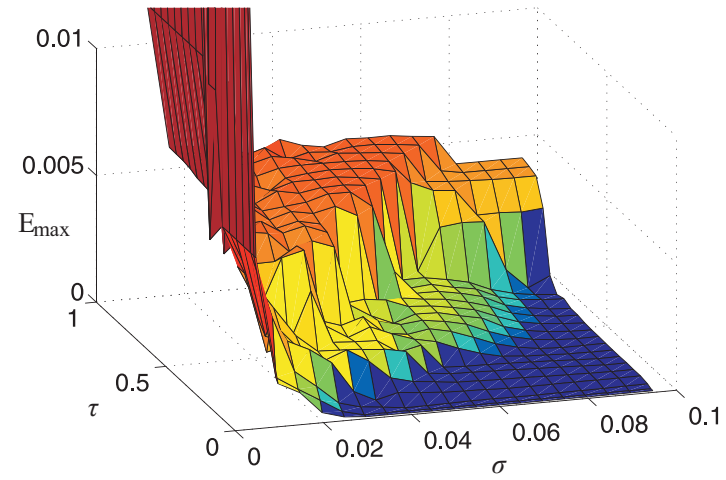

Figure 27: Maximum SVC effort as a function of σ and τ on the time-varying 118 bus benchmark system with an AFF fitting algorithm.

7.3.4 Robustness of the decentralized control scheme

This section aims to evaluate the decentralized scheme when the benchmark system is subjected to a severe disturbance or demand prediction error. Although these types of events would also affect a system controlled through a centralized optimization scheme, this section aims to illustrate the robustness properties of the decentralized control scheme with respect to these two types of unexpected events.

First, it is supposed that a transmission line is disconnected on January 28, 2008 and reconnected 12 hours later. Two cases are considered, the loss of the transmission line between bus 1 and bus 2 (case 1), and between bus 3 and bus 4 (case 2). This kind of disturbance may affect the performance and robustness of the scheme as the parameter fitting procedures rely on the measurements at the interconnections, which were made with other network configurations.

Second, it is supposed that one of the TSOs incorrectly predicts the load demand $r(k+1)$ and optimizes its control settings with an inexact knowledge on the future state of the power system. Two types of prediction errors are considered for TSO_1 during the period January 28-31, 2008: a 5% underestimation (case 3) and 5% overestimation (case 4) of the load demand.

Simulations were run for the four cases presented above. The three types of parameter fitting procedures were applied using the values of β, σ, and τ that are leading to the best performance in the time-varying system studied in Section 7.3. More specifically, $\beta = 0.575$ for the ERLS fitting procedure, $\sigma = 0.025$ for the EDERLS fitting procedure, and $\sigma = 0.095$ and $\tau = 0.35$ for the VFF fitting procedure. The evolution of the performance index $D(k)$ and SVC effort $E(k)$ with the ERLS, ED-ERLS, and AFF fitting procedures are displayed for each case under consideration.

7.3.4.1 Change in the system configuration

Figures 28 and 29 display the performance index $D(k)$ and the SVC effort $E(k)$ over the evaluation period, when the IEEE 118 bus is subjected to case 1. Figures 30 and 31 display the same indexes, respectively, with case 2.

It can be observed that the decentralized control scheme with VFF fitting procedure leads to the best performance and the smallest SVC effort, although the performance remains slightly worse than with the centralized control scheme that is presented in Chapter 5. However, case 2 shows that an unexpected event could induce poorer performance and higher SVC effort (see D(k) and E(k) on Figures 30 and 31 with k from 1300 through 1330, for example).

Theoretically, it can be noticed that an important change in the system configuration might lead, with too selective parameter fitting procedures, to parameters for the external network equivalents that cause non-convergent local optimizations. In that particular case, the decentralized control scheme faces some robustness issues, which could be tackled by refreshing the measurements at the interconnections several times before running the local optimizations.

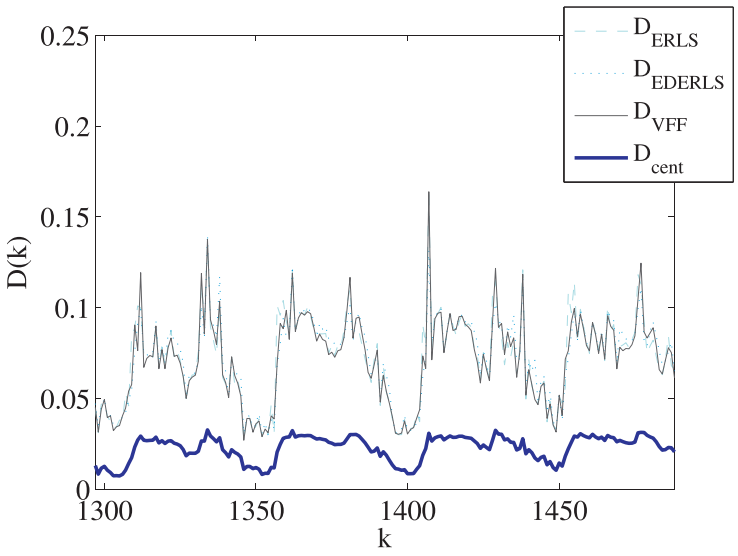

Figure 28: Evolution of the performance index $D(k)$ with the 118 bus benchmark system subjected to case 1.

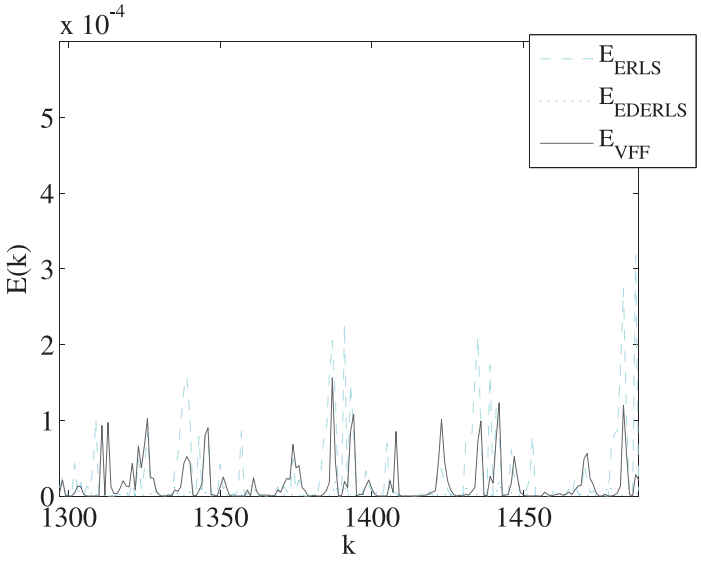

Figure 29: Evolution of the performance index $E(k)$ with the 118 bus benchmark system subjected to case 1.

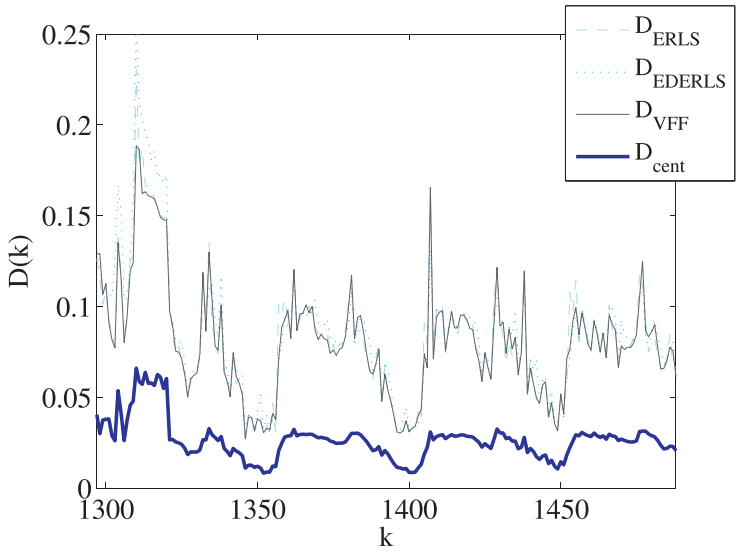

Figure 30: Evolution of the performance index $D(k)$ with the 118 bus benchmark system subjected to case 2.

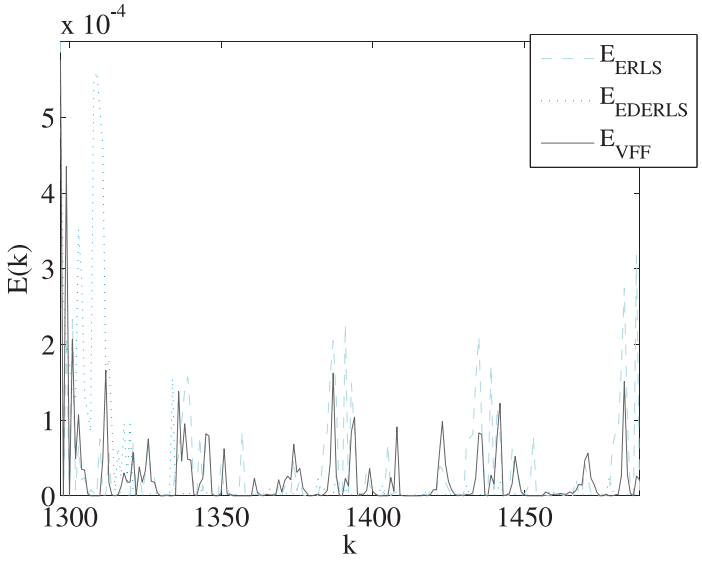

Figure 31: Evolution of the performance index $E(k)$ with the 118 bus benchmark system subjected to case 2.

7.3.4.2 Misprediction of the load demand

Figures 32 and 33 display the performance index $D(k)$ and the SVC effort $E(k)$ over the evaluation period, when the IEEE 118 bus is subjected to case 3 (5% underestimation of the load demand). Figures 32 and 33 display the same indexes with case 4 (5% overestimation of the load demand).

It can be observed that a misprediction of the load demand by one TSO does not significantly affect the performance in terms of the index $D(k)$ for the entire system. On the contrary, it may even lead to a better performance. However, a misprediction induces higher SVC effort. By comparing Figure 29 and Figure 33, one can observe an SVC effort increase of 200%. On the other hand, it must be recalled that such a misprediction would also affect the performance and the SVC effort obtained with a centralized control scheme.

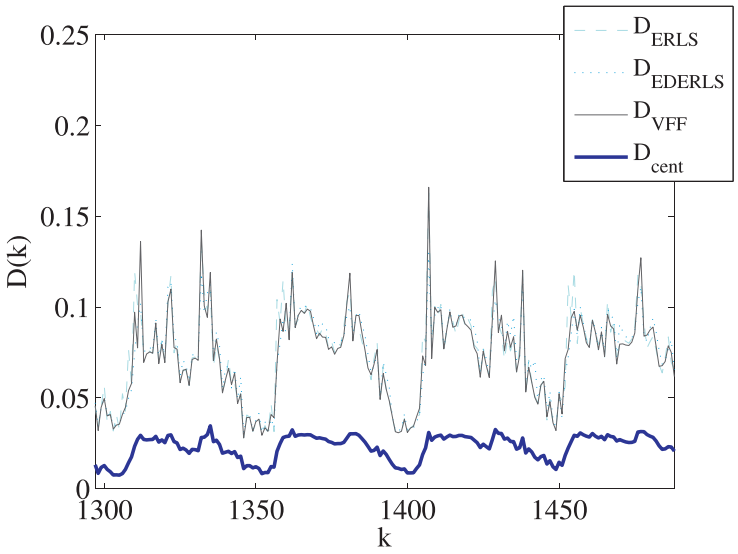

Figure 32: Evolution of the performance index $D(k)$ with the 118 bus benchmark system subjected to case 3.

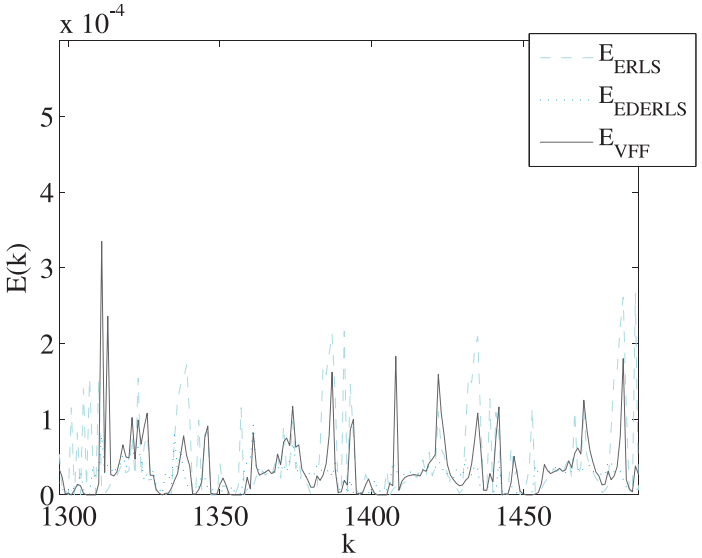

Figure 33: Evolution of the performance index $E(k)$ with the 118 bus benchmark system subjected to case 3.

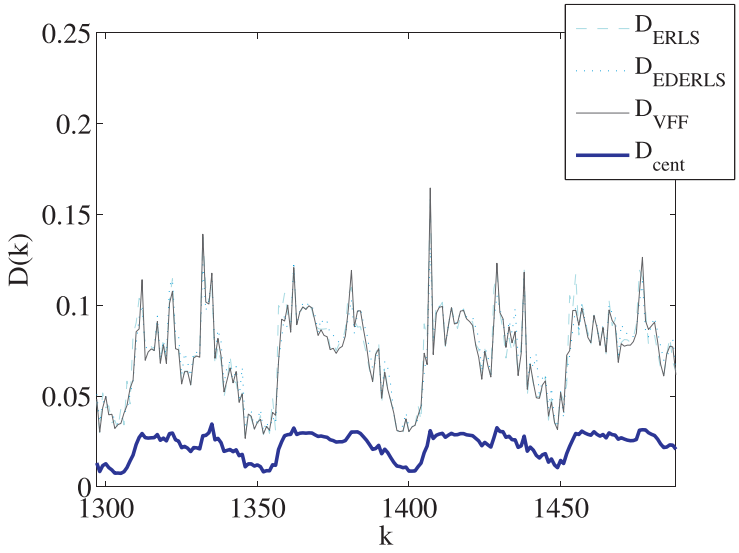

Figure 34: Evolution of the performance index $D(k)$ with the 118 bus benchmark system subjected to case 4.

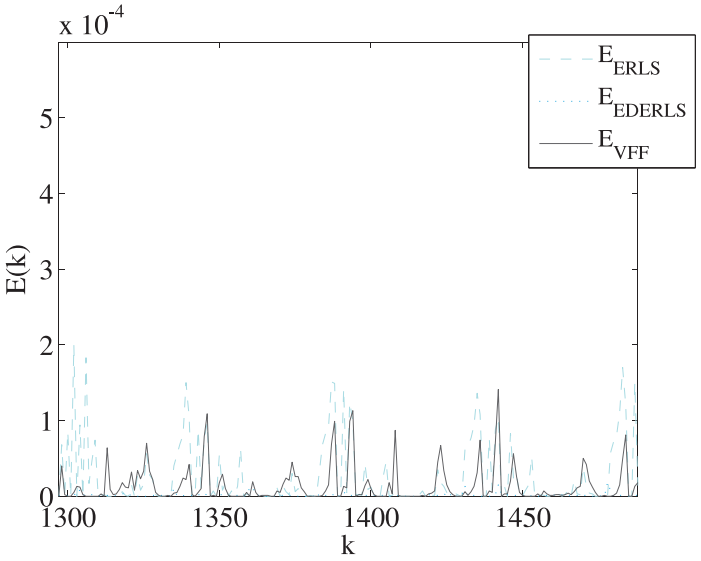

Figure 35: Evolution of the performance index $E(k)$ with the 118 bus benchmark system subjected to case 4.

CHAPTER VIII

APPLICATION TO A LARGE-SCALE SYSTEM

This chapter proposes an evaluation of the performance that can be obtained when the decentralized control scheme is applied to a large-scale system. Simulations are run on a UCTE-like system with 4141 buses and seven TSOs, whose data were provided by RTE, the French TSO. As computation costs are significantly higher than for the IEEE 39 and 118 bus systems, only PQ and PV equivalents with the ERLS fitting procedure are evaluated.

This chapter is organized as follows. First, the test power system is described. Second, the performance of the scheme for a time-invariant power system is detailed. Third, the performance of the scheme is analyzed in the context of a time-varying power system.

8.1 Benchmark system

The time-invariant large-scale test system under consideration is a reduction of the UCTE system that focuses on the western part of the UCTE system (including Spain, France, Belgium, Netherlands, Germany, Switzerland, and Italy) on December 17, 2007 at 10.30 a.m. It is composed of 4141 buses, 624 generators, 6419 branches, and seven TSOs. Due to higher computation complexity, the specific solver SPI developed by RTE has been used to run the optimizations. The simulation time is around 40 seconds for a load flow over the interconnected system and 50 seconds for an optimal power flow.

As minimizing reactive power support requires more computation resources, new objective formulations have been defined. More precisely, the objective of each TSO_i can either be the minimization of active power losses or voltage profiles with respect to a reference value V_{ref}. This latter type of objective is defined as follows.

$$C_{V_{ref}}(\mathbf{u}, \mathbf{x}) = \sum_{i \in [1,\ldots,N_G]} (V_{G_i} - V_{ref})^2 \tag{73}$$

The type of objective of each TSO is arbitrarily chosen as detailed in Table 11.

Table 11: Objective function of every TSO_i in the test power system.

i	1	2	3	4	5	6	7
C_i	$C_{V_{ref}}$	$C_{V_{ref}}$	$C_{V_{ref}}$	$C_{V_{ref}}$	$C_{V_{ref}}$	C_L	C_L
V_{ref} (p.u.)	0.97	0.97	1.01	1.01	1.01		

8.2 Evaluation for a time-invariant large-scale system

Figures 36 and 37 present the evolution of the performance index $D(k)$ and SVC effort $E(k)$, respectively, for PQ and PV equivalents with an ERLS parameter fitting strategy with $\beta = 0.575$.

On the one hand, the SVC effort is large with PV equivalents ($E_{PV_{max}} = 0.0468$), while it remains almost null with PQ equivalents ($E_{PQ_{max}} = 0.0350$, for the first iteration that starts from a non-optimized state and $AE_{PQ} = 0.0005$).

One the other hand, as for the smaller test systems, it can be observed that the PQ equivalent performs better than the PV equivalent and leads to close to optimal performance. Indeed, the average distance AD is equal to 0.2875 with PQ equivalents, 0.6835 with PV equivalents, and 0.1319 with the centralized optimization scheme. Hence, whereas the performance index is higher with the large-scale benchmark system, the decentralized optimization schemes leads to nearly optimal operation conditions. The time to convergence TC is equal to 12 with PQ equivalents, and 1 with PV equivalents.

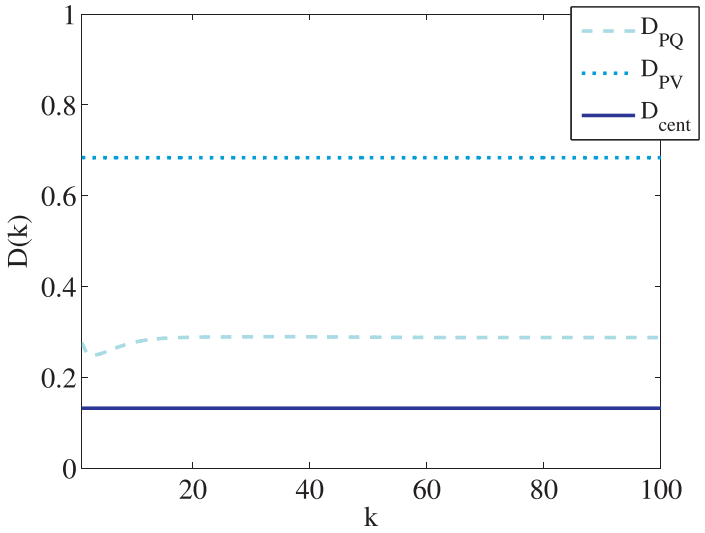

Figure 36: Evolution of the performance index $D(k)$ with the 4141 bus benchmark system under time-invariant operation conditions.

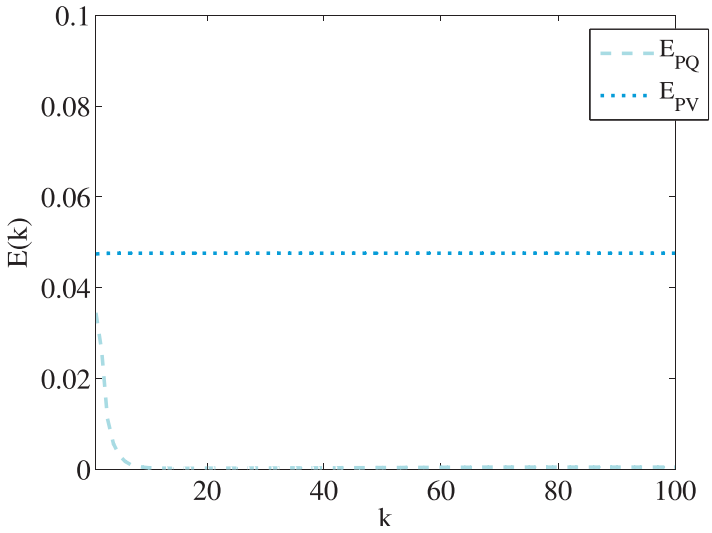

Figure 37: Evolution of the SVC effort index $E(k)$ with the 4141 bus benchmark system under time-invariant operation conditions.

8.3 Evaluation for a time-varying large-scale system

To model a time-varying large-scale system, each region has been allocated a different time-varying load factor $r_i(k)$. As for the IEEE 39 and 118 bus system used in Chapter 7, it is assumed that those load factors $r_i(k)$ are perfectly predicted by each TSO_i at the instant $k-1$. The values of $r_i(k)$ are selected from the ETSO (European Transmission System Operators) website [121]. They correspond to the period April 1, 2008 through April 30, 2008.

In addition, the system configuration evolves on a daily basis based on four snapshots of the UCTE system on December 17, 2007 at 3.30 a.m., 10.30 a.m., 12.30 p.m., and 7.30 p.m.

The time delay between two iterations is defined equal to one hour, and simulations are run for a one month period, where the training period corresponds to the first 15 days and the evaluation period corresponds to the last 15 days.

Figures 38 and 39, display the evolution of the performance index $D(k)$ and SVC effort $E(k)$, respectively, with the PQ and PV equivalents and an ERLS fitting procedure with $\beta = 0.575$. It can be observed that the average performance index is $AD_{cent} = 0.1139$ with the centralized scheme, $AD_{PQ} = 0.0570$ with PQ equivalents, and $AD_{PV} = 0.5112$ with PV equivalents. In addition, the maximum SVC effort is $E_{PV_{max}} = 0.0562$ with PV equivalents and $E_{PQ_{max}} = 0.0072$ with PQ equivalents.

Those figures suggest that, for time-varying large-scale systems, the decentralized optimization scheme leads to nearly optimal performance while inducing low additional SVC effort. Moreover, according to the observations made in Chapter 7, more sophisticated parameter fitting strategies could slightly improve the performance of the proposed optimization scheme.

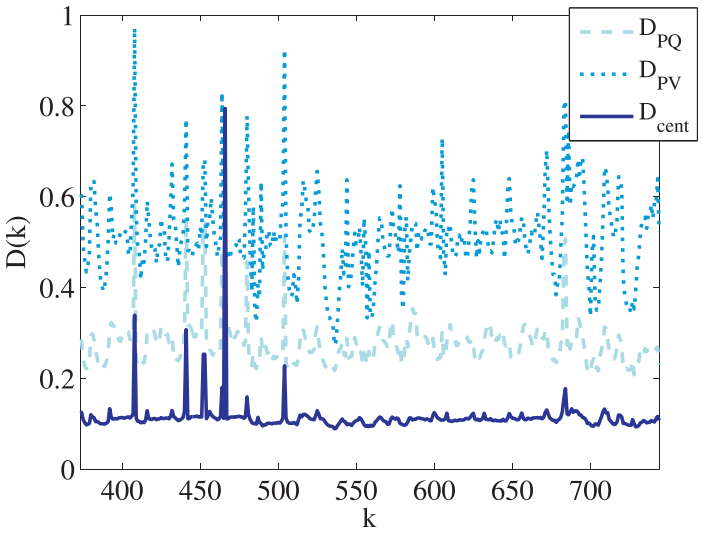

Figure 38: Evolution of the performance index $D(k)$ with the 4141 bus benchmark system under time-varying operation conditions.

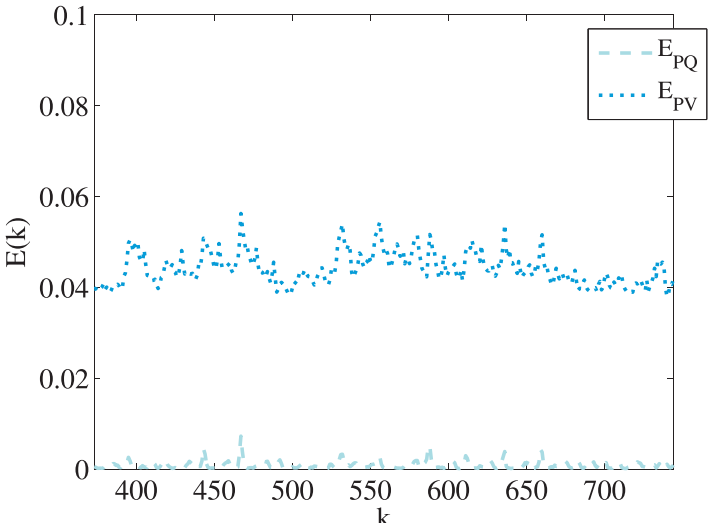

Figure 39: Evolution of the SVC effort index $E(k)$ with the 4141 bus benchmark system under time-varying operation conditions.

CHAPTER IX

CONCLUSIONS

In this thesis, the problem of reactive power dispatch in a multi-TSO system has been formalized as a multi-TSO optimization problem, where each TSO focuses on its own objective. It was shown that a new scheme to coordinate the control actions of the different TSOs should exhibit some properties of fairness, and a centralized optimization scheme was proposed in this respect. As a centralized control scheme inherently raises some issues of robustness, a decentralized scheme with no information exchange has also been proposed.

The principle of this new scheme is as follows. Every TSO assumes an external network equivalent for its neighboring areas at the interconnections and optimizes at every iteration its control actions in a greedy way, i.e. without taking into consideration the impact that its actions may have on the other TSOs' objectives. The communication is done implicitly, by measuring voltage and current values at the interconnections, which depend on the actions taken by different TSOs. Those data are used later to fit the parameters of the equivalents through adaptive parameter fitting procedures.

The study has mainly focused on the single interconnection based equivalents, which model a particular interconnection with a set of equality constraints between the voltage and the current at this interconnection. Also, the adopted fitting procedures assesses the parameters of the equivalents by using only local measurements. Several power system models, types of equivalents, and parameter fitting procedures have been considered. Simulations in time-invariant and time-varying systems have shown that the performance of the decentralized control scheme is strongly dependent

on the functional form of the equality constraints and the fitting procedure. However, one pair of equivalent/fitting procedure, namely a PQ equivalent and an adaptive forgetting factor procedure were identified as consistently performing well in the context of voltage optimization, regardless of the benchmark or the objective functions used. More precisely, that pair was always leading to a decentralized optimization scheme that converged rapidly to a nearly optimal solution while, at the same time, ensuring a good compliance with the system constraints.

Those results suggest on the one hand that a decentralized coordination based on PQ equivalents and adaptive parameter fitting procedure could be a close to optimal solution, easy to implement because it does not add complexity to actual practices of TSOs for reactive power scheduling. On the other hand, results also show that fair settings would be obtained with the centralized coordination scheme. But this scheme may involve large computational complexity, and incentives for TSOs to adopt biased strategies, and would thus require the design of appropriate optimization tools for large-scale systems.

CHAPTER X

CONTRIBUTIONS

As of today, the contributions of the presented research are emphasized below:

- First, a methodology was developed for identifying issues related to MVAr scheduling in multi-TSO systems with poor coordination. Simulation results have been presented in the Strategic Energy Initiative poster session at Georgia Tech in 2006 and in the student poster session of the IEEE PES General Meeting 2006 with a poster entitled "Global coordination of MVAr planning."

- Second, the multi-TSO MVAr scheduling has been formalized as an OPF problem on the basis of a scheduled generation/demand dispatch. New constraints were introduced such as constant active power export for each TSO and the OPF problem was programmed in Matlab and AMPL. The consistency of the optimization scheme was verified by comparing its outcome with industrial software. Based on this program, it was shown that a lack of coordination in the choice of the local objective functions may be a concern in a multi-TSO power system. This study has been presented in the session on ancillary services of the IEEE PES General Meeting 2007 in Tampa, Fl. The associated paper is entitled "Impact of non coordinated MVAr scheduling strategies in multi-area power systems" [70].

- A decentralized coordination algorithm based on single-interconnection based equivalents was proposed, and presented in the Power Tech Conference 2007 in Lausanne, Switzerland. The associated paper is "External network modeling for MVAr scheduling in multi-area power systems" [75].

- This coordination scheme has been further developed through the mathematical formulation of simple equivalents as analytical constraints in the OPF problem. The associated fitting procedures were also developed. This iterative scheme was proposed in the paper entitled "Evaluation of network equivalents for voltage optimization in multi-area power systems," which published in the IEEE Transactions on Power Systems in May 2009 [106].

- Adaptive parameter fitting procedures were developed and applied to the above mentioned decentralized optimization scheme. In addition, the performance obtained with such parameter fitting procedures was analyzed and commented on in a paper entitled "Decentralized reactive power dispatch for a time-varying multi-TSO system" [112], which was presented at the HICSS 2009, in Waikoloa, HI. The robustness of this new scheme has been analyzed in Section 7.3.4 of this thesis.

- A method for fairness analysis of a multi-party optimization scheme in an economic sense was developed. This was presented in the PSCC 2008 in Glasgow, Scotland, in a paper entitled " On the fairness of centralized decision-making strategies for multi-TSO power systems" [7]. This paper was selected among the best papers of the PSCC 2008 for further publication in a special issue of the International Journal of Electric Power and Energy Systems (IJEPES).

- Based on the fairness criteria defined in [7], a fair scheme for centralized optimization of a multi-party system was developed and a journal paper entitled "A fair method for centralized optimization of multi-TSO power systems" [122] was submitted to the IJEPES. This paper was accepted in March 2009.

- In addition, a fairness index for evaluating multi-TSO coordination schemes was developed in collaboration with D. Marinakis and T. Van Cutsem, from the University of Liège. This index will be discussed in a transactions letter

entitled "Fairness and optimization of power systems operated by several system operators." This letter will be submitted shortly to the IEEE Transactions on Power Systems.

- Finally, an advanced decentralized coordination scheme was applied to a large-scale system. Simulation results obtained in this context and some recommendations for an effective implementation of the proposed coordination technique will be submitted for publication in a journal paper in the forthcoming weeks.

The contributions of the presented research are detailed hereafter.

1. Y. Phulpin, S. Plumel, and M. Begovic, "Global coordination of MVAr Planning," Poster in the IEEE Power Engineering Society General Meeting, Montreal, Canada, June 2006.

2. Y. Phulpin, M. Begovic, and M. Petit, "Impact of non-coordinated MVAr scheduling strategies in multi-area power systems," in IEEE Power Engineering Society General Meeting, Tampa, Florida, June 2007.

3. Y. Phulpin, M. Begovic, and M. Petit, "External network modeling for MVAr scheduling in multi-area power systems," in Proceedings of the Power Tech 2007, Lausanne, Switzerland, July 2007.

4. Y. Phulpin, M. Begovic, M. Petit, J.B. Heyberger, and D. Ernst, "Evaluation of network equivalents for voltage optimization in multi-area power systems," IEEE Transactions on Power Systems, Vol. 24, No. 2, pp. 729-743, May 2009.

5. Y. Phulpin, M. Begovic, and M. Petit, and D. Ernst, "On the fairness of centralized decision-making strategies for multi-TSO power systems," in Proceedings of the PSCC 2008, Glasgow, Scotland, July 2008.

6. Y. Phulpin, M. Begovic, and M. Petit, and D. Ernst, "Decentralized reactive power dispatch for a time-varying multi-TSO system," in Proceedings of the HICSS 2009, Waikoloa, Hawaii, January 2009.

7. Y. Phulpin, M. Begovic, and M. Petit, and D. Ernst, "A fair method for centralized optimization of multi-TSO power systems," submitted to the International Journal of Electrical Power and Energy Systems in October 2008, accepted for publication.

8. Y. Phulpin, D. Marinakis, M. Begovic, T. Van Cutsem, and D. Ernst, "Fairness and optimization of power systems operated by several system operators," to be submitted to the IEEE Transactions on Power Systems in August 2009.

CHAPTER XI

FUTURE RESEARCH

This thesis emphasizes that centralized optimization of multi-TSO power systems may achieve settings that could satisfy every TSO. While new types of control centers are created to co-ordinate emergency control actions among several TSOs [123], this scheme is clearly of interest for implementing long-term control actions at the scale of the interconnected system. However, appropriate optimization tools need to be developed to handle optimization of settings for the entire system with respect to an individual objective that covers a single area of the system. In addition, further work should study the potential biased behaviors that TSOs could adopt to turn the optimization scheme in their favor.

The contributions of this research in terms of decentralized coordination could lead to new rules for operating large-scale power systems. For example, one could propose to incorporate the use of PQ equivalents in the operation handbook of interconnected power systems. There are, however, two main issues that should be investigated before using the outcome of this work as a guideline for optimizing power systems in a decentralized way.

The first issue is about the robustness of the proposed control scheme. Indeed, as emphasized in this thesis, the ability of the scheme to constantly lead to secure operation conditions mostly relies on the secondary reactive power reserves quantity and location. Whereas those resources are also explored with traditional practices in reactive power management to compensate for local inconsistencies of the control settings, they are mainly intended to track fast variations of the operation conditions. Therefore, it would be very interesting to compare the different optimization schemes

with regard to an evaluation index that can reflect the location of secondary voltage control reserves. Further research should thus investigate the design of such an index.

The second issue concerns the parameter tracking procedure. This issue is twofold. First, as the amount of data to be taken into account within the parameter fitting process may exceed the computation resources for local optimization of the reactive power dispatch, the computational burden involved by the decentralized scheme should be studied. While the record of the measurements at the interconnections could be truncated to limit the number of cases under consideration, this could also limit the effectiveness of the scheme. Second, the optimal settings identified in this thesis are those that minimize the performance index over certain scenarios. One could thus attempt to design a systematic method to assess settings that would be optimal in any case.

While those new issues may open new research directions, it would also be interesting to investigate other aspects of this research, for example, to set up functional forms of equality constraints that would define optimal types of equivalents. One way to address this problem would be to cast it as an optimization problem. The objective function would then use some of the criteria dealt with in this paper to assess the performance of the control schemes, and a search space composed of a large set of functional equality constraints (based on current and voltage measurements at the interconnections). Another possible research direction is to compare the proposed decentralized optimization scheme with other types of coordination, such as multi-agent model predictive control [124] for example, in the context of reactive power scheduling of multi-area power systems. The comparison could then be extended to other types of coordination problems, such as the setting of phase changers located at interconnections, for example.

APPENDIX A

AMPL FILES FOR A SINGLE-TSO REACTIVE POWER SCHEDULING PROBLEM

This section details the ampl files "problem.run," "problem.dat," and "problem.mod" that are used for a single-TSO optimization. As described in [76], comments are preceded by the symbol #.

A.1 Main file "problem.run"

```
# List of the associated files
model problem.mod; #name of the model file
data problem.dat; #name of the data file


    # Resolution of the problem
solve objective_optim; #name of the objective variable


# Printing the output file (bus voltage magnitudes and angles in this case)
printf "%s \n",'# no: bus_phase: bus_voltage:'> problem.out;
for {i in BUS : i > 0 }{
printf "%4d %6.6f %6.6f\n",i,bus_angle[i],bus_voltage[i] >> problem.txt;};
```

A.2 Data file "problem.dat"

Introduction

data;

Description of the organization of the data files

param: BUS: bus_type bus_voltage0 bus_angl0 bus_p_gen bus_q_gen bus_q_min bus_q_max bus_v_min bus_v_max := include bus.txt; #bus parameters

param: BRANCH: branch_type branch_r branch_x branch_c branch_tap_0 branch_tap_max branch_def_0 branch_def_min branch_def_max := include branch.txt;#branch parameters

param: OBJ: objectif_tso := include objectif.txt; #objective of the TSO

A.3 Model file "problem.mod"

Definition of the sets of data

set BUS; # set of buses

set BRANCH within {1..4000} cross BUS cross BUS; # set of branches

set OBJ; # set of objectives

Definition of the bus parameters

param bus_type {BUS}; #bus type

param bus_voltage0 {BUS}; #initial bus voltage magnitude

param bus_angl0 {BUS}; #initial bus voltage angle

param bus_p_load {BUS}; #initial active power demand at the bus

param bus_q_qload {BUS}; #initial reactive power demand at the bus

param bus_p_gen {BUS}; #initial active power generation at the bus

param bus_q_gen_0 {BUS}; #initial reactive power generation at the bus

```
param bus_q_min {BUS}; #minimum reactive power generation at the bus
param bus_q_max {BUS}; #maximum reactive power generation at the bus
param bus_v_min {BUS}; #minimum bus voltage magnitude
param bus_v_max {BUS}; #maximum bus voltage magnitude

#Definition of the branch parameters
param branch_type {BRANCH}; #branch type
param branch_r {BRANCH}; #branch resistance (in p.u.)
param branch_x {BRANCH}; #branch reactance (in p.u.)
param branch_c {BRANCH}; #branch capacitance (in p.u.)
param branch_tap_0 {BRANCH}; #initial tap setting of the branch (if applicable)
param branch_tap_min {BRANCH}; #minimum tap setting of the branch
param branch_tap_max {BRANCH}; #maximum tap setting of the branch
param branch_def_0 {BRANCH}; #initial angle shift of the branch (if applicable)
param branch_def_min {BRANCH}; #minimum angle shift of the branch
param branch_def_max {BRANCH}; #maximum angle shift of the branch

param branch_g {(l,k,m) in BRANCH} :=
branch_r[l,k,m]/(branch_r[l,k,m]^2+branch_x[l,k,m]^2);
param branch_b {(l,k,m) in BRANCH} :=
-branch_x[l,k,m]/(branch_r[l,k,m]^2+branch_x[l,k,m]^2);

# Definition of the objective weight factor
param objectif_tso {OBJ}; #value of γ for the TSO

# Definition of the state variables
var bus_voltage {i in BUS} ≥ bus_v_min[i], ≤ bus_v_max[i];
```

```
var bus_q_gen {i in BUS} ≥ bus_q_min[i], ≤ bus_q_max[i];
var bus_angle {i in BUS};
var branch_tap {(l,k,m) in BRANCH}
≥ branch_tap_min[l,k,m], ≤ branch_tap_max[l,k,m];
var branch_def {(l,k,m) in BRANCH}
≥ branch_def_min[l,k,m], ≤ branch_def_max[l,k,m];

# Definition of auxiliar variables
# matrix YBUS
set YBUS := setof{i in BUS} (i,i) union
setof {(l,k,m) in BRANCH} (k,m) union
setof {(l,k,m) in BRANCH} (m,k);

var G{(k,m) in YBUS} =
if(k == m) then (sum{(l,k,i) in BRANCH}
branch_g[l,k,i]*branch_tap[l,k,i]∧2 + sum{(l,i,k) in BRANCH} branch_g[l,i,k])
else if(k != m) then (sum{(l,k,m) in BRANCH}
(-branch_g[l,k,m]*cos(branch_def[l,k,m])
-branch_b[l,k,m]*sin(branch_def[l,k,m]))*branch_tap[l,k,m]
+sum{(l,m,k) in BRANCH} (-branch_g[l,m,k]*cos(branch_def[l,m,k])
+branch_b[l,m,k]*sin(branch_def[l,m,k]))*branch_tap[l,m,k]);

var B{(k,m) in YBUS} =
if(k == m) then (sum{(l,k,i) in BRANCH}
(branch_b[l,k,i]*branch_tap[l,k,i]∧2 + branch_c[l,k,i]/2)
+ sum(l,i,k) in BRANCH (branch_b[l,i,k]+branch_c[l,i,k]/2))
else if(k != m) then (sum{(l,k,m) in BRANCH}
```

```
(branch_g[l,k,m]*sin(branch_def[l,k,m])
-branch_b[l,k,m]*cos(branch_def[l,k,m]))*branch_tap[l,k,m]
+sum{(l,m,k) in BRANCH} (-branch_g[l,m,k]*sin(branch_def[l,m,k])
-branch_b[l,m,k]*cos(branch_def[l,m,k]))*branch_tap[l,m,k]);

# Definition of the objective variables
var losses = sum{(l,k,m) in BRANCH} (branch_g[l,k,m]*
(bus_voltage[k]^2*branch_tap[l,k,m]^2+bus_voltage[m]^2
-2*bus_voltage[k]*bus_voltage[m]*branch_tap[l,k,m]*cos(bus_angle[k]-bus_angle[m])));
#active power losses
var support_reactif = sumk in BUS : bus_type[k] == 2 —— bus_type[k] == 3
( bus_q_load[k] + sum(k,m) in YBUS (bus_voltage[k]*bus_voltage[m]*
(G[k,m]*sin(bus_angle[k]-bus_angle[m])-B[k,m]*cos(bus_angle[k]-bus_angle[m])))^2;
var objective = (1-objectif_tso[1])*support_reactif+objectif_tso[1]*losses;

# Definition of the objective name
minimize objective_optim : objective;

# Definition of the constraints
subject to bus_Ref : bus_angle[1]=0;
#sets the phase reference
subject to Sum_Active {k in BUS}:
bus_Compen*bus_p_gen[k] - bus_p_load[k]- sum{(k,m) in YBUS}
(bus_voltage[k]*bus_voltage[m]*(G[k,m]*cos(bus_angle[k]-bus_angle[m])
+B[k,m]*sin(bus_angle[k]-bus_angle[m]))) = 0;
#sets the sum of active power flows = 0, for each bus
subject to Sum_Reactive {k in BUS}:
```

```
bus_q_gen[k] - bus_q_load[k] - sum{(k,m) in YBUS}
(bus_voltage[k]*bus_voltage[m]*(G[k,m]*sin(bus_angle[k]-bus_angle[m])
-B[k,m]*cos(bus_angle[k]-bus_angle[m]))) = 0;
#sets the sum of reactive power flows = 0, for each bus
```

APPENDIX B

NUMERICAL DATA FOR THE IEEE 118 BUS BENCHMARK SYSTEM

Table 12: Bus data for the IEEE 118 bus system with three TSOs.

i	P_i (MW)	Q_i (MW)	V_{maxi} (p.u.)	V_{mini} (p.u.)	TSO
1	51	27	1.06	0.94	2
2	20	9	1.06	0.94	2
3	39	10	1.06	0.94	2
4	39	12	1.06	0.94	2
5	0	0	1.06	0.94	2
6	52	22	1.06	0.94	2
7	19	2	1.06	0.94	2
8	28	0	1.06	0.94	2
9	0	0	1.06	0.94	2
10	0	0	1.06	0.94	2
11	70	23	1.06	0.94	2
12	47	10	1.06	0.94	2
13	34	16	1.06	0.94	2
14	14	1	1.06	0.94	2
15	90	30	1.06	0.94	2
16	25	10	1.06	0.94	2
17	11	3	1.06	0.94	2
18	60	34	1.06	0.94	2
19	45	25	1.06	0.94	2
20	18	3	1.06	0.94	2
21	14	8	1.06	0.94	2
22	10	5	1.06	0.94	2
23	7	3	1.06	0.94	2
24	13	0	1.06	0.94	1
25	0	0	1.06	0.94	2
26	0	0	1.06	0.94	2
27	71	13	1.06	0.94	2
28	17	7	1.06	0.94	2
29	24	4	1.06	0.94	2
30	0	0	1.06	0.94	2
31	43	27	1.06	0.94	2

i	P_i (MW)	Q_i (MW)	V_{maxi} (p.u.)	V_{mini} (p.u.)	TSO
32	59	23	1.06	0.94	2
33	23	9	1.06	0.94	1
34	59	26	1.06	0.94	1
35	33	9	1.06	0.94	1
36	31	17	1.06	0.94	1
37	0	0	1.06	0.94	1
38	0	0	1.06	0.94	1
39	27	11	1.06	0.94	1
40	66	23	1.06	0.94	1
41	37	10	1.06	0.94	1
42	96	23	1.06	0.94	1
43	18	7	1.06	0.94	1
44	16	8	1.06	0.94	1
45	53	22	1.06	0.94	1
46	28	10	1.06	0.94	1
47	34	0	1.06	0.94	1
48	20	11	1.06	0.94	1
49	87	30	1.06	0.94	1
50	17	4	1.06	0.94	1
51	17	8	1.06	0.94	1
52	18	5	1.06	0.94	1
53	23	11	1.06	0.94	1
54	113	32	1.06	0.94	1
55	63	22	1.06	0.94	1
56	84	18	1.06	0.94	1
57	12	3	1.06	0.94	1
58	12	3	1.06	0.94	1
59	277	113	1.06	0.94	1
60	78	3	1.06	0.94	1
61	0	0	1.06	0.94	1
62	77	14	1.06	0.94	1
63	0	0	1.06	0.94	1
64	0	0	1.06	0.94	1
65	0	0	1.06	0.94	1
66	39	18	1.06	0.94	1
67	28	7	1.06	0.94	1
68	0	0	1.06	0.94	1
69	0	0	1.06	0.94	1
70	66	20	1.06	0.94	1
71	0	0	1.06	0.94	1
72	12	0	1.06	0.94	1
73	6	0	1.06	0.94	1
74	68	27	1.06	0.94	3
75	47	11	1.06	0.94	3

i	P_i (MW)	Q_i (MW)	V_{maxi} (p.u.)	V_{mini} (p.u.)	TSO
76	68	36	1.06	0.94	3
77	61	28	1.06	0.94	3
78	71	26	1.06	0.94	3
79	39	32	1.06	0.94	3
80	130	26	1.06	0.94	3
81	0	0	1.06	0.94	3
82	54	27	1.06	0.94	3
83	20	10	1.06	0.94	3
84	11	7	1.06	0.94	3
85	24	15	1.06	0.94	3
86	21	10	1.06	0.94	3
87	0	0	1.06	0.94	3
88	48	10	1.06	0.94	3
89	0	0	1.06	0.94	3
90	163	42	1.06	0.94	3
91	10	0	1.06	0.94	3
92	65	10	1.06	0.94	3
93	12	7	1.06	0.94	3
94	30	16	1.06	0.94	3
95	42	31	1.06	0.94	3
96	38	15	1.06	0.94	3
97	15	9	1.06	0.94	3
98	34	8	1.06	0.94	3
99	42	0	1.06	0.94	3
100	37	18	1.06	0.94	3
101	22	15	1.06	0.94	3
102	5	3	1.06	0.94	3
103	23	16	1.06	0.94	3
104	38	25	1.06	0.94	3
105	31	26	1.06	0.94	3
106	43	16	1.06	0.94	3
107	50	12	1.06	0.94	3
108	2	1	1.06	0.94	3
109	8	3	1.06	0.94	3
110	39	30	1.06	0.94	3
111	0	0	1.06	0.94	3
112	68	13	1.06	0.94	3
113	6	0	1.06	0.94	2
114	8	3	1.06	0.94	2
115	22	7	1.06	0.94	2
116	184	0	1.06	0.94	1
117	20	8	1.06	0.94	2
118	33	15	1.06	0.94	3

Table 13: Generator data for the IEEE 118 bus system with three TSOs.

j	Bus #	$P_{G_j}^0$ (MW)	Q_{Gmax_j} (MVAr)	Q_{Gmin_j} (MVAr)	V_j^0 (p.u.)
1	1	0.00	15.00	-5.00	0.96
2	4	0.00	300.00	-300.00	1.00
3	6	0.00	50.00	-13.00	0.99
4	8	0.00	300.00	-300.00	1.02
5	10	450.00	200.00	-147.00	1.05
6	12	85.00	120.00	-35.00	0.99
7	15	0.00	30.00	-10.00	0.97
8	18	0.00	50.00	-16.00	0.97
9	19	0.00	-8.00	-8.00	0.96
10	24	0.00	300.00	-300.00	0.99
11	25	220.00	140.00	-47.00	1.05
12	26	314.00	1000.00	-1000.00	1.02
13	27	0.00	300.00	-300.00	0.97
14	31	7.00	300.00	-300.00	0.97
15	32	0.00	-14.00	-14.00	0.96
16	34	0.00	-8.00	-8.00	0.98
17	36	0.00	24.00	-8.00	0.98
18	40	0.00	300.00	-300.00	0.97
19	42	0.00	300.00	-300.00	0.99
20	46	19.00	100.00	-100.00	1.01
21	49	204.00	210.00	-85.00	1.03
22	54	48.00	300.00	-300.00	0.96
23	55	0.00	23.00	-8.00	0.95
24	56	0.00	15.00	-8.00	0.95
25	59	155.00	0.00	0.00	0.99
26	61	160.00	300.00	-100.00	1.00
27	62	0.00	20.00	-20.00	1.00
28	65	391.00	200.00	-67.00	1.01
29	66	392.00	200.00	-67.00	1.05
30	69	513.87	300.00	-300.00	1.04
31	70	0.00	32.00	-10.00	0.98
32	72	0.00	100.00	-100.00	0.98
33	73	0.00	100.00	-100.00	0.99
34	74	0.00	9.00	-6.00	0.96
35	76	0.00	23.00	-8.00	0.94
36	77	0.00	70.00	-20.00	1.01
37	80	477.00	280.00	-165.00	1.04
38	85	0.00	23.00	-8.00	0.99
39	87	4.00	1000.00	-100.00	1.02
40	89	607.00	300.00	-210.00	1.01

j	Bus #	$P_{G_j}^0$ (MW)	Q_{Gmax_j} (MVAr)	Q_{Gmin_j} (MVAr)	V_j^0 (p.u.)
41	90	0.00	300.00	-300.00	0.99
42	91	0.00	100.00	-100.00	0.98
43	92	0.00	-3.00	-3.00	0.99
44	99	0.00	100.00	-100.00	1.01
45	100	252.00	155.00	-50.00	1.02
46	103	40.00	40.00	40.00	1.01
47	104	0.00	23.00	-8.00	0.97
48	105	0.00	-8.00	-8.00	0.97
49	107	0.00	200.00	-200.00	0.95
50	110	0.00	23.00	-8.00	0.97
51	111	36.00	1000.00	-100.00	0.98
52	112	0.00	1000.00	-100.00	0.98
53	113	0.00	200.00	-100.00	0.99
54	116	0.00	1000.00	-1000.00	1.01

Table 14: Branch data for the IEEE 118 bus system with three TSOs.

k	From bus #	To bus #	r_k (p.u.)	x_k (p.u.)	g_k (p.u.)	ρ_k
1	1	2	0.0303	0.0999	0.0254	0
2	1	3	0.0129	0.0424	0.01082	0
3	4	5	0.00176	0.00798	0.0021	0
4	3	5	0.0241	0.108	0.0284	0
5	5	6	0.0119	0.054	0.01426	0
6	6	7	0.00459	0.0208	0.0055	0
7	8	9	0.00244	0.0305	1.162	0
8	8	5	0	0.0267	0	0.985
9	9	10	0.00258	0.0322	1.23	0
10	4	11	0.0209	0.0688	0.01748	0
11	5	11	0.0203	0.0682	0.01738	0
12	11	12	0.00595	0.0196	0.00502	0
13	2	12	0.0187	0.0616	0.01572	0
14	3	12	0.0484	0.16	0.0406	0
15	7	12	0.00862	0.034	0.00874	0
16	11	13	0.02225	0.0731	0.01876	0
17	12	14	0.0215	0.0707	0.01816	0
18	13	15	0.0744	0.2444	0.06268	0
19	14	15	0.0595	0.195	0.0502	0
20	12	16	0.0212	0.0834	0.0214	0
21	15	17	0.0132	0.0437	0.0444	0
22	16	17	0.0454	0.1801	0.0466	0
23	17	18	0.0123	0.0505	0.01298	0
24	18	19	0.01119	0.0493	0.01142	0
25	19	20	0.0252	0.117	0.0298	0

k	From bus #	To bus #	r_k (p.u.)	x_k (p.u.)	g_k (p.u.)	ρ_k
26	15	19	0.012	0.0394	0.0101	0
27	20	21	0.0183	0.0849	0.0216	0
28	21	22	0.0209	0.097	0.0246	0
29	22	23	0.0342	0.159	0.0404	0
30	23	24	0.0135	0.0492	0.0498	0
31	23	25	0.0156	0.08	0.0864	0
32	26	25	0	0.0382	0	0.96
33	25	27	0.0318	0.163	0.1764	0
34	27	28	0.01913	0.0855	0.0216	0
35	28	29	0.0237	0.0943	0.0238	0
36	30	17	0	0.0388	0	0.96
37	8	30	0.00431	0.0504	0.514	0
38	26	30	0.00799	0.086	0.908	0
39	17	31	0.0474	0.1563	0.0399	0
40	29	31	0.0108	0.0331	0.0083	0
41	23	32	0.0317	0.1153	0.1173	0
42	31	32	0.0298	0.0985	0.0251	0
43	27	32	0.0229	0.0755	0.01926	0
44	15	33	0.038	0.1244	0.03194	0
45	19	34	0.0752	0.247	0.0632	0
46	35	36	0.00224	0.0102	0.00268	0
47	35	37	0.011	0.0497	0.01318	0
48	33	37	0.0415	0.142	0.0366	0
49	34	36	0.00871	0.0268	0.00568	0
50	34	37	0.00256	0.0094	0.00984	0
51	38	37	0	0.0375	0	0.935
52	37	39	0.0321	0.106	0.027	0
53	37	40	0.0593	0.168	0.042	0
54	30	38	0.00464	0.054	0.422	0
55	39	40	0.0184	0.0605	0.01552	0
56	40	41	0.0145	0.0487	0.01222	0
57	40	42	0.0555	0.183	0.0466	0
58	41	42	0.041	0.135	0.0344	0
59	43	44	0.0608	0.2454	0.06068	0
60	34	43	0.0413	0.1681	0.04226	0
61	44	45	0.0224	0.0901	0.0224	0
62	45	46	0.04	0.1356	0.0332	0
63	46	47	0.038	0.127	0.0316	0
64	46	48	0.0601	0.189	0.0472	0
65	47	49	0.0191	0.0625	0.01604	0
66	42	49	0.0715	0.323	0.086	0
67	42	49	0.0715	0.323	0.086	0
68	45	49	0.0684	0.186	0.0444	0

k	From bus #	To bus #	r_k (p.u.)	x_k (p.u.)	g_k (p.u.)	ρ_k
69	48	49	0.0179	0.0505	0.01258	0
70	49	50	0.0267	0.0752	0.01874	0
71	49	51	0.0486	0.137	0.0342	0
72	51	52	0.0203	0.0588	0.01396	0
73	52	53	0.0405	0.1635	0.04058	0
74	53	54	0.0263	0.122	0.031	0
75	49	54	0.073	0.289	0.0738	0
76	49	54	0.0869	0.291	0.073	0
77	54	55	0.0169	0.0707	0.0202	0
78	54	56	0.00275	0.00955	0.00732	0
79	55	56	0.00488	0.0151	0.00374	0
80	56	57	0.0343	0.0966	0.0242	0
81	50	57	0.0474	0.134	0.0332	0
82	56	58	0.0343	0.0966	0.0242	0
83	51	58	0.0255	0.0719	0.01788	0
84	54	59	0.0503	0.2293	0.0598	0
85	56	59	0.0825	0.251	0.0569	0
86	56	59	0.0803	0.239	0.0536	0
87	55	59	0.04739	0.2158	0.05646	0
88	59	60	0.0317	0.145	0.0376	0
89	59	61	0.0328	0.15	0.0388	0
90	60	61	0.00264	0.0135	0.01456	0
91	60	62	0.0123	0.0561	0.01468	0
92	61	62	0.00824	0.0376	0.0098	0
93	63	59	0	0.0386	0	0.96
94	63	64	0.00172	0.02	0.216	0
95	64	61	0	0.0268	0	0.985
96	38	65	0.00901	0.0986	1.046	0
97	64	65	0.00269	0.0302	0.38	0
98	49	66	0.018	0.0919	0.0248	0
99	49	66	0.018	0.0919	0.0248	0
100	62	66	0.0482	0.218	0.0578	0
101	62	67	0.0258	0.117	0.031	0
102	65	66	0	0.037	0	0.935
103	66	67	0.0224	0.1015	0.02682	0
104	65	68	0.00138	0.016	0.638	0
105	47	69	0.0844	0.2778	0.07092	0
106	49	69	0.0985	0.324	0.0828	0
107	68	69	0	0.037	0	0.935
108	69	70	0.03	0.127	0.122	0
109	24	70	0.00221	0.4115	0.10198	0
110	70	71	0.00882	0.0355	0.00878	0
111	24	72	0.0488	0.196	0.0488	0

k	From bus #	To bus #	r_k (p.u.)	x_k (p.u.)	g_k (p.u.)	ρ_k
112	71	72	0.0446	0.18	0.04444	0
113	71	73	0.00866	0.0454	0.01178	0
114	70	74	0.0401	0.1323	0.03368	0
115	70	75	0.0428	0.141	0.036	0
116	69	75	0.0405	0.122	0.124	0
117	74	75	0.0123	0.0406	0.01034	0
118	76	77	0.0444	0.148	0.0368	0
119	69	77	0.0309	0.101	0.1038	0
120	75	77	0.0601	0.1999	0.04978	0
121	77	78	0.00376	0.0124	0.01264	0
122	78	79	0.00546	0.0244	0.00648	0
123	77	80	0.017	0.0485	0.0472	0
124	77	80	0.0294	0.105	0.0228	0
125	79	80	0.0156	0.0704	0.0187	0
126	68	81	0.00175	0.0202	0.808	0
127	81	80	0	0.037	0	0.935
128	77	82	0.0298	0.0853	0.08174	0
129	82	83	0.0112	0.03665	0.03796	0
130	83	84	0.0625	0.132	0.0258	0
131	83	85	0.043	0.148	0.0348	0
132	84	85	0.0302	0.0641	0.01234	0
133	85	86	0.035	0.123	0.0276	0
134	86	87	0.02828	0.2074	0.0445	0
135	85	88	0.02	0.102	0.0276	0
136	85	89	0.0239	0.173	0.047	0
137	88	89	0.0139	0.0712	0.01934	0
138	89	90	0.0518	0.188	0.0528	0
139	89	90	0.0238	0.0997	0.106	0
140	90	91	0.0254	0.0836	0.0214	0
141	89	92	0.0099	0.0505	0.0548	0
142	89	92	0.0393	0.1581	0.0414	0
143	91	92	0.0387	0.1272	0.03268	0
144	92	93	0.0258	0.0848	0.0218	0
145	92	94	0.0481	0.158	0.0406	0
146	93	94	0.0223	0.0732	0.01876	0
147	94	95	0.0132	0.0434	0.0111	0
148	80	96	0.0356	0.182	0.0494	0
149	82	96	0.0162	0.053	0.0544	0
150	94	96	0.0269	0.0869	0.023	0
151	80	97	0.0183	0.0934	0.0254	0
152	80	98	0.0238	0.108	0.0286	0
153	80	99	0.0454	0.206	0.0546	0
154	92	100	0.0648	0.295	0.0472	0

k	From bus #	To bus #	r_k (p.u.)	x_k (p.u.)	g_k (p.u.)	ρ_k
155	94	100	0.0178	0.058	0.0604	0
156	95	96	0.0171	0.0547	0.01474	0
157	96	97	0.0173	0.0885	0.024	0
158	98	100	0.0397	0.179	0.0476	0
159	99	100	0.018	0.0813	0.0216	0
160	100	101	0.0277	0.1262	0.0328	0
161	92	102	0.0123	0.0559	0.01464	0
162	101	102	0.0246	0.112	0.0294	0
163	100	103	0.016	0.0525	0.0536	0
164	100	104	0.0451	0.204	0.0541	0
165	103	104	0.0466	0.1584	0.0407	0
166	103	105	0.0535	0.1625	0.0408	0
167	100	106	0.0605	0.229	0.062	0
168	104	105	0.00994	0.0378	0.00986	0
169	105	106	0.014	0.0547	0.01434	0
170	105	107	0.053	0.183	0.0472	0
171	105	108	0.0261	0.0703	0.01844	0
172	106	107	0.053	0.183	0.0472	0
173	108	109	0.0105	0.0288	0.0076	0
174	103	110	0.03906	0.1813	0.0461	0
175	109	110	0.0278	0.0762	0.0202	0
176	110	111	0.022	0.0755	0.02	0
177	110	112	0.0247	0.064	0.062	0
178	17	113	0.00913	0.0301	0.00768	0
179	32	113	0.0615	0.203	0.0518	0
180	32	114	0.0135	0.0612	0.01628	0
181	27	115	0.0164	0.0741	0.01972	0
182	114	115	0.0023	0.0104	0.00276	0
183	68	116	0.00034	0.00405	0.164	0
184	12	117	0.0329	0.14	0.0358	0
185	75	118	0.0145	0.0481	0.01198	0
186	76	118	0.0164	0.0544	0.01356	0

APPENDIX C

NUMERICAL DATA FOR THE IEEE 39 BUS BENCHMARK SYSTEM

Table 15: Bus data for the IEEE 39 bus system with three TSOs.

i	P_i (MW)	Q_i (MW)	V_{maxi} (p.u.)	V_{mini} (p.u.)	TSO
1	0	0	1.06	0.94	1
2	0	0	1.06	0.94	2
3	322	2.4	1.06	0.94	2
4	500	184	1.06	0.94	1
5	0	0	1.06	0.94	1
6	0	0	1.06	0.94	1
7	233.8	84	1.06	0.94	1
8	522	176.6	1.06	0.94	1
9	0	0	1.06	0.94	1
10	0	0	1.06	0.94	1
11	0	0	1.06	0.94	1
12	8.5	88	1.06	0.94	1
13	0	0	1.06	0.94	1
14	0	0	1.06	0.94	1
15	320	153	1.06	0.94	3
16	329.4	32.3	1.06	0.94	3
17	0	0	1.06	0.94	2
18	158	30	1.06	0.94	2
19	0	0	1.06	0.94	3
20	680	103	1.06	0.94	3
21	274	115	1.06	0.94	3
22	0	0	1.06	0.94	3
23	247.5	84.6	1.06	0.94	3
24	308.6	-92.2	1.06	0.94	3
25	224	47.2	1.06	0.94	2
26	139	17	1.06	0.94	2
27	281	75.5	1.06	0.94	2
28	206	27.6	1.06	0.94	2
29	283.5	26.9	1.06	0.94	2
30	0	0	1.06	0.94	2
31	9.2	4.6	1.06	0.94	1

i	P_i (MW)	Q_i (MW)	V_{maxi} (p.u.)	V_{mini} (p.u.)	TSO
32	0	0	1.06	0.94	1
33	0	0	1.06	0.94	3
34	0	0	1.06	0.94	3
35	0	0	1.06	0.94	3
36	0	0	1.06	0.94	3
37	0	0	1.06	0.94	2
38	0	0	1.06	0.94	2
39	1104	250	1.06	0.94	1

Table 16: Generator data for the IEEE 39 bus system with three TSOs.

j	Bus #	P_{Gj}^0 (MW)	Q_{Gmaxj} (MVAr)	Q_{Gminj} (MVAr)	V_j^0 (p.u.)
1	30	250	9999.00	-9999.00	1.05
2	31	573.2359	9999.00	-9999.00	0.98
3	32	650	9999.00	-9999.00	0.98
4	33	632	9999.00	-9999.00	1.00
5	34	508	9999.00	-9999.00	1.01
6	35	650	9999.00	-9999.00	1.05
7	36	560	9999.00	-9999.00	1.06
8	37	540	9999.00	-9999.00	1.03
9	38	830	9999.00	-9999.00	1.03
10	39	1000	9999.00	-9999.00	1.03

Table 17: Branch data for the IEEE 39 bus system with three TSOs.

k	From bus #	To bus #	r_k (p.u.)	x_k (p.u.)	g_k (p.u.)	ρ_k
1	1	2	0.0035	0.0411	0.6987	0
2	1	39	0.001	0.025	0.75	0
3	2	3	0.0013	0.0151	0.2572	0
4	2	25	0.007	0.0086	0.146	0
5	3	4	0.0013	0.0213	0.2214	0
6	3	18	0.0011	0.0133	0.2138	0
7	4	5	0.0008	0.0128	0.1342	0
8	4	14	0.0008	0.0129	0.1382	0
9	5	6	0.0002	0.0026	0.0434	0
10	5	8	0.0008	0.0112	0.1476	0

k	From bus #	To bus #	r_k (p.u.)	x_k (p.u.)	g_k (p.u.)	ρ_k
11	6	7	0.0006	0.0092	0.113	0
12	6	11	0.0007	0.0082	0.1389	0
13	7	8	0.0004	0.0046	0.078	0
14	8	9	0.0023	0.0363	0.3804	0
15	9	39	0.001	0.025	1.2	0
16	10	11	0.0004	0.0043	0.0729	0
17	10	13	0.0004	0.0043	0.0729	0
18	13	14	0.0009	0.0101	0.1723	0
19	14	15	0.0018	0.0217	0.366	0
20	15	16	0.0009	0.0094	0.171	0
21	16	17	0.0007	0.0089	0.1342	0
22	16	19	0.0016	0.0195	0.304	0
23	16	21	0.0008	0.0135	0.2548	0
24	16	24	0.0003	0.0059	0.068	0
25	17	18	0.0007	0.0082	0.1319	0
26	17	27	0.0013	0.0173	0.3216	0
27	21	22	0.0008	0.014	0.2565	0
28	22	23	0.0006	0.0096	0.1846	0
29	23	24	0.0022	0.035	0.361	0
30	25	26	0.0032	0.0323	0.513	0
31	26	27	0.0014	0.0147	0.2396	0
32	26	28	0.0043	0.0474	0.7802	0
33	26	29	0.0057	0.0625	1.029	0
34	28	29	0.0014	0.0151	0.249	0
35	12	11	0.0016	0.0435	0	1.006
36	12	13	0.0016	0.0435	0	1.006
37	6	31	0	0.025	0	1.07
38	10	32	0	0.02	0	1.07
39	19	33	0.0007	0.0142	0	1.07
40	20	34	0.0009	0.018	0	1.009
41	22	35	0	0.0143	0	1.025
42	23	36	0.0005	0.0272	0	1
43	25	37	0.0006	0.0232	0	1.025
44	2	30	0	0.0181	0	1.025
45	29	38	0.0008	0.0156	0	1.025
46	19	20	0.0007	0.0138	0	1.06

REFERENCES

[1] Y. Rebours, D. Kirschen, M. Trotignon, and S. Rossignol, "A survey of frequency and voltage control ancillary services - part I: technical features," *IEEE Transactions on Power Systems*, vol. 22, pp. 350–357, February 2007.

[2] J. Bialek, "Are blackouts contagious?," *IEE Power Engineer*, vol. 17, pp. 10–13, December 2003.

[3] UCTE, "Final Report - system disturbance on 4 November 2006," tech. rep., UCTE, January 2007.

[4] C. Taylor, "Improving grid behaviour," *IEEE Spectrum*, vol. 36, pp. 40–45, June 1999.

[5] L. Day, "Control area trends: principles and responses," *IEEE Computer Applications in Power*, vol. 8, pp. 34–39, April 1995.

[6] J. Aguado and V. Quintana, "Inter-utilities power-exchange coordination: a market-oriented approach," *IEEE Transactions on Power Systems*, vol. 16, pp. 513–519, August 2001.

[7] Y. Phulpin, M. Begovic, M. Petit, and D. Ernst, "On the fairness of centralised decision-making strategies for multi-TSO power systems," in *Proceedings of the PSCC 2008*, (Glasgow, Scotland), July 2008.

[8] Y. Li and V. Venkatasubramanian, "Coordination of transmission path transfers," *IEEE Transactions on Power systems*, vol. 19, pp. 1607–1615, August 2004.

[9] P. Panciatici, F. Bena, P. Pruvot, N. Janssens, J. Deuse, and M. Stubbe, "Centralized voltage control: a key point for optimal operation of power systems," in *Cigre Paper 39-116*, (Paris, France), September 1998.

[10] UCTE, "UCTE Operation Handbook," 2007.

[11] L. Dubins and E. Spanier, "How to cut a cake fairly," *American mathematical monthly*, vol. 68, pp. 1–17, January 1961.

[12] A. Feldman and A. Kirman, "Fairness and envy," *American economic review*, vol. 64, pp. 995–1005, December 1974.

[13] J. Konow, "A positive theory of economic fairness," *Journal of Behavior and Organization*, vol. 31, pp. 13–35, October 1996.

[14] C. Liu, J. Jung, G. Heydt, and V. Vittal, "The strategic power infrastructure defense (SPID) system," *IEEE Control System Magazine*, vol. 20, pp. 40–52, 2000.

[15] A. Marinakis, M. Glavic, and T. Van Cutsem, "Control of phase shifting transformers by multiple transmission system operators," in *Proceedings of the Power Tech 2007*, (Lausanne, Switzerland), July 2007.

[16] G. Hug-Glanzmann and G. Andersson, "Decentralized optimal power flow control for overlapping areas in power systems," *IEEE Transactions on Power Systems*, vol. 24, pp. 327–336, February 2009.

[17] M. Zima and D. Ernst, "On multi-area control in electric power systems," in *Proceedings of the PSCC 2005*, (Liege, Belgium), August 2005.

[18] A. Conejo and J. Aguado, "Multi-area coordinated decentralized DC optimal power flow," *IEEE Transactions on Power Systems*, vol. 13, pp. 1272–1278, November 1998.

[19] M. Ilic, E. Allen, J. Chapman, C. King, J. Lang, and E. Litvinov, "Preventing future blackouts by means of enhanced electric power systems control: From complexity to order," *Proceedings of the IEEE*, vol. 93, pp. 1920–1941, November 2005.

[20] IEEE/CIGRE Joint Task Force on Stability Terms and Definitions, "Definition and classification of power system stability," *IEEE Transactions on Power Systems*, vol. 19, pp. 1387–1401, May 2004.

[21] T. Van Cutsem and C. Vournas, *Voltage Stability of Electric Power Systems*. Kluwer Academic Publishers, 1998.

[22] C. Barbier and J. Barret, "An analaysis of phenomena of voltage collapse on a transmission system," *Revue Générale de l'Electricité*, vol. 89, pp. 672–690, October 1980.

[23] V. Venikov, V. Stroev, V. Idelchick, and V. Tarasov, "Estimation of electrical power system steady-state stability by load flow calculations," *IEEE Transactions on Power Apparatus and Systems*, vol. PAS-94, no. 3, pp. 1034–1041, 1975.

[24] H. Kwatny, A. Pasrija, and L. Bahar, "Static bifurcation in electric power networks: loss of steady-state stability and voltage collapse," *IEEE Transactions on Circuits and Systems*, vol. 33, pp. 981–991, October 1986.

[25] J. Medanic, M. Ilic, and J. Christensen, "Discrete models of slow voltage dynamics for under load tap-changing transformer coordination," *IEEE Transactions on Power Systems*, vol. 2, no. 4, pp. 873–880, 1987.

[26] T. Zhu, S. Tso, and K. Lo, "An investigation into the OLTC effects on voltage collapse," *IEEE Transactions on Power Systems*, vol. 15, pp. 515–521, May 2000.

[27] C. Liu and K. Vu, "Analysis of tap-changer dynamics and contruction of voltage stability regions," *IEEE Transactions on Circuits and Systems*, vol. 36, pp. 575–590, April 1989.

[28] H. Ohtsuki, A. Yokoyama, and Y. Sekine, "Reverse action of on-load tap changer in association with voltage collapse," *IEEE Transactions on Power Systems*, vol. 6, pp. 300–306, February 1991.

[29] F. Capitanescu, B. Otomega, H. Lefebvre, V. Sermanson, and T. Van Cutsem, "Prospects of an improved system protection scheme against voltage instability in the RTE system," in *Proceedings of the PSCC 2008*, (Glasgow, Scotland), July 2008.

[30] B. Milosevic, *On Voltage Stability Monitoring and Control Using Multiagent Systems*. PhD thesis, Georgia Institute of Technology, USA, December 2002.

[31] J. Sotomayor, *Generic Bifurcations of dynamical systems*. Academic Press, New York, 1973.

[32] H. Kwatny, R. Fischl, and C. Nwankpa, "Local bidufrcation in power systems: theory, computation, and application," *Proceedings of the IEEE*, vol. 83, pp. 1456–1483, November 1995.

[33] V. Ajjarapu and B. Lee, "Bifurcation theory and its application to nonlinear dynamical phenomena in an electrical power system," *IEEE Transactions on Power Systems*, vol. 7, pp. 424–431, February 1992.

[34] J. Guckenheimer and P. Holmes, *Nonlinear oscillations, dynamical systems, and bifurcation of vector fields*. Springer Verlag, New York, 1983.

[35] S. Greene, I. Dobson, and F. Alvarado, "Sensitivity of the loading margin to voltage collapse with respect to arbitrary parameters," *IEEE Transactions on Power Systems*, vol. 12, pp. 262–268, February 1997.

[36] C. Canizares and F. Alvardo, "Point of collapse and continuation methods for large AC/DC systems," *IEEE Transactions on Power Systems*, vol. 7, pp. 1–8, February 1993.

[37] T. Van Cutsem, "Voltage instability: phenomena, coutermeasures, and analysis methods," *Proceedings of the IEEE*, vol. 88, pp. 208–227, February 2000.

[38] C. Taylor, *Power System Voltage, Stability*. New York: McGraw Hill, 1994.

[39] C. Noe, G. Richerme., G. Blanchon, and F. Maury, "Le reglage automatique de la tension du reseau de transport d'EDF," *Revue Generale de l'Electricite*, pp. 333–347, 1972.

[40] T. Hughes, *Networks of Power: Electrification in Western Society, 1880-1930*. The Johns Hopkins University Press, 1993.

[41] C. Bouneau, "Les reseaux de tranpsort d'electricite en europe occidentale depuis la fin du XIXeme sciecle: de la diversite des modeles nationaux a la recherche de la convergence europeenne," *L'Electricite en reseaux, Networks of Power, Annales historiques de l'electricite*, pp. 23–37, June 2004.

[42] M. Huneault and F. Galiana, "A survey of the optimal power flow literature," *IEEE Transactions on Power Systems*, vol. 6, pp. 762–770, May 1991.

[43] N. Martins, N. Macedo, L. Lima, and H. Pinto, "Control strategies for multiple static VAr compensators in long distance voltage supported transmission systems," *IEEE Transactions on Power Systems*, vol. 8, pp. 1107–1117, August 1993.

[44] S. Corsi, M. Pozzi, C. Sabelli, and A. Serrani, "The coordinated automatic voltage control of the Italian transmission grid - part I: Reasons of the choice and overview of the consolidated hierarchical system," *IEEE Transactions on Power Systems*, vol. 19, pp. 1723–1732, November 2004.

[45] Cigre Task Force 39-02, "Reglage de la tension et de la puissance reactive," in *Cigre Paper 39-203*, (Paris, France), September 1992.

[46] S. Hao, "A reactive power management proposal for transmission operators," *IEEE Transactions on Power Systems*, vol. 18, pp. 1374–1381, November 2002.

[47] C. Taylor, "Reactive power today, best practices to prevent blackouts," *IEEE Power and Energy Magazine*, vol. 4, pp. 104–102, September 2006.

[48] S. Corsi, P. Marannino, N. Losignore, G. Moreschini, and G. Piccini, "Coordination between the reactive power scheduling function and the hierarchical voltage control of the EHV ENEL system," *IEEE Transactions on Power Systems*, vol. 10, pp. 686–694, May 1995.

[49] M. Ilic, "New approaches to voltage monitoring and control," *IEEE Control Systems Magazine*, vol. 9, pp. 5–11, January 1989.

[50] N. Martins, "The new cigre task force on coordinated voltage control in transmission networks," in *IEEE Power Engineering Society General Meeting*, pp. 305–306, June 2000.

[51] P. Vovos, A. Kiprakis, A. Wallace, and G. Harrison, "Centralized and distributed voltage control: Impact on distributed generation penetration," *IEEE Transactions on Power Systems*, vol. 22, pp. 476–483, February 2007.

[52] H. Vu, P. Pruvot, C. Launay, and Y. Harmand, "An improved voltage control on large scale power system," *IEEE Transactions on Power Systems*, vol. 11, pp. 1295–1303, August 1996.

[53] J. Paul, J. Leost, and J. Tesseron, "Survey on the secondary voltage control in France: a present realization and investigations," *IEEE Transactions on Power Systems*, vol. 2, pp. 505–511, May 1987.

[54] J. Thorp, M. Ilic, and M. Verghese, "An optimal secondary voltage-VAr control technique," *IFAC Automatica*, vol. 22, no. 2, pp. 217–221, 1986.

[55] P. Lagonotte, J. Sabonnadiere, J. Leost, and J. Paul, "Structural analysis of the electrical system: Application to secondary voltage control in France," *IEEE Transactions on Power Systems*, vol. 4, pp. 479–486, May 1989.

[56] A. Stankovic, M. Ilic, and D. Maratukulam, "Recent results in secondary voltage control of power systems," *IEEE Transactions on Power Systems*, vol. 6, pp. 94–101, February 1991.

[57] A. Conejo and M. Aguilar, "Secondary voltage control: Non-linear selection of pilot buses, design of an optimal control law, and simulation results," *IEE Proceedings on Generation Transmission and Distribution*, vol. 145, pp. 123–131, January 1998.

[58] H. Lefebvre, D. Fragnier, J. Boussion, P. Mallet, and M. Bulot, "Advantages of coordinated secondary voltage control in a deregulated environment," in *Cigre Paper 39-208*, (Paris, France), September 2000.

[59] M. Ilic, X. Liu, G. Leung, M. Athans, C. Vialas, and P. Pruvot, "Improved secondary and new tertiary voltage control," *IEEE Transactions on Power Systems*, vol. 10, pp. 1851–1862, November 1995.

[60] H. Song, B. Lee, and Y. Moon, "Reactive optimal power flow incorporating margin enhancement constraints with non linear interior point method," *IEE Proceedings on Generation Transmission and Distribution*, vol. 152, pp. 961–968, November 2005.

[61] D. Thukaram, L. Jenkins, and K. Visakha, "Optimum allocation of reactive power for voltage stability improvement in AC-DC power systems," *IEE Proceedings on Generation Transmission and Distribution*, vol. 153, pp. 237–246, March 2006.

[62] T. Menezes, T. Da Silva, C. Affonso, and V. Da Costa, "MVAr management on the pre-dispatch problem for improving voltage stability margin," *IEE Proceedings on Generation Transmission and Distribution*, vol. 151, pp. 665–672, November 2004.

[63] N. Janssens, "Tertiary and secondary voltage control for the Belgian HV system," in *Proceedings of the IEE Colloquium on International Practices in Reactive Power Control*, (London, UK), pp. 81–84, April 1993.

[64] F. Graf, "Real-time application of an optimal power flow algorithm for reactive power allocation of the RWE energy control center," in *Proceedings of the IEE Colloquium on International Practices in Reactive Power Control*, (London, UK), pp. 71–74, April 1993.

[65] J. Sancha, J. Fernandez, F. Martinez, and C. Salle, "Spanish practices in reactive power management and voltage control," in *Proceedings of the IEE Colloquium on International Practices in Reactive Power Control*, (London, UK), pp. 31–34, April 1993.

[66] C. Launay, "Prevention of voltage collapse on the French power system," in *Proceedings of the IEE Colloquium on International Practices in Reactive Power Control*, (London, UK), pp. 21–27, April 1993.

[67] F. Milano, C. Canizares, and A. Conejo, "Sensitivity-based security-constrained OPF market clearing model," *IEEE Transactions on Power Systems*, vol. 20, pp. 2051–2060, November 2005.

[68] R. Pritchard, "The contemporary rationale for interconnection of power systems," *Oil Gas and Energy Law Intelligence*, vol. 1, January 2003.

[69] A. Adamson, A. Dessel, and L. Garver, "Generation reserve value of interconnections," *IEEE Transactions on Power Apparatus and Systems*, vol. PAS-96, no. 2, pp. 337–346, 1977.

[70] Y. Phulpin, M. Begovic, and M. Petit, "Impact of non coordinated MVAr scheduling strategies in multi-area power systems," in *IEEE Power Engineering Society General Meeting*, (Tampa, Florida), June 2007.

[71] H. Dommel and W. Tinney, "Optimal power flow solutions," *IEEE Transactions on Power Apparatus and Systems*, vol. PAS-87, no. 10, pp. 1866–1876, 1968.

[72] F. Capitanescu, M. Glavic, D. Ernst, and L. Wehenkel, "Interior-point based algorithms for the solution of optimal power flow problems," *Electric Power Systems Research*, vol. 77, pp. 508–517, April 2007.

[73] R. Salgado and M. Irving, "Framework for the analysis of reactive power dispatch in energy pools," *IEE Proc. on Generation, Transmission, Distribution*, vol. 151, pp. 167–174, March 2004.

[74] E. Miguelez, F. Echavarren Cerezo, and L. Rodriguez, "On the assignment of voltage control ancillary service of generators in Spain," *IEEE Transactions on Power Systems*, vol. 22, pp. 367–375, February 2007.

[75] Y. Phulpin, M. Begovic, and M. Petit, "External network modeling for MVAr scheduling in multi-area power systems," in *Proceedings of the Power Tech 2007*, (Lausanne, Switzerland), July 2007.

[76] R. Fourer, D. Gay, and B. Kernighan, *AMPL: A Modeling Language for Mathematical Programming*. Duxbury Press / Brooks/Cole Publishing Company, 2002.

[77] R. Vanderbei, "Non linear models for power system optimization." Available at: http://www.sor.princeton.edu/ rvdb/ampl/nlmodels/, 2007.

[78] R. Zimmerman, C. Murillo-Sanchez, and D. Gan, *Matpower User's Manual*. School of Electrical Engineering, Cornell University, Ithaca, 2005.

[79] V. Quintana, G. Torres, and J. Medina-Palomo, "Interior-point methods and their applications to power systems: A classification of publications and software codes," *IEEE Transactions on Power Systems*, vol. 15, pp. 170–176, November 2000.

[80] B. Murtagh and M. Saunders, "Minos 5.4 user's guide," tech. rep., Systems Optimization Laboratory, Stanford University, 1983, Revised 1995.

[81] T. Orfanogianni and R. Bacher, "Increased OPF code development efficiency by integration of general purpose optimization and derivative computation tools," in *Proceedings of the 21st IEEE International Conference on Power Industry Computer Applications, PICA '99*, pp. 123–129, May 1999.

[82] R. Vanderbei, "LOQO: An interior point code for quadratic programming," tech. rep., Princeton University, School of Engineering and Operations Research, Princeton, NJ, May 1997.

[83] K. Miettinen, *Nonlinear Multiobjective Optimization*. Kluwer Academic Publishers, 1999.

[84] Y. Censor, "Pareto optimality in multi-objective problems," *Applied Mathematics and Optimization*, vol. 4, no. 1, pp. 41–59, 1977.

[85] C. Coello Coello, "Evolutionary multi-objective optimization: a historical view of the field," *IEEE Computational Intelligence Magazine*, vol. 1, pp. 28–36, February 2006.

[86] Y. Collette and P. Siarry, *Optimisation multiobjectif*. Eyrolles, 2002.

[87] I. Das and J. Dennis, "Normal-boundary intersection: a new method for generating the pareto surface in nonlinear multicriteria optimization problems," *SIAM Journal on Optimization*, vol. 8, pp. 631–657, August 1998.

[88] C. Roman and W. Rosehart, "Evenly distributed pareto points in multiobjective optimal power flow," *IEEE Transactions on Power Systems*, vol. 21, pp. 1011–1012, May 2006.

[89] E. Ulungu, J. Teghem, P. Fortemps, and D. Tuyttens, "MOSA method: a tool for solving multiobjective combinatorial optimization problems," *Journal of multicriteria decision analysis*, vol. 8, no. 4, pp. 221–236, 1999.

[90] F. Glover and M. Laguna, *Tabu Search*. Kluwer Academic Publishers, 1997.

[91] K. Deb, A. Pratap, S. Agarwal, and T. Meyarivan, "A fast and elitist multiobjective genetic algorithm: NSGA-II," *IEEE Transactions on Evolutionary Computation*, vol. 6, pp. 182–197, April 2002.

[92] S. Small and B. Jeyasura, "Multi-objective reactive power planning: a pareto optimization approach," in *Intelligent Systems Applications to Power Systems, ISAP 2007*, (Niigata, Japan), pp. 1–6, November 2007.

[93] K. Miettinen, "Some methods for nonlinear multi-objective optimization," in *Evolutionary Multi-Criterion Optimization, EMO 2001* (E. Zitzler, K. Deb, L. Thiele, C. A. Coello Coello, and D. Corne, eds.), (Berlin, Heidelberg), pp. 1–20, Springer-Verlag, March 2001.

[94] S. Zionts and J. Wallenius, "An interactive programming method for solving the multiple-criteria problem," *Management sceince*, vol. 22, pp. 652–663, February 1976.

[95] Y. Chen and C. Liu, "Multiobjective var planning using the goal-attainment method," *IEE Proceedings on Generation Transmission Distribution*, vol. 141, pp. 227–232, May 1994.

[96] Y. Hsiao, H. Chiang, C. Liu, and Y. Chen, "A computer package for optimal multi-objective VAR planning in large-scale power systems," *IEEE Transactions on Power Systems*, vol. 9, pp. 668–676, May 1994.

[97] Y. Haimes, L. Lasdon, and D. Wismer, "On a bicriterion formulation of the problems of integrated system identification and system optimization," *IEEE Transactions on Systems, Man and Cybernetics*, vol. 1, pp. 296–297, 1971.

[98] F. Gembicki, *Performance and Sensitivity Optimization: A Vector Index Approach*. PhD thesis, Case Western Research University, Cleveland, Ohio, 1974.

[99] M. Salukvadze, *Vector Valued Optimization in Control Theory*. New York Academic Press, 1979.

[100] R. Marler and J. Arora, "Survey of multi-objective optimization methods for engineering," *Structural and Multidisciplinary Optimization*, vol. 26, no. 6, pp. 369–395, 2004.

[101] L. Lim and I. Benbasat, "From negotiation to negotiation support systems: a theoretical perspective," in *Proceedings of the HICSS 1992*, (Hawaii, USA), pp. 153 – 163, January 1992.

[102] D. Dickinson and J. Tiefenthaler, "What is fair? experimental evidence," *Southern Economic Journal*, vol. 69, pp. 214–428, October 2002.

[103] M. Rabin, "Incorporating fairness into game theory and economics," *American Economic Review*, vol. 83, pp. 1281–1302, 1993.

[104] B. Rubenstein-Montano and R. Malaga, "A weighted sum genetic algorithm to support multiple-party multiple-objective negotiations," *IEEE Transactions on Evolutionary Computations*, vol. 6, pp. 366–377, August 2002.

[105] H. Wang, C. Murillo-Sanchez, R. Zimmerman, and R. Thomas, "On computational issues of market-based optimal power flow," *IEEE Transactions on Power Systems*, vol. 22, pp. 1185–1193, August 2007.

[106] Y. Phulpin, M. Begovic, M. Petit, J. Heyberger, and D. Ernst, "Evaluation of network equivalents for voltage optimization in multi-area power systems," *IEEE Transactions on Power Systems*, vol. 24, pp. 729–743, May 2009.

[107] K. Allstrom, U. Borisson, L. Ljung, and B. Wittemark, "Theory and applications of self-tuning regulators," *Automatica*, vol. 13, pp. 457–476, 1977.

[108] D. Pierre, "A perspective on adaptive control of power systems," *IEEE Transactions on Power Systems*, vol. 2, pp. 387–395, May 1987.

[109] R. Majumder, B. Chaudhuri, and B. Pal, "A probabilistic approach to model-based adaptive control for damping of interarea oscillations," *IEEE Transactions on Power Systems*, vol. 20, pp. 367–374, February 2005.

[110] S. Jain, F. Khorrami, and B. Fardanesh, "Adaptive nonlinear excitation control of power systems with unknown interconnections," *IEEE Transactions on Control Systems Technology*, vol. 2, pp. 436–446, December 1994.

[111] T. Fortescue, L. Kershenbaum, and B. Ydstie, "Implementation of self-tuning regulators with variable forgetting factors," *Automatica*, vol. 17, no. 6, pp. 831–835, 1981.

[112] Y. Phulpin, M. Begovic, M. Petit, and D. Ernst, "Decentralized reactive power dispatch for a time-varying multi-TSO system," in *Proceedings of the HICSS 2009*, (Hawaii, USA), pp. 1 – 8, January 2009.

[113] B. Milosevic and M. Begovic, "A network of phasor measurement units for voltage stability monitoring and control," *IEEE Transactions on Power Systems*, vol. 18, pp. 121–127, February 2003.

[114] P. Dimo, *Node Analysis of Power Systems*. Abacus Press, United Kingdom, 1975.

[115] M. Oatts, S. Erwin, and J. Hart, "Application of the REI equivalent for operations planning analysis of interchange schedules," *IEEE Transactions on Power Systems*, vol. 5, pp. 547–555, May 1990.

[116] E. Davison and W. Gesing, "Sequential stability and optimization of large scale decentralized systems," *Automatica*, vol. 15, pp. 307–324, 1979.

[117] D. Gavel and D. Siljak, "Decentralized adaptive control: structural conditions for stablity," *IEEE Transactions on Automatic Control*, vol. 34, pp. 413–426, April 1989.

[118] W. Kim and K. Lee, "The existence of Nash equilibrium in n-person games with C-concavity," *Computers and Mathematics with Applications*, vol. 44, pp. 1219–1228, November 2002.

[119] K. Tan, J. Yu, and X. Yuan, "Existence theorems of Nash equilibria for non-cooperative n-person games," *International Journal of Game Theory*, vol. 24, pp. 217–222, September 1995.

[120] G. Inalhan, D. Stipanovic, and C. Tomlin, "Decentralized optimization, with application to multiple aircraft coordination," in *Proceedings of the 41st IEEE Conference on Decision and Control*, (Las Vegas, Nevada), pp. 1147–1155, December 2002.

[121] European Transmission System Operators, "System vertical load data." Available at : http://www.etsovsita.org, 2008.

[122] Y. Phulpin, M. Begovic, M. Petit, and D. Ernst, "A fair method for centralized optimization of multi-TSO power systems," *International Journal of Electric Power and Energy Systems*, pp. 1–7, 2009.

[123] Coreso, "http://www.coreso.eu."

[124] R. Negenborn, *Multi-Agent Model Predictive Control with Applications to Power Networks*. PhD thesis, TU Delft, Delft, Netherlands, 2007.